Towards optimal lung volume in high-frequency oscillatory ventilation

Cover design: Femke Hiemstra
Reproduction: PrintPartners Ipskamp
ISBN: 90-9018619-0

VRIJE UNIVERSITEIT

Towards optimal lung volume in high-frequency oscillatory ventilation

ACADEMISCH PROEFSCHRIFT

ter verkrijging van de graad van doctor aan
de Vrije Universiteit Amsterdam,
op gezag van de rector magnificus
prof.dr. T. Sminia,
in het openbaar te verdedigen
ten overstaan van de promotiecommissie
van de faculteit der Geneeskunde
op vrijdag 28 januari 2005 om 13.45 uur
in de aula van de universiteit,
De Boelelaan 1105

door

Désiré Godwin Markhorst

geboren te Apeldoorn

promotoren:	prof.dr. J.J. Roord
	prof.dr. A.J. van Vught
copromotor:	dr. ir. H.R. van Genderingen

CONTENTS

Chapter 1

General introduction

Background

Mechanical ventilation is one of the cornerstones of modern intensive care practice. Mechanical ventilation may, however, result in secondary lung damage, also referred to as ventilator-induced lung injury (VILI) and multi-organ failure.[1-6] In a small number of patients, pulmonary gas exchange cannot sufficiently be improved by conventional mechanical ventilation.[7-9]

Attempts have been made to develop new ventilatory strategies and modes of mechanical ventilation with the purpose of overcoming these limitations and adverse effects of conventional mechanical ventilation.[10-24] One of these relatively new modes of mechanical ventilation is high-frequency oscillatory ventilation (HFOV).

At the end of the 1960 s Öberg and Sjöstrand, while studying blood pressure regulation and the carotid sinus reflex in ventilated animals, found their measurements disturbed by respiratory synchronous variations in blood pressure.[25,26] Therefore, they needed a method of artificial ventilation that would reduce this effect. Insufflation of the ventilating gas deep into the trachea via an endotracheal catheter reduced the anatomical dead space and, consequently, smaller tidal volumes at higher frequencies, 60 – 120 min^{-1}, could be used. This reduced pressure variations in the airways and in the intrathoracic space, and diminished the cyclic circulatory effects of ventilation. The circulation remained stable and adequate gas exchange was obtained at lower inspiratory peak pressures, lower mean airway pressure and lower transpulmonary pressures. Experimental animals and later on newborns and small children accepted these ventilatory conditions without significant breathing against the ventilator. For this mode of ventilation Sjöstrand and co-workers introduced the term high-frequency positive pressure ventilation (HFPPV).[25] Although originally designed for experimental physiological studies, HFPPV was recognised to have important clinical advantages and the method has since been developed for clinical application. In 1977 Klain et al. described the insufflation of small volumes of gas under high pressures (jets) with frequencies up to 200 min^{-1}, later up to 600 min^{-1}, into the trachea of dogs.[27] This method was referred to as high-frequency jet ventilation (HFJV). In 1980 Bohn et al. and Butler et al. demonstrated that adequate gas exchange was also possible by generating oscillations in the airways at a frequency of 15 Hz.[28,29] The oscillations could be generated either by a loudspeaker or an electronically driven piston pump. Earlier, Lunkenheimer et al. had found adequate CO_2 elimination by comparable methods with frequencies between 20 – 40 Hz.[30] This method, high-frequency oscillatory ventilation (HFOV), is characterised by the generation of pressure swings with, in contrast to HFPPV

and HFJV, an active withdrawal of air from the airways. Following experimental work in animals, the first large studies on the use of HFOV in human newborn patients were published at the end of the 1980s early 1990s.[31-37] A few years later, its use in small paediatric patients was reported. [38,39] Based on the positive experiences in paediatric patients and with evolving technology, HFOV has now also found its way into adult and adolescent intensive care.[40] High-frequency oscillatory ventilation has gained a definite place in the treatment of severe respiratory insufficiency. Although the use of this ventilation mode is not limited to acute respiratory distress syndrome (ARDS), most experience with HFOV in paediatric intensive care has been gained in this disease entity. However, it is well recognised that future studies should compare different algorithms of applying HFOV to determine the optimal techniques for achieving oxygenation and ventilation, and that the potential role of adjunctive therapies used with HFOV, including inhaled nitric oxide, requires further research.[41]

In this thesis, we investigated the safety and efficacy of HFOV in paediatric patients and focussed on monitoring of effects during HFOV.

Respiratory distress syndrome

Acute respiratory distress syndrome

Adult respiratory distress syndrome was first described in 1967 by Ashbaugh et al. in a series of 12 patients who developed a sudden onset of respiratory failure characterised by dyspnea, reduced respiratory system compliance and diffuse alveolar infiltrates on the chest radiograph, that resembled pulmonary oedema without evidence of prior lung disease or congestive heart failure.[42] Later, it was recognised that the syndrome is not limited to adults, but also occurs in children. This led to a change in terminology to *acute* respiratory distress syndrome (ARDS).[43] An important characteristic of ARDS is the inactivation of lung surfactant, covering the surface of alveoli and small airways in normal lungs and mainly consisting of lipoproteins. Surfactant reduces the surface tension of the alveolar liquid-air interface and prevents alveolar collapse. The absence or inactivation of surfactant causes alveolar collapse (atelectasis), leading to a reduction of functional residual capacity (FRC), an increase of right-to-left shunt, a decrease in respiratory system compliance and an increase in physiological dead space. These cumulative events eventually lead to a life threatening decrease in arterial oxygenation and increase in work of breathing. ARDS is a severe form of acute lung injury (ALI), a term that covers a wide spectrum of disease

severity between mild dyspnea and tachypnea to a rapidly fatal respiratory failure. Criteria for the diagnosis have been defined as: [44]

- Acute onset of impaired oxygenation;
- Severe hypoxemia defined as a ratio of PaO_2 / FIO_2 of $\leq$ 300 mmHg (40 kPa);
- Bilateral diffuse infiltration on the chest radiograph;
- Pulmonary artery wedge pressure $\leq$ 18 mm Hg to exclude cardiogenic causes of pulmonary oedema.

ARDS is defined as for ALI except for a greater degree of impairment of gas exchange, such that the PaO_2 / FIO_2 ratio is $\leq$ 200 mm Hg (26.7 kPa).

Neonatal respiratory distress syndrome

A surfactant deficiency may lead to the neonatal respiratory distress syndrome (nRDS), the most common cause of acute respiratory failure in newborns, especially premature infants.[45-47] Besides surfactant deficiency, structural immaturity of lung development plays a role in this disease. These abnormalities may lead to deteriorating lung mechanics and gas exchange, resulting in dyspnea, tachypnea and cyanosis in ambient air.
New therapies have been developed, including antenatal glucocorticoid administration and endotracheal surfactant administration. Other, additional, strategies aim at reducing damaging effects of mechanical ventilation and exposure to high oxygen concentrations in the immature lung. One of these strategies is HFOV. Probably, however, a ventilator strategy aimed at optimising lung volume is more important than the specific ventilator used, for reducing the incidence of chronic lung disease.[48,49]

Lung mechanics in ARDS

The mechanical properties of the respiratory system are altered in ARDS. Compliance of either lung, its surrounding chest wall or both is decreased. Furthermore, FRC is decreased. A schematic representation of these changes is shown in Fig. 1.1.

In ARDS, pulmonary oedema causes an increase in alveolar surface tension.[50] The pressure needed to open a collapsed lung unit in ARDS is increased.[51] Both phenomena lead to a shift of the pressure-volume (PV) curve to the right and a decrease in lung volume at zero airway pressure (FRC).

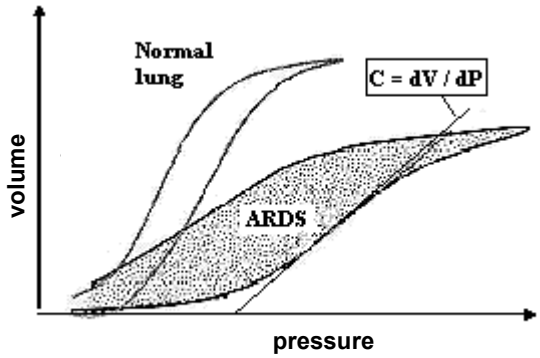

Fig. 1.1. Schematic static pressure-volume curves in health and ARDS.

ARDS is characterised by considerable regional differences in lung aeration (Fig 1.2).[52] In general, in a supine patient, the dependent lung zone (dorsal) is mostly affected and prone to atelectasis at low distending pressures. The non-dependent lung zone (ventral) is relatively healthy. Superimposed pressure by the gravitational force of the overlying tissue is thought to be one of the contributing factors to explain these regional differences.
Alveolar *closing* pressures may be substantially smaller than alveolar *opening* pressures, yielding hysteresis in the PV curve (Fig 1.3).[53,54] Lung volume and lung compliance at a given end-expiratory pressure will be higher following a manoeuvre aimed at opening previously collapsed lung units.

Mechanical ventilation

The majority of patients suffering from acute respiratory insufficiency require respiratory

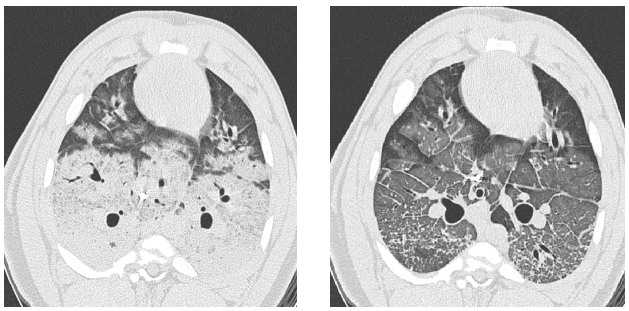

Fig. 1.2. CT scan of an animal with acute lung injury, induced by lung lavage, at two different static airway pressures: 5 cm H_2O (left) and 40 cm H_2O (right). The dark lung areas are well aerated, the light areas indicate atelectasis (from N. Weiler, with permission).

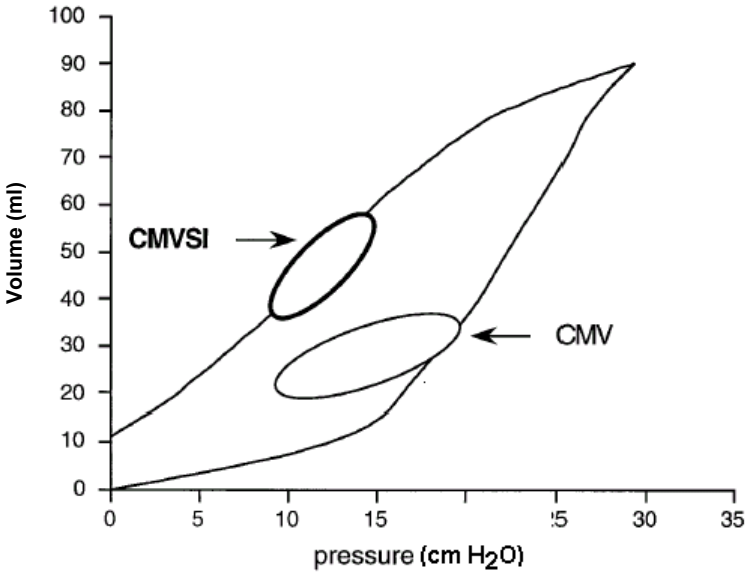

Figure 1.3. Schematic drawing illustrating the position of dynamic pressure volume loops to the overall pressure volume curve during conventional ventilation before (CMV) and after a sustained inflation (CMVSI). (From [54] with permission).

support, with positive airway pressure and increased levels of inspired oxygen concentration to increase lung volume and improve oxygenation. These patients are intubated and mechanically ventilated. However, mechanical ventilation has adverse effects and, therefore, has limitations. It has been demonstrated that low end-expiratory pressure can augment lung injury, explained by repetitive opening and closure of distal lung units, leading to increased forces on adjacent tissue zones (atelectrauma).[55] In rabbits it has been demonstrated that atelectasis leads to migration and activation of granulocytes, giving rise to a local pulmonary inflammatory response and damage of distant organs (biotrauma).[56-58] It was suggested that an increased positive end-expiratory pressure (PEEP) is indicated in mechanical ventilation of the atelectasis-prone lung. However, together with high tidal volumes, this may lead to lung injury as a result of high end-inspiratory pressures (barotrauma) [59] and lung overstretching (volutrauma).[60] High airway pressures may also lead to important detrimental haemodynamic effects.[61] High airway pressure may increase intrathoracic pressure, thereby increasing central venous pressure, causing a decrease in venous return and a decrease in right and left cardiac preload. As a consequence, cardiac output and oxygen delivery to the body may decrease substantially.[62] Limitation of positive airway pressure may therefore minimise the depression of oxygen delivery.

Based on the above-mentioned considerations, a lung protective ventilation strategy with maintenance of adequate tissue oxygenation should aim at avoiding both alveolar end-expiratory collapse and end-inspiratory overdistention. Although there is a large amount of experimental evidence, there is a limited number of clinical studies in which the beneficial effect on lung protection by an increased PEEP level and/or limited tidal volumes was convincingly demonstrated.[63] Experimental studies have shown that ventilation with low tidal volumes by itself does not prevent lung injury and may even worsen lung injury when repetitive collapse of lung tissue is not prevented. PEEP levels currently employed in intensive care units around the world are below 6 cm H_2O in 78% patients receiving mechanical ventilation,[64] whereas it is known that high PEEP levels above 15 cm H_2O may be needed to prevent repetitive collapse of alveoli and thus reduce shear stress.[65]

Alternative and adjunctive therapy

Recruitment

In a diseased lung the reduction of atelectasis is based on two principles. First, collapsed alveoli need to be recruited by application of sufficient airway pressures. Secondly, once alveoli are open, sufficient end-expiratory pressure needs to be applied to prevent subsequent collapse during expiration. Staub et al. proposed that the behaviour of alveoli is quantal in nature.[66] Once a critical opening pressure is reached, the collapsed alveolus pops open, resulting in an immediate large volume increase. As follows from the law of Laplace, which states that the pressure (P) necessary to keep a spherical structure with radius r open is twice the surface tension (T) divided by the radius (P=2T/r), the critical closing pressure will be lower than the opening pressure.

The pressure volume relationship of the entire lung, as shown in Figures 1.1 and 1.3, will be the cumulative relationship of all alveoli within the lung, each with a different degree of injury, and thus of the opening and closure pressure.

The inflation limb of the PV curve shows the lung volume changes during incremental airway pressures; initially the lung volume does not increase significantly despite an increasing airway pressure. Next, the lung volume increases and once the lung volume approaches the total lung capacity (TLC), the volume increase per unit pressure increase diminishes: the inflation limb flattens. The deflation limb represents changes in lung volume during decremental changes in airway pressures, starting at TLC. Again, as explained by the law of Laplace, lung volume is initially maintained as pressures are lowered, but eventually

decreases due to progressive alveolar collapse. It is now known that opening of collapsed lung units or recruitment occurs along the entire inflation limb of the PV curve.[67] Mathematical models and animal experiments have shown that adequate recruitment of collapsed alveoli, followed by optimal stabilisation with adequate PEEP levels will place ventilation on the deflation limb of the PV curve.[68,69] This will improve compliance and limit end-expiratory atelectasis, repetitive reopening of collapsed alveoli, end-inspiratory pressures and regional overstretching.

Spontaneous breathing efforts help to distribute tidal volume to the dependent zones in the proximity of the diaphragm that are most susceptible to collapse.[70] Prone positioning of the ventilated patient is an especially attractive adjunct to recruitment, in that it applies and sustains rather high tractive forces in dorsal regions that are compressed in the supine position by the locally higher pleural pressure and the weight of the heart and mediastinal contents.[71-73]

From these basic principles, various methods have been suggested to accomplish recruitment without repetitive tidal cyclic forces. How best to perform episodic recruitment manoeuvres, however, has not yet been determined and may well vary with the underlying pathophysiology. Recruitment of collapsed alveoli, as well as collapse of previously open alveoli, are not only pressure dependent, but also time dependent.[74-76] Episodic PEEP increases,[77] intermittent sighs,[78-80] and sustained application of a pressure that achieves total lung capacity have been proposed and tested. Since most underlying lung diseases are inhomogeneous, regional overdistention of relatively healthy lung units is a major concern during lung recruitment. There is, however, little evidence that recruitment manoeuvres damage the lung when accompanied by sufficient end-expiratory pressure. Most experiments indicate that derecruitment is more harmful than recruitment.[81,82] When successful, the benefits of each manoeuvre tend to fade over time, unless a sufficient end-expiratory pressure is sustained by PEEP and/or prone positioning.[83]

Although the concept of the “open-lung approach” is supported by increasing evidence, it should be stated that recruitment of collapsed lung units is not always possible. ARDS may result from direct pulmonary injury (pulmonary ARDS) or may be the result of indirect pulmonary injury by extrapulmonary causes. Diseases like pneumonia and ARDS caused by pulmonary disease are associated with predominant consolidation, whereas ARDS caused by extrapulmonary disease is associated with prevalent interstitial oedema and alveolar

collapse. In diseases characterised predominantly by consolidation, application of PEEP induces only moderate lung recruitment, increased elastance of the respiratory system (reduction of respiratory compliance) and potential alveolar overdistention. When, on the other hand, interstitial oedema and alveolar collapse predominate, PEEP application induces lung recruitment with a decrease of respiratory system elastance (increase of respiratory compliance).[84,85]

High-frequency oscillatory ventilation

HFOV is a ventilatory mode in which an oscillator at a high frequency (5-15 Hz, 300-900 breaths/min) administers a small tidal volume (around 2 ml/kg). These oscillations are superimposed upon a mean airway pressure, referred to as the continuous distending pressure (CDP). Lung volume and thus oxygenation is mainly determined by CDP, whereas ventilation is provided by the oscillations. Theoretically, HFOV is an ideal method for the ventilatory treatment of ARDS patients: The increased end-expiratory lung volume prevents alveolar collapse in the dependent lung zone, whereas the low tidal volume prevents end-inspiratory overstretching of the relatively healthy alveoli in the non-dependent lung zone. However, early multi-centre studies showed increased morbidity in neonates when HFOV was compared to conventional mechanical ventilation (CMV). This was attributed to the lack of an adequate lung volume recruitment strategy and other methodological flaws. In the 1990s, the safety of HFOV has been demonstrated in a number of studies in newborns, children and more recently in adults.[86-89] At present, various experimental and clinical investigations are conducted to find the best lung-protective strategy, both for HFOV and CMV.

Optimal lung volume

One of the difficulties in the practical implementation of open lung ventilation is the lack of consensus on the definition of optimal lung volume. Lachmann et al. proposed the use of the physiological shunt fraction (Q'_S/Q'_T) to assess an open-lung condition. At a Q'_S/Q'_T below 0.1, the lungs are assumed to be adequately recruited, an optimal lung volume is reached at the lowest airway pressure needed to achieve this condition, thereby minimising lung overdistention and cardiac output depression. In HFOV, the lowest ratio of pressure swings at the distal end and the proximal opening of the endotracheal tube (OPR), as well as the lowest oxygenation index (OI) have been described as indicators of optimal airway pressure.[90,91] Determination of Q'_S/Q'_T requires access to the pulmonary artery for mixed venous blood sampling, which is not always suitable in adults and is usually not performed

in most paediatric patients. For the clinical assessment of lung volume, only indirect methods are currently available, such as chest X-ray and measurement of oxygenation. Direct measurement of lung volume during HFOV has not been established yet. Only by interruption of HFOV, and application of a gas dilution method during subsequent conventional mechanical ventilation, lung volume can be determined.[92] Lung volume assessment through FRC measurement is difficult at the bedside, but alternative methods such as inductive plethysmography and electrical impedance tomography are promising.[93-96] Computed tomography was demonstrated to give information on regional lung aeration in a thoracic cross-section, to assess atelectasis and hyperinflation. It is, however, not available at the bedside, requires transportation of an often unstable patient and is associated with increased radiation load. Recently, two methods were proposed and tested experimentally to provide information to find the optimal CDP: Analysis of a quasi-static pressure-volume curve by supersyringe, obtained *prior* to HFOV application and estimation of mean lung volume change by respiratory inductive plethysmography *during* HFOV.[97] The value of the pressure volume curve as a guide for mechanical ventilation has been disputed and currently is not available at the bedside.[98]

Nitric oxide

As was outlined above, the “open-lung approach” is not feasible in all patients. This may lead to failing mechanical ventilation as a result of decreased ventilation-perfusion matching. Inhalation of nitric oxide (NO) reduces pulmonary artery pressure and increases arterial oxygenation by improving ventilation-perfusion matching, without producing systemic vasodilatation in newborns with severe persistent hypertension of the newborn (PPHN), in children with pulmonary hypertension and in patients with severe ARDS.[99-104] In adults with severe ARDS, however, clinical trials have shown no beneficial outcome.[105-108] Nevertheless, NO is still in use for rescue therapy in adults.[109,110] In newborns suffering from PPHN, inhaled NO (iNO) improves oxygenation, reduces the amount of ventilatory support needed, and prevents progression to severe PPHN.[111]
The effect of iNO is augmented by optimal recruitment of lung volume, as has been described in the combination of HFOV and iNO.[112,113]

Outline of this thesis

The aim of this thesis was to develop and evaluate a number of methods to improve volume targeted HFOV and the combination of HFOV and iNO:

- *High-frequency oscillatory ventilation in paediatric patients.* Three HFOV strategies were described. First, the "open-lung strategy" in diffuse alveolar disease, secondly the "low-volume strategy" in air leak syndromes and thirdly the "open airway strategy" in obstructive small airway disease (*Chapter 2*).
- In *Chapter 3*, *a system for integrated measurement of ventilator settings, lung volume change and blood gases during high-frequency oscillatory ventilation* is described. As outlined above, lung volume measurements are currently not available at the bedside, and lung volume optimisation during HFOV requires combined analysis of vital parameters, blood gas analysis and close observation of the patient. We tried to provide a method of facilitating this process both for clinical and research purposes.
- The accuracy of respiratory inductive plethysmography (RIP) to estimate lung volume changes has been addressed in *Chapter 4*: *accuracy of respiratory inductive plethysmography at varying PEEP levels and during different degrees of acute lung injury*.
- Given a reliable method of measuring lung volume changes with the potential to be used at the bedside, we questioned the value of the use of pressure volume curves to predict pressures needed to obtain and maintain an "open lung", as has been described in the literature. This was done in a mathematical model of ARDS lungs (*Chapter 5, static pressure-volume curve characteristics are moderate estimators of optimal airway pressures in a mathematical model of ARDS*).
- In the analysis of respiratory inductive plethysmography signals, obtained in piglet experiments and clinical application, we noticed airway pressure-dependent changes in ribcage and abdominal motion. We hypothesised that maximal breath-to-breath chest wall displacement measured with RIP would coincide with maximal respiratory system compliance (*Chapter 6, breath-to-breath analysis of abdominal and rib cage motion in surfactant depleted piglets during high-frequency oscillatory ventilation*).
- As described above, the "open lung approach" is not feasible for all patients or may be insufficient in a selected group of patients. Some of these patients may benefit form the combination of HFOV and iNO therapy. It was speculated that the effect of iNO therapy was augmented by ventilating the lung at its optimal volume.[112] In an attempt to provide an accurate means of dosing NO during HFOV we described the accuracy of nitric oxide dosage and measurement during HFOV comparing various set-ups (*Chapter 7, bench test assessment of dosage accuracy and measurement inaccuracy in nitric oxide inhalational therapy during high-frequency oscillatory ventilation*).

- Since large continuous gas flows are employed during HFOV, application of nitric oxide during HFOV may lead to the use of significant quantities of nitric oxide. In *Chapter 8 (occupational exposure during nitric oxide inhalational therapy in a paediatric intensive care setting)*, we describe the environmental consequences of this combined therapy.
- In *Chapter 9*, the results are summarised and discussed, conclusions are given and future perspectives are presented.

REFERENCES

1. Dreyfuss D, Saumon G. From ventilator-induced lung injury to multiple organ dysfunction? *Intensive Care Med* 1998; 24: 102 - 104.
2. Slutsky AS, Tremblay LN. Multiple system organ failure. Is mechanical ventilation a contributing factor? *Am J Respir Crit Care Med* 1998; 157: 1721 - 1725.
3. Muscedere JG, Mullen JB, Gan K, Slutsky AS. Tidal ventilation at low airway pressures can augment lung injury. *Am J Respir Crit Care Med* 1994; 149: 1327 - 1334.
4. Tremblay LN, Miatto D, Hamid Q, Govindarajan A, Slutsky AS. Injurious ventilation induces widespread pulmonary epithelial expression of tumor necrosis factor-alpha and interleukin-6 messenger RNA. *Crit Care Med* 2002; 30: 1693 - 1700.
5. Tremblay LN, Slutsky AS. Ventilator-induced injury: from barotrauma to biotrauma. *Proc Assoc Am Physician*s 1998; 110: 482 - 488.
6. Suchyta MR, Orme JF, Jr., Morris AH. The changing face of organ failure in ARDS. *Chest* 2003; 124: 1871 - 1879.
7. Lewandowski K. Extracorporeal membrane oxygenation for severe acute respiratory failure. *Crit Care* 2000; 4: 156 - 168.
8. Zobel G, Kuttnig-Haim M, Urlesberger B, Dacar D, Reiterer F, Riccabona M. Extracorporeal lung support in pediatric patients. *Acta Anaesthesiol Scand Suppl* 1996; 109: 122 - 125.
9. Zobel G, Rodl S, Gamillscheg A, Urlesberger B, Trop M, Grubbauer HM. Inhaled nitric oxide in pediatric intensive care. *Acta Anaesthesiol Scand Suppl* 1996; 109: 92 - 96.
10. Lachmann B. Open up the lung and keep the lung open. *Intensive Care Med* 1992; 18: 319 - 321.
11. Barbas CS, de Matos GF, Okamoto V, Borges JB, Amato MB, de Carvalho CR. Lung recruitment maneuvers in acute respiratory distress syndrome. *Respir Care Clin N Am* 2003; 9: 401 - 18, vii.
12. Amato MB, Barbas CS, Medeiros DM, Schettino GP, Lorenzi FG, Kairalla RA, Deheinzelin D, Morais C, Fernandes EO, Takagaki TY, . Beneficial effects of the "open lung approach" with low distending pressures in acute respiratory distress syndrome. A prospective randomized study on mechanical ventilation. *Am J Respir Crit Care Med* 1995; 152: 1835 - 1846.
13. Amato MB, Barbas CS, Medeiros DM, Magaldi RB, Schettino GP, Lorenzi-Filho G, Kairalla RA, Deheinzelin D, Munoz C, Oliveira R, Takagaki TY, Carvalho CR. Effect of a protective-ventilation strategy on mortality in the acute respiratory distress syndrome. *N Engl J Med* 1998; 338: 347 - 354.
14. Stewart TE, Meade MO, Cook DJ, Granton JT, Hodder RV, Lapinsky SE, Mazer CD, McLean RF, Rogovein TS, Schouten BD, Todd TR, Slutsky AS. Evaluation of a ventilation strategy to prevent barotrauma in patients at high risk for acute respiratory distress syndrome. Pressure- and Volume-Limited Ventilation Strategy Group. *N Engl J Med* 1998; 338: 355 - 361.
15. Brower RG, Shanholtz CB, Fessler HE, Shade DM, White P, Jr., Wiener CM, Teeter JG, Dodd-o JM, Almog Y, Piantadosi S. Prospective, randomized, controlled clinical trial comparing traditional versus reduced tidal volume ventilation in acute respiratory distress syndrome patients. *Crit Care Med* 1999; 27: 1492 - 1498.
16. Brochard L, Roudot-Thoraval F, Roupie E, Delclaux C, Chastre J, Fernandez-Mondejar E, Clementi E, Mancebo J, Factor P, Matamis D, Ranieri M, Blanch L, Rodi G, Mentec H, Dreyfuss D, Ferrer M, Brun-Buisson C, Tobin M, Lemaire F. Tidal volume reduction for prevention of ventilator-induced lung injury in acute respiratory distress syndrome. The Multicenter Trail Group on Tidal Volume reduction in ARDS. *Am J Respir Crit Care Med* 1998; 158: 1831 - 1838.

17. Ventilation with lower tidal volumes as compared with traditional tidal volumes for acute lung injury and the acute respiratory distress syndrome. The Acute Respiratory Distress Syndrome Network. *N Engl J Med* 2000; 342: 1301 - 1308.

18. Singh JM, Stewart TE. High-frequency oscillatory ventilation in adults with acute respiratory distress syndrome. *Curr Opin Crit Care* 2003; 9: 28 - 32.

19. Arnold JH, Anas NG, Luckett P, Cheifetz IM, Reyes G, Newth CJ, Kocis KC, Heidemann SM, Hanson JH, Brogan TV, Bohn DJ. High-frequency oscillatory ventilation in pediatric respiratory failure: a multicenter experience. *Crit Care Med* 2000; 28: 3913 - 3919.

20. Mehta S, Lapinsky SE, Hallett DC, Merker D, Groll RJ, Cooper AB, MacDonald RJ, Stewart TE. Prospective trial of high-frequency oscillation in adults with acute respiratory distress syndrome. *Crit Care Med* 2001; 29: 1360 - 1369.

21. Derdak S, Mehta S, Stewart TE, Smith T, Rogers M, Buchman TG, Carlin B, Lowson S, Granton J. High-frequency oscillatory ventilation for acute respiratory distress syndrome in adults: a randomized, controlled trial. *Am J Respir Crit Care Med* 2002; 166: 801 - 808.

22. Dreyfuss D, Soler P, Basset G, Saumon G. High inflation pressure pulmonary edema. Respective effects of high airway pressure, high tidal volume, and positive end-expiratory pressure. *Am Rev Respir Dis* 1988; 137: 1159 - 1164.

23. Varkul MD, Stewart TE, Lapinsky SE, Ferguson ND, Mehta S. Successful use of combined high-frequency oscillatory ventilation, inhaled nitric oxide, and prone positioning in the acute respiratory distress syndrome. *Anesthesiology* 2001; 95: 797 - 799.

24. Hirschl RB, Croce M, Gore D, Wiedemann H, Davis K, Zwischenberger J, Bartlett RH. Prospective, randomized, controlled pilot study of partial liquid ventilation in adult acute respiratory distress syndrome. *Am J Respir Crit Care Med* 2002; 165: 781 - 787.

25. Jonzon A, Oberg PA, Sedin G, Sjostrand U. High-frequency positive-pressure ventilation by endotracheal insufflation. *Acta Anaesthesiol Scand* 1971; 43: Suppl - 43.

26. Sjostrand U. Review of the physiological rationale for and development of high-frequency positive-pressure ventilation--HFPPV. A*cta Anaesthesiol Scand Suppl* 1977; 64: 7 - 27.

27. Klain M, Smith RB. High frequency percutaneous transtracheal jet ventilation. *Crit Care Med* 1977; 5: 280 - 287.

28. Bohn DJ, Miyasaka K, Marchak BE, Thompson WK, Froese AB, Bryan AC. Ventilation by high-frequency oscillation. *J Appl Physiol* 1980; 48: 710 - 716.

29. Butler WJ, Bohn DJ, Bryan AC, Froese AB. Ventilation by high-frequency oscillation in humans. *Anesth Analg* 1980; 59: 577 - 584.

30. Lunkenheimer PP, Rafflenbeul W, Keller H, Frank I, Dickhut HH, Fuhrmann C. Application of transtracheal pressure oscillations as a modification of "diffusing respiration". *Br J Anaesth* 1972; 44: 627

31. High-frequency oscillatory ventilation compared with conventional mechanical ventilation in the treatment of respiratory failure in preterm infants. The HIFI Study Group. *N Engl J Med* 1989; 320: 88 - 93.

32. Bryan AC, Froese AB. Reflections on the HIFI trial. Pediatrics 1991; 87: 565 - 567.

33. Carter JM, Gerstmann DR, Clark RH, Snyder G, Cornish JD, Null DM, Jr., deLemos RA. High-frequency oscillatory ventilation and extracorporeal membrane oxygenation for the treatment of acute neonatal respiratory failure. *Pediatrics* 1990; 85: 159 - 164.

34. Clark RH, Gerstmann DR, Null DM, Jr., deLemos RA. Prospective randomized comparison of high-frequency oscillatory and conventional ventilation in respiratory distress syndrome. *Pediatrics* 1992; 89: 5 - 12.

35. Gerstmann DR, Minton SD, Stoddard RA, Meredith KS, Monaco F, Bertrand JM, Battisti O, Langhendries JP, Francois A, Clark RH. The Provo multicenter early high-frequency oscillatory ventilation trial: improved pulmonary and clinical outcome in respiratory distress syndrome. Pediatrics 1996; 98: 1044 - 1057.

36. Kalenga M, Battisti O, Francois A, Langhendries JP, Gerstmann DR, Bertrand JM. High-frequency oscillatory ventilation in neonatal RDS: initial volume optimization and respiratory mechanics. *J Appl Physiol* 1998; 84: 1174 - 1177.

37. Rettwitz-Volk W, Veldman A, Roth B, Vierzig A, Kachel W, Varnholt V, Schlosser R, von L, V. A prospective, randomized, multicenter trial of high-frequency oscillatory ventilation compared with conventional ventilation in preterm infants with respiratory distress syndrome receiving surfactant. *J Pediatr* 1998; 132: 249 - 254.

38. Arnold JH, Truog RD, Thompson JE, Fackler JC. High-frequency oscillatory ventilation in pediatric respiratory failure. *Crit Care Med* 1993; 21: 272 - 278.

39. Arnold JH, Hanson JH, Toro-Figuero LO, Gutierrez J, Berens RJ, Anglin DL. Prospective, randomized comparison of high-frequency oscillatory ventilation and conventional mechanical ventilation in pediatric respiratory failure. *Crit Care Med* 1994; 22: 1530 - 1539.

40. Derdak S. High-frequency oscillatory ventilation for acute respiratory distress syndrome in adult patients. *Crit Care Med* 2003; 31: S317 - S323.

41. Derdak S. High-frequency oscillatory ventilation for acute respiratory distress syndrome in adult patients. *Crit Care Med* 2003; 31: S317 - S323.

42. Ashbaugh DG, Bigelow DB, Petty TL, Levine BE. Acute respiratory distress in adults. *Lancet* 1967; 2: 319 - 323.

43. Petty TL, Ashbaugh DG. The adult respiratory distress syndrome. Clinical features, factors influencing prognosis and principles of management. *Chest* 1971; 60: 233 - 239.

44. Bernard GR, Artigas A, Brigham KL, Carlet J, Falke K, Hudson L, Lamy M, LeGall JR, Morris A, Spragg R. The American-European Consensus Conference on ARDS. Definitions, mechanisms, relevant outcomes, and clinical trial coordination. *Am J Respir Crit Care Med* 1994; 149: 818 - 824.

45. Horbar JD, Badger GJ, Carpenter JH, Fanaroff AA, Kilpatrick S, LaCorte M, Phibbs R, Soll RF. Trends in mortality and morbidity for very low birth weight infants, 1991-1999. *Pediatrics* 2002; 110: 143 - 151.

46. Dani C, Reali MF, Bertini G, Wiechmann L, Spagnolo A, Tangucci M, Rubaltelli FF. Risk factors for the development of respiratory distress syndrome and transient tachypnoea in newborn infants. Italian Group of Neonatal Pneumology. *Eur Respir J* 1999; 14: 155 - 159.

47. Lemons JA, Bauer CR, Oh W, Korones SB, Papile LA, Stoll BJ, Verter J, Temprosa M, Wright LL, Ehrenkranz RA, Fanaroff AA, Stark A, Carlo W, Tyson JE, Donovan EF, Shankaran S, Stevenson DK. Very low birth weight outcomes of the National Institute of Child health and human development neonatal research network, January 1995 through December 1996. NICHD Neonatal Research Network. *Pediatrics* 2001; 107: E1 -

48. Bollen CW, Uiterwaal CS, van Vught AJ. Cumulative metaanalysis of high-frequency versus conventional ventilation in premature neonates. *Am J Respir Crit Care Med* 2003; 168: 1150 - 1155.

49. Henderson-Smart DJ, Bhuta T, Cools F, Offringa M. Elective high frequency oscillatory ventilation versus conventional ventilation for acute pulmonary dysfunction in preterm infants. *Cochrane Database Syst Rev* 2003; CD000104 -

50. Pelosi P, Goldner M, McKibben A, Adams A, Eccher G, Caironi P, Losappio S, Gattinoni L, Marini JJ. Recruitment and derecruitment during acute respiratory failure: an experimental study. *Am J Respir Crit Care Med* 2001; 164: 122 - 130.

51. Crotti S, Mascheroni D, Caironi P, Pelosi P, Ronzoni G, Mondino M, Marini JJ, Gattinoni L. Recruitment and derecruitment during acute respiratory failure: a clinical study. *Am J Respir Crit Care Med* 2001; 164: 131 - 140.

52. Gattinoni L, Pesenti A, Avalli L, Rossi F, Bombino M. Pressure-volume curve of total respiratory system in acute respiratory failure. Computed tomographic scan study. *Am Rev Respir Dis* 1987; 136: 730 - 736.

53. Slutsky AS. Lung injury caused by mechanical ventilation. *Chest* 1999; 116: 9S - 15S.

54. Rimensberger PC, Pristine G, Mullen BM, Cox PN, Slutsky AS. Lung recruitment during small tidal volume ventilation allows minimal positive end-expiratory pressure without augmenting lung injury. *Crit Care Med* 1999; 27: 1940 - 1945.

55. Froese AB, McCulloch PR, Sugiura M, Vaclavik S, Possmayer F, Moller F. Optimizing alveolar expansion prolongs the effectiveness of exogenous surfactant therapy in the adult rabbit. *Am Rev Respir Dis* 1993; 148: 569 - 577.

56. McCulloch PR, Forkert PG, Froese AB. Lung volume maintenance prevents lung injury during high frequency oscillatory ventilation in surfactant-deficient rabbits. *Am Rev Respir Dis* 1988; 137: 1185 - 1192.

57. Sugiura M, McCulloch PR, Wren S, Dawson RH, Froese AB. Ventilator pattern influences neutrophil influx and activation in atelectasis-prone rabbit lung. *J Appl Physiol* 1994; 77: 1355 - 1365.

58. Dreyfuss D, Soler P, Basset G, Saumon G. High inflation pressure pulmonary edema. Respective effects of high airway pressure, high tidal volume, and positive end-expiratory pressure. *Am Rev Respir Dis* 1988; 137: 1159 - 1164.

59. Dreyfuss D, Saumon G. Barotrauma is volutrauma, but which volume is the one responsible? *Intensive Care Med* 1992; 18: 139 - 141.

60. Pinsky MR. The hemodynamic consequences of mechanical ventilation: an evolving story. *Intensive Care Med* 1997; 23: 493 - 503.

61. Suter PM, Fairley B, Isenberg MD. Optimum end-expiratory airway pressure in patients with acute pulmonary failure. *N Engl J Med* 1975; 292: 284 - 289.

62. Hickling KG, Walsh J, Henderson S, Jackson R. Low mortality rate in adult respiratory distress syndrome using low-volume, pressure-limited ventilation with permissive hypercapnia: a prospective study. *Crit Care Med* 1994; 22: 1568 - 1578.

63. Esteban A, Anzueto A, Alia I, Gordo F, Apezteguia C, Palizas F, Cide D, Goldwaser R, Soto L, Bugedo G, Rodrigo C, Pimentel J, Raimondi G, Tobin MJ. How is mechanical ventilation employed in the intensive care unit? An international utilization review. *Am J Respir Crit Care Med* 2000; 161: 1450 - 1458.

64. Gattinoni L, Pelosi P, Crotti S, Valenza F. Effects of positive end-expiratory pressure on regional distribution of tidal volume and recruitment in adult respiratory distress syndrome. *Am J Respir Crit Care Me*d 1995; 151: 1807 - 1814.

65. Staub NC, Nagano H, Pearce ML. Pulmonary edema in dogs, especially the sequence of fluid accumulation in lungs. *J Appl Physiol* 1967; 22: 227 - 240.

66. Jonson B, Richard JC, Straus C, Mancebo J, Lemaire F, Brochard L. Pressure-volume curves and compliance in acute lung injury: evidence of recruitment above the lower inflection point. *Am J Respir Crit Care Med* 1999; 159: 1172 - 1178.

67. Hickling KG. The pressure-volume curve is greatly modified by recruitment. A mathematical model of ARDS lungs. *Am J Respir Crit Care Med* 1998; 158: 194 - 202.

68. Hickling KG. Best compliance during a decremental, but not incremental, positive end-expiratory pressure trial is related to open-lung positive end-expiratory pressure: a mathematical model of acute respiratory distress syndrome lungs. *Am J Respir Crit Care Med* 2001; 163: 69 - 78.

69. Putensen C, Mutz NJ, Putensen-Himmer G, Zinserling J. Spontaneous breathing during ventilatory support improves ventilation-perfusion distributions in patients with acute respiratory distress syndrome. *Am J Respir Crit Care Med* 1999; 159: 1241 - 1248.

70. Relvas MS, Silver PC, Sagy M. Prone positioning of pediatric patients with ARDS results in improvement in oxygenation if maintained > 12 h daily. *Chest* 2003; 124: 269 - 274.

71. Casado-Flores J, Martinez dA, Ruiz-Lopez MJ, Ruiz M, Serrano A. Pediatric ARDS: effect of supine-prone postural changes on oxygenation. *Intensive Care Med* 2002; 28: 1792 - 1796.

72. Albert RK, Hubmayr RD. The prone position eliminates compression of the lungs by the heart. *Am J Respir Crit Care Me*d 2000; 161: 1660 - 1665.

73. Neumann P, Berglund JE, Mondejar EF, Magnusson A, Hedenstierna G. Dynamics of lung collapse and recruitment during prolonged breathing in porcine lung injury. *J Appl Physiol* 1998; 85: 1533 - 1543.

74. Markstaller K, Eberle B, Kauczor HU, Scholz A, Bink A, Thelen M, Heinrichs W, Weiler N. Temporal dynamics of lung aeration determined by dynamic CT in a porcine model of ARDS. *Br J Anaesth* 2001; 87: 459 - 468.

75. Allen G, Lundblad LK, Parsons P, Bates JH. Transient mechanical benefits of a deep inflation in the injured mouse lung. *J Appl Physiol* 2002; 93: 1709 - 1715.

76. Foti G, Cereda M, Sparacino ME, De Marchi L, Villa F, Pesenti A. Effects of periodic lung recruitment maneuvers on gas exchange and respiratory mechanics in mechanically ventilated acute respiratory distress syndrome (ARDS) patients. *Intensive Care Med* 2000; 26: 501 - 507.

77. Pelosi P, Bottino N, Chiumello D, Caironi P, Panigada M, Gamberoni C, Colombo G, Bigatello LM, Gattinoni L. Sigh in supine and prone position during acute respiratory distress syndrome. *Am J Respir Crit Care Med* 2003; 167: 521 - 527.

78. Pelosi P, Bottino N, Panigada M, Eccher G, Gattinoni L. The sigh in ARDS (acute respiratory distress syndrome). *Minerva Anestesiol* 1999; 65: 313 - 317.

79. Pelosi P, Cadringher P, Bottino N, Panigada M, Carrieri F, Riva E, Lissoni A, Gattinoni L. Sigh in acute respiratory distress syndrome. *Am J Respir Crit Care Med* 1999; 159: 872 - 880.

80. Bond DM, Froese AB. Volume recruitment maneuvers are less deleterious than persistent low lung volumes in the atelectasis-prone rabbit lung during high-frequency oscillation. *Crit Care Med* 1993; 21: 402 - 412.

81. Fujino Y, Goddon S, Dolhnikoff M, Hess D, Amato MB, Kacmarek RM. Repetitive high-pressure recruitment maneuvers required to maximally recruit lung in a sheep model of acute respiratory distress syndrome. *Crit Care Med* 2001; 29: 1579 - 1586.

82. Cakar N, der Kloot TV, Youngblood M, Adams A, Nahum A. Oxygenation response to a recruitment maneuver during supine and prone positions in an oleic acid-induced lung injury model. *Am J Respir Crit Care Med* 2000; 161: 1949 - 1956.

83. Gattinoni L, Pelosi P, Suter PM, Pedoto A, Vercesi P, Lissoni A. Acute respiratory distress syndrome caused by pulmonary and extrapulmonary disease. Different syndromes? *Am J Respir Crit Care Med* 1998; 158: 3 - 11.

84. Pelosi P, D'Onofrio D, Chiumello D, Paolo S, Chiara G, Capelozzi VL, Barbas CS, Chiaranda M, Gattinoni L. Pulmonary and extrapulmonary acute respiratory distress syndrome are different. *Eur Respir J Suppl* 2003; 42: 48s - 56s.

85. Fort P, Farmer C, Westerman J, Johannigman J, Beninati W, Dolan S, Derdak S. High-frequency oscillatory ventilation for adult respiratory distress syndrome--a pilot study. *Crit Care Med* 1997; 25: 937 - 947.

86. Cartotto R, Ellis S, Gomez M, Cooper A, Smith T. High frequency oscillatory ventilation in burn patients with the acute respiratory distress syndrome. *Burns* 2004; 30: 453 - 463.

87. Ritacca FV, Stewart TE. Clinical review: high-frequency oscillatory ventilation in adults--a review of the literature and practical applications. *Crit Care* 2003; 7: 385 - 390.

88. David M, Weiler N, Heinrichs W, Neumann M, Joost T, Markstaller K, Eberle B. High-frequency oscillatory ventilation in adult acute respiratory distress syndrome. *Intensive Care Med* 2003; 29: 1656 - 1665.

89. van Genderingen HR, van Vught JA, Jansen JR, Duval EL, Markhorst DG, Versprille A. Oxygenation index, an indicator of optimal distending pressure during high-frequency oscillatory ventilation? *Intensive Care Med* 2002; 28: 1151 - 1156.

90. van Genderingen HR, Versprille A, Leenhoven T, Markhorst DG, van Vught AJ, Heethaar RM. Reduction of oscillatory pressure along the endotracheal tube is indicative for maximal respiratory compliance during high-frequency oscillatory ventilation: a mathematical model study. *Pediatr Pulmonol* 2001; 31: 458 - 463.

91. Thome U, Topfer A, Schaller P, Pohlandt F. Effects of mean airway pressure on lung volume during high-frequency oscillatory ventilation of preterm infants. *Am J Respir Crit Care Med* 1998; 157: 1213 - 1218.

92. Gothberg S, Parker TA, Griebel J, Abman SH, Kinsella JP. Lung volume recruitment in lambs during high-frequency oscillatory ventilation using respiratory inductive plethysmography. *Pediatr Res* 2001; 49: 38 - 44.

93. Brazelton TB, III, Watson KF, Murphy M, Al Khadra E, Thompson JE, Arnold JH. Identification of optimal lung volume during high-frequency oscillatory ventilation using respiratory inductive plethysmography. *Crit Care Med* 2001; 29: 2349 - 2359.

94. Frerichs I, Dargaville PA, Dudykevych T, Rimensberger PC. Electrical impedance tomography: a method for monitoring regional lung aeration and tidal volume distribution? *Intensive Care Med* 2003; 29: 2312 - 2316.

95. Victorino JA, Borges JB, Okamoto VN, Matos GF, Tucci MR, Caramez MP, Tanaka H, Sipmann FS, Santos DC, Barbas CS, Carvalho CR, Amato MB. Imbalances in regional lung ventilation: a validation study on electrical impedance tomography. *Am J Respir Crit Care Med* 2004; 169: 791 - 800.

96. Goddon S, Fujino Y, Hromi JM, Kacmarek RM. Optimal mean airway pressure during high-frequency oscillation: predicted by the pressure-volume curve. *Anesthesiology* 2001; 94: 862 - 869.

97. Kallet RH. Pressure-volume curves in the management of acute respiratory distress syndrome. *Respir Care Clin N Am* 2003; 9: 321 - 341.

98. Kinsella JP, Neish SR, Shaffer E, Abman SH. Low-dose inhalation nitric oxide in persistent pulmonary hypertension of the newborn. *Lancet* 1992; 340: 819 - 820.

99. Kinsella JP, Neish SR, Ivy DD, Shaffer E, Abman SH. Clinical responses to prolonged treatment of persistent pulmonary hypertension of the newborn with low doses of inhaled nitric oxide. *J Pediatr* 1993; 123: 103 - 108.

100. Roberts JD, Polaner DM, Lang P, Zapol WM. Inhaled nitric oxide in persistent pulmonary hypertension of the newborn. *Lancet* 1992; 340: 818 - 819.

101. Lonnqvist PA, Winberg P, Lundell B, Sellden H, Olsson GL. Inhaled nitric oxide in neonates and children with pulmonary hypertension. *Acta Paediatr* 1994; 83: 1132 - 1136.

102. Winberg P, Lundell BP, Gustafsson LE. Effect of inhaled nitric oxide on raised pulmonary vascular resistance in children with congenital heart disease. *Br Heart J* 1994; 71: 282 - 286.

103. Rossaint R, Falke KJ, Lopez F, Slama K, Pison U, Zapol WM. Inhaled nitric oxide for the adult respiratory distress syndrome. *N Engl J Med* 1993; 328: 399 - 405.

104. Michael JR, Barton RG, Saffle JR, Mone M, Markewitz BA, Hillier K, Elstad MR, Campbell EJ, Troyer BE, Whatley RE, Liou TG, Samuelson WM, Carveth HJ, Hinson DM, Morris SE, Davis BL, Day RW. Inhaled nitric oxide versus conventional therapy: effect on oxygenation in ARDS. *Am J Respir Crit Care Med* 1998; 157: 1372 - 1380.

105. Dellinger RP, Zimmerman JL, Taylor RW, Straube RC, Hauser DL, Criner GJ, Davis K, Jr., Hyers TM, Papadakos P. Effects of inhaled nitric oxide in patients with acute respiratory distress syndrome: results of a randomized phase II trial. Inhaled Nitric Oxide in ARDS Study Group. *Crit Care Med* 1998; 26: 15 - 23.

106. Lundin S, Mang H, Smithies M, Stenqvist O, Frostell C. Inhalation of nitric oxide in acute lung injury: results of a European multicentre study. The European Study Group of Inhaled Nitric Oxide. *Intensive Care Med* 1999; 25: 911 - 919.

107. Payen DM. Is nitric oxide inhalation a "cosmetic" therapy in acute respiratory distress syndrome? *Am J Respir Crit Care Med* 1998; 157: 1361 - 1362.

108. Baxter FJ, Randall J, Miller JD, Higgins DA, Powles AC, Choi PT. Rescue therapy with inhaled nitric oxide in critically ill patients with severe hypoxemic respiratory failure (Brief report). *Can J Anaesth* 2002; 49: 315 - 318.

109. Decoene C, Bourzoufi K, Moreau D, Narducci F, Crepin F, Krivosic-Horber R. Use of inhaled nitric oxide for emergency Cesarean section in a woman with unexpected primary pulmonary hypertension. *Can J Anaesth* 2001; 48: 584 - 587.

110. Sadiq HF, Mantych G, Benawra RS, Devaskar UP, Hocker JR. Inhaled nitric oxide in the treatment of moderate persistent pulmonary hypertension of the newborn: a randomized controlled, multicenter trial. J *Perinatol* 2003; 23: 98 - 103.

111. Hoehn T, Krause M, Hentschel R. High-frequency ventilation augments the effect of inhaled nitric oxide in persistent pulmonary hypertension of the newborn. *Eur Respir J* 1998; 11: 234 - 238.

112. Kinsella JP, Truog WE, Walsh WF, Goldberg RN, Bancalari E, Mayock DE, Redding GJ, deLemos RA, Sardesai S, McCurnin DC, Moreland SG, Cutter GR, Abman SH. Randomized, multicenter trial of inhaled nitric oxide and high-frequency oscillatory ventilation in severe, persistent pulmonary hypertension of the newborn. *J Pediatr* 1997; 131: 55 - 62.

Chapter 2

High-frequency oscillatory ventilation in paediatric patients

ELIM Duval, DG Markhorst, RJBJ Gemke, AJ van Vught

Netherlands Journal of Medicine 2000; 56: 177 - 185

SUMMARY

Background: High-frequency oscillatory ventilation (HFOV) is a ventilatory mode using small tidal volumes with low phasic pressures at supraphysiologic frequencies. Beyond the neonatal period there are distinct lung diseases for which HFOV is used. Data of 35 children who deteriorated on conventional ventilation were retrospectively analysed in two tertiary paediatric intensive care units.

Methods: Depending on the underlying pulmonary pathophysiology, three strategies were employed. First, the “open-lung strategy” designed to rapidly recruit and maintain optimal lung volume in diffuse alveolar disease (DAD) (n=27) and pulmonary haemorrhage (n=5). Second, the “low-volume”-strategy in persistent airleak (n=1) where after an initial identical approach, continuous distending pressure (CDP) is reduced until the airleak ceases. Third, the “open-airway”-strategy in obstructive airway disease (n=5) where CDP is used to recruit and stent the airways.

Results: Seven patients died, two due to respiratory failure. Three patients developed an airleak. Nine patients developed chronic lung disease. There was a significant decrease of the oxygenation index (OI) in the survivors. In the two patients who died of respiratory failure, the OI increased.

Conclusion: If certain conditions are met, HFOV appears a safe and effective mode of ventilation in paediatric respiratory failure.

INTRODUCTION

Despite improvements in respiratory care, pulmonary disease remains an important cause of morbidity and mortality in children as well as in adults. Although positive pressure ventilation has reduced mortality, pulmonary complications due to oxygen toxicity and baro- or volutrauma remain high.[1-4] High-frequency oscillatory ventilation (HFOV) has been suggested as an alternative for treatment of various forms of respiratory failure.[5-11] In HFOV small tidal volumes with low phasic pressure changes are used at supraphysiological frequencies, superimposed on an adjustable continuous distending pressure (CDP). In 1980, Bohn et al.[12] and Butler et al.[13] showed that it was possible to achieve adequate gas exchange with this mode of ventilation.

In contrast to other forms of HFV, HFOV has an active expiratory phase.[14] HFOV effectively decouples oxygenation from ventilation. As there is a near linear relationship between lung volume and oxygenation, changes in oxygenation are achieved by modulating the CDP. Ventilation depends on the oscillatory volume, determined by the amplitude and frequency.[15] During HFOV, higher mean airway pressures than those tolerated with conventional mechanical ventilation (CMV) can be applied to keep the lung open. Lower peak pressures and lower pressure swings cause less lung damage.

While in 1989 the HIFI-trial, a prospective study including 10 neonatal intensive care units, did not demonstrate a benefit to the use of HFOV compared to CMV, much was learned during that and other studies which has altered the way we apply this therapy today.[16-18] Different modes of HFV and different strategies will lead to marked differences in outcome. Consequently, more recent studies show better results. In preterm infants with hyaline membrane disease, HFOV decreases the incidence of chronic lung injury.[6,10,19] Furthermore, the effectiveness of HFOV in paediatric patients with airleak or diffuse alveolar disease (DAD) was demonstrated in a randomised clinical study.[8,9]

We report our experience with HFOV in 35 paediatric patients who deteriorated on CMV. Three different HFOV-strategies were employed: the *"high-volume"* or *"open-lung"* strategy for DAD and pulmonary haemorrhage, the *"low-volume"* strategy for airleak and the *"open-airway"* strategy for obstructive lung disease. Our objectives were to evaluate the safety and efficacy of HFOV using specific strategies according to the underlying disorder.

Table 2.1. Patient characteristics.[a]

Number of patients	35	
Male : Female	15:20	
HFOV runs	38	
Main diagnosis	ARDS	17
	Pneumonia	10
	Pulmonary haemorrhage	5
	Bronchiolitis	4
	Airleak	1
	PPHN	1
	Median	*range*
Decimal age	0.390	0.03 - 13.8
Weight (kg)	5.750	2.6 - 65.0
Days prior to CMV	2.0	0.2 – 36

[a]*: ARDS, acute respiratory distress syndrome; PPHN, persistent pulmonary hypertension of the newborn; CMV, conventional mechanical ventilation.*

PATIENTS AND METHODS

Patients

Between January 1994 and January 1998, we treated 35 children with HFOV in two tertiary care paediatric intensive care units. We retrospectively analysed the chart records. Patients characteristics are listed in Table 2.1. The main diagnosis was DAD in 27 patients (77%), of which 10 had pneumonia and 17 ARDS (11 due to sepsis, two due to mediastinitis after oesophageal surgery, one after anti-thymocyte-globuline treatment, one after submersion and two after neurotrauma). One patient showed both small airway disease and persistent airleak. She was put on HFOV primarily to hasten resolution of the airleak.
The course of three children with severe ARDS was complicated by airleaks during CMV, which were drained with chest tubes and considered stable before starting oscillation. One patient had severe bronchopulmonary dysplasia (BPD), with continuous oxygen need at home before admission. Two other patients had mild BPD, one with intermittent oxygen

need at home (two episodes on HFOV), the other was already without oxygen supply before admission.

Conventional Mechanical Ventilation.

All patients were ventilated with either pressure regulated volume controlled or pressure controlled ventilation (Servo 300 and 900C, Siemens, Solna, Sweden). In our units severe respiratory failure is treated using a strategy that utilises increases in end-expiratory pressure and inspiratory time to increase mean airway pressure. If felt appropriate patients with DAD were put in prone position to improve their oxygenation. Furthermore, low tidal volumes were used to prevent overdistention, regardless of $PaCO_2$-values, as long as pH was above 7.25 with a bicarbonate level above 19 mmol/l (permissive hypercapnia).
All patients had arterial and central venous lines. They were sedated with a continuous infusion of midazolam and, if necessary, paralysed with vecuronium. According to arterial blood pressure, central venous pressure, diuresis, peripheral temperature and serum lactate levels, intravenous fluids and inotropes were administered.

High-frequency oscillatory ventilation

Informed consent was obtained before HFOV was instituted. HFOV was started, when clinical and radiological deterioration occurred on CMV and 1 or both of the following criteria were met: intractable respiratory failure with peak inspiratory pressures of more than 30 cm water despite the use of permissive hypercapnia for at least 2 h, or an oxygenation index (OI) above 13 demonstrated by two consecutive arterial blood gas measurements over a 6-h period. The OI is calculated as: FIO_2 x 100 x CDP (cm water) divided by the PaO_2 (mm Hg). HFOV was also started in patients with persistent pulmonary haemorrhage despite the use of high end-expiratory pressures, or radiographic evidence of barotrauma with unstable airleak, requiring additional chest tubes or continuing for more than 72 h. Former prematurity with residual BPD was not considered to be a contraindication for HFOV. Neither was obstructive airway disease with clinical evidence of increased expiratory resistance or hyperinflation on chest X-ray. We used an electromagnetically driven membrane oscillator (3100 A, SensorMedics Critical Care, Yorba Linda, California, USA). Three main strategies for HFOV were employed:

1. *The "high-volume strategy or open-lung strategy" for DAD and pulmonary haemorrhage.*

We aimed at an oxygen saturation (SaO_2) above 90% at an FIO_2 of less than 0.6, an arterial pH above 7.25 with a bicarbonate level above 19 mmol/l irrespective of the $PaCO_2$, and

stable haemodynamics. Circulatory compromise was treated with optimising preload (CVP above 12 mm Hg) and by inotropic support. General supportive care remained unchanged during the transition. In children less than 10 kg, we used a frequency of 10 Hz, above 10 kg 8 Hz. With persistent respiratory acidosis frequency was decreased to 8, 6 or 4 Hz - frequencies. Pressure swings were adjusted according to chest wall vibrations and $PaCO_2$. Inspiratory time was set at 33%. In one patient with persistent respiratory acidosis an inspiratory time of 50% was used. Since CO_2 elimination is very sensitive to mucus accumulation in the endotracheal tube or airways, sudden rises in $PaCO_2$ were treated by immediate suctioning. Bias gas flow was 20, 30 or 40 l/min as necessary to maintain CDP. We started with an FIO_2 of 1.0 on the oscillator. CDP was initially set 3-4 cm higher than mean airway pressure on CMV, and subsequently increased according to SaO_2 and chest X-ray. Priority was given to reduction of FIO_2 above pressure. Lung inflation was considered satisfactory with diaphragm margins projected at the 9th posterior rib on chest X-ray. In patients with persistent hypoxemia with adequate circulation and no radiographic signs of lung overinflation, CDP was increased further until oxygenation targets were reached. Eventually, prone position was used, most of the time successfully. Management of hypoxemia in patients with suspected cardiac dysfunction was treated by optimising preload and contractility. If the therapeutic goals were not attained, the patient was considered a treatment failure. Once adequate oxygenation was achieved with an FIO_2 below 0.4, attempts were made to reduce the CDP in 1-2 cm decrements.

2. *The "low-volume strategy" in airleak syndrome.*

Initial settings and management were the same as in the *"open-lung"* strategy. Once adequate oxygenation was achieved, immediate attempts were made to reduce CDP until the airleak ceased. Higher oxygen concentrations were accepted to keep CDP as low as possible with a PaO_2 of at least 55 mm Hg. Priority was given to reduction of CDP above FIO_2.

3. *The "open-airway strategy" for small airway disease.*

In patients with small airway disease, we used the same initial settings as described in the *"open-lung"* strategy, but high CDP was now used to up the small airways, allowing oscillations to move freely in and out the alveolus. Once the airways were opened, careful attention was paid to overinflation since the normal compliant alveoli were faced with relatively high CDP. Management of hypoxemia in these patients was directed at optimising preload (CVP>15-20 mm Hg) and contractility. The degree of lung hyperinflation on chest X-

ray was not used to modify CDP. To minimise dynamic airtrapping by spontaneous breaths, these patients were paralysed. In addition inspiratory times no longer than 33% were used and, if necessary, pressure swings were reduced as much as possible by the use of permissive hypercapnia.

Nitric oxide administration during HFOV

In 2 patients nitric oxide (NO) was added during HFOV because of persistent hypoxemia (persistent OI above 13 in 2 consecutive blood gas measurements despite adequate lung inflation and optimal haemodynamics). In 2 other patients NO was added because of pulmonary hypertension. NO was administered by a ball valve flow meter into the inspiratory limb of the circuit, 25 cm proximal to the endotracheal tube. NO flow was calculated according to the formula: NO flow = (V_{vent} x NO_{del}) / (NO_{tank} - NO_{del}), where V_{vent} is the ventilator flow, NO_{del} the required NO concentration in parts per million (ppm) and NO_{tank} the NO concentration in ppm in the delivery tank. We have previously found this method to be accurate.[20] In 3 patients, NO and nitric dioxide concentrations were measured with a monitor based on electrochemical cells (SensorNOx, SensorMedics Critical Care, Yorba Linda, California, USA). In these children a dose response curve was obtained with NO concentrations from 1 to 40 ppm. With each step measurements were made of PaO_2, SaO_2 and, if available, the pulmonary artery pressure (PAP).

Statistical analysis.

Data in Tables 2.1 and 2.2 are reported as median and ranges. The oxygenation indices in Figs 2.1 and 2.2 are reported as mean values with standard deviation. The OI and $PaCO_2$ values were compared to baseline values on CMV. Data were compared using Wilcoxon's signed ranks test (SPSS 7.0 for Windows, SPSS Software, Chicago, IL, USA). Statistical significance was assumed when the p-value was less than 0.05.

RESULTS

Conventional Mechanical Ventilation

Median duration of CMV before beginning the high-frequency protocol was 2 days, ranging from a few hours to 36 days. Characteristics of CMV just prior to HFOV are listed in Table 2.2. The OI at that time ranged from 6 to 42. The highest mean OI was found in the group of DAD.

Table 2.2. Characteristics on CMV 1 h prior to transition.[a]

	Median (ranges)
PIP (cm water)	34 (21-50)
PEEP (cm water)	8 (2-19)
MAP (cm water)	18 (9-35)
PaO_2 (mm Hg)	68 (37-190)
$PaCO_2$ (mm Hg)	47 (30-92)
pH	7.33 (7.07-7.63)
FIO_2	0.8 (0.4-1.0)
OI	20.5 (6.2-42.2)

[a]*: PIP, peak inspiratory pressure; PEEP, positive end expiratory pressure; MAP, mean airway pressure; OI, oxygenation index.*

Indications to start HFOV were: OI above 13 in 18 patients, PIP above 30 cm water despite the use of permissive hypercapnia in five patients, and the combination of both in five patients. In the remaining 10 patients, there was persistent pulmonary bleeding in one patient and persistent airleak in another. Three other patients had PIP above 30 cm water with high $PaCO_2$ but with a pH still above 7.25. Because of the risk to increase the already existing pulmonary hypertension after cardiac surgery in two patients and due to persistent foetal circulation in the other patient, we did not allow the $PaCO_2$ to rise further. In the remaining 5 patients, although mean airway pressure on CMV was not recorded, we assumed an OI >13. All of these patients either had a low PaO_2 despite the use of high PEEP and high FIO_2, either peak pressures above 30 cm water. At that time the children were clinically and radiologically rapidly deteriorating.

High-frequency oscillatory ventilation

Three patients had two episodes of HFOV, with a total of 38 HFOV episodes. Two patients were oscillated on a tracheotomy, in one of them HFOV was used twice. The median duration on HFOV was 11 days, the longest being 37 days. Prone position was used in eight patients. The highest CDP used was 45 cm water, the highest delta P 77 cm water. Twenty-five (66%) patients, including the 5 patients with small airway disease, were paralysed. Thirteen patients never received muscle relaxants.

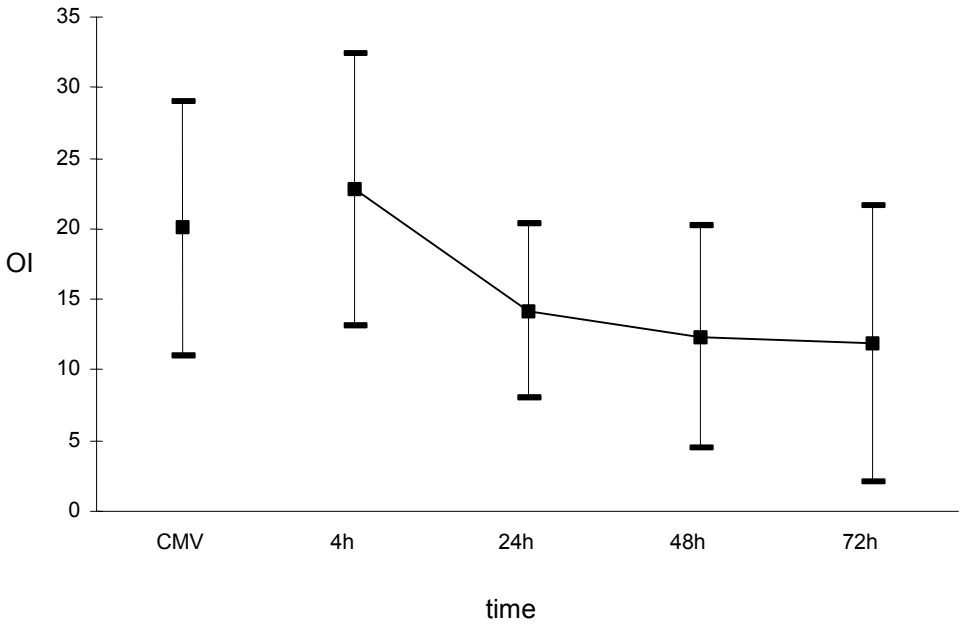

Fig. 2.1: The oxygenation index (OI) prior to (CMV) and during the first 72 h on HFOV of all survivors: 4, 24, 48 and 72h represent the OI after stabilisation within 4 h on HFOV, and after 24, 48 and 72 h on HFOV respectively. Data are mean ± S.D. Compared to the OI during CMV, differences with the OI at 4, 24, 48 and 72 h were significant (p<0.02).

Gas-exchange variables

Fig. 2.1 shows the OI prior to HFOV and 4, 24, 48 and 72 h after initiation in all survivors. The OI initially increased during transition to oscillatory ventilation. Subsequently there was a steady decrease of the OI in the survivor group from 20.1 ± 9.0 to 11.9 ± 9.8 (mean ± SD). Compared to the OI on CMV, differences with OI after 4, 24, 48 and 72 h on HFOV were significant ($p<0.02$).

Fig. 2.2 shows the individual OI of the non-survivors. In patients 3 and 6 who died from respiratory failure, a continuous increase of the OI is recorded. In the remaining patients, dying from non-pulmonary causes, no such increase is seen. Changes in $PaCO_2$ values compared to baseline value on CMV were not significant.

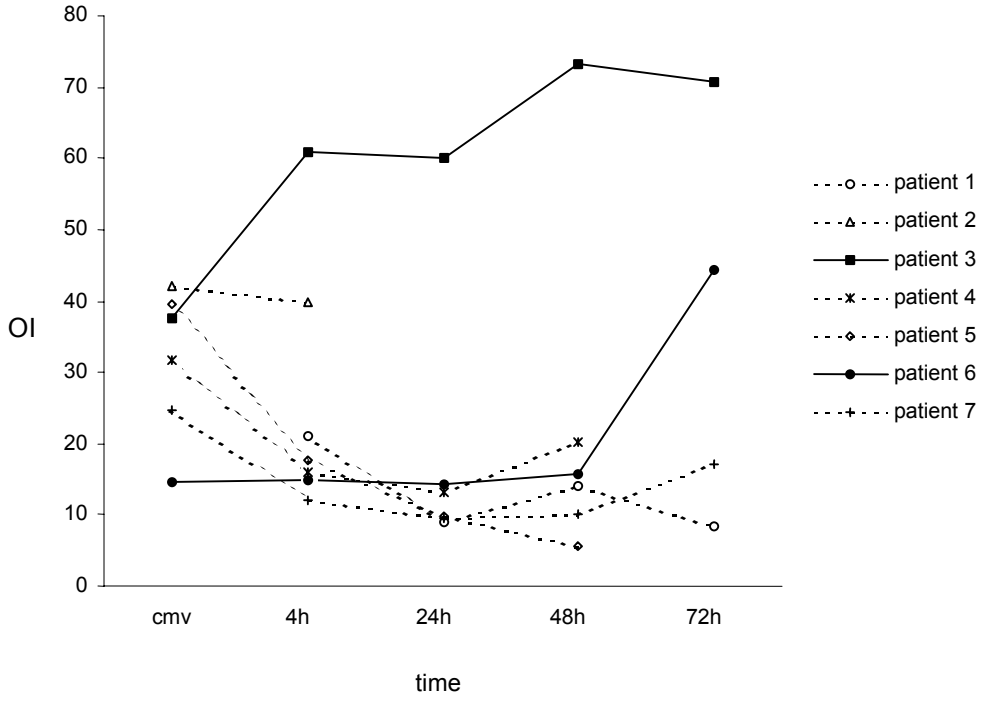

Fig. 2.2: The individual OI of the non-survivors prior to and during the first 72 h on HFOV. Time points are the same as indicated in the legend to Fig. 2.1. Patients 3 and 6 died from respiratory failure.

Effect of NO inhalational therapy during HFOV

Four patients received NO during HFOV. The first patient was a 3-year-old girl admitted with severe ARDS, who developed pulmonary hypertension. HFOV and NO were started at the same time, NO in a dosage of 2 ppm gradually increasing to 40 ppm in two h. There was no effect of NO on the PaO_2 or PAP. The second patient was a 2.5-month old girl with RSV bronchiolitis. NO (20 ppm) was started because of clinical deterioration with haemodynamic instability, pulmonary interstitial emphysema (PIE) and increasing OI. Within 6 h, there was a marked decrease in OI. NO was gradually weaned and could be stopped after 14 days. The third patient was admitted with a severe viral pneumonia. The course on HFOV was complicated by the development of PIE. Despite the combined use of HFOV, NO and corticosteroids, the patient died from respiratory failure (Table 2.3 patient 3). The last patient was a one-year-old boy with a complex congenital heart defect admitted with ARDS due to a super-infected RSV bronchiolitis. The course was complicated by a severe exacerbation of

Table 2.3. Non-survivors characteristics.[a]

Patient	Sex	Diagnosis leading to HFOV	Days on HFOV	Cause of death
1	M	ARDS post BMX	14	FEL, bleeding after liver biopsy, limitation further treatment
2	M	ARDS post submersion	0.2	Circulatory collapse after initiation HFOV, died on CMV, brain death
3	F	Pneumonia	9	Progressive respiratory failure despite HFOV, NO and corticoid treatment
4	F	ARDS after ATG exposure	2	FEL relapse, sepsis, gut bleeding, limitation further treatment
5	F	Pulmonary haemorrhage	5	Withdrawal therapy in Omen syndrome
6	F	Pulmonary haemorrhage	8	CMV pneumonia after renal transplantation, progressive respiratory failure despite HFOV
7	M	Neurogenic ARDS	4	Brain death

[a]*: ARDS, acute respiratory distress syndrome; BMX, bone marrow transplantation; FEL, familial erythrophagocytic lymphohistiocytosis; CMV, conventional mechanical ventilation; NO, nitric oxide; ATG, anti-thymocyte globulines*.

an already existing pulmonary hypertension. One day after initiation of HFOV, NO was administered in increasing dosages up to 40 ppm without any effect on the PaO_2 or PAP.

Complications and outcome

There were 31 survivors, 19 of them without chronic lung disease defined as more than 30% oxygen need 28 days after starting HFOV. Among the 12 patients with chronic lung disease, 3 patients had pre-existing BPD, the 9 other patients had no prior lung disease. All patients except one were ultimately discharged home without supplemental oxygen.
Table 2.3 shows the characteristics of the 7 non-survivors. Two patients can be considered as respiratory failure in spite of HFOV. Patient 3 died from progressing multi-organ failure including respiratory failure despite the use of HFOV, NO and steroids. Although initially responding well, patient 6 died after a third period of pulmonary haemorrhage in persisting respiratory acidosis, despite using the maximal power of the device.

Three patients developed an airleak during HFOV. Twelve (32%) needed additional fluids or more inotropic support during transition to improve their oxygenation. Twenty-one patients (68%) were weaned directly from HFOV to CPAP before extubation. The remaining patients were weaned on a conventional ventilator. In paralysed patients improving lung compliance sometimes resulted in higher $PaCO_2$ and prompted to increase the pressure swings, improperly suggesting respiratory deterioration. In these patients, decreasing CDP resulted in better ventilation. Non-paralysed patients started to breathe spontaneously.

DISCUSSION

HFOV has been studied extensively in the treatment of neonatal respiratory failure. In preterm infants, early use of HFOV utilising a strategy designed to recruit and maintain optimal lung volume, has proved to lower the incidence of chronic lung disease.[6,10,19] HFOV was also successfully used as a "rescue" treatment in term and near term infants with respiratory failure.[21,22] Beyond the neonatal period there are two distinct groups of pulmonary diseases for which HFOV could be used effectively: DAD and airleak syndromes, with a ventilatory strategy depending on the underlying disorder.[7-9] In paediatric patients, aggressive lung volume recruitment resulted in a significant improvement in oxygenation compared with a conventional ventilatory strategy designed to limit increases in peak airway pressures.[8] Furthermore, despite of the use of higher mean airway pressures, the "open lung" strategy was associated with a lower frequency of barotrauma, indicated by the oxygen requirement at 30 days.[8]

Recently, Fort et al reported the beneficial use of HFOV in adults in the treatment of ARDS utilising the lung volume optimisation protocol.[5] A multicentre prospective trial comparing HFOV and CMV is currently in progress in adults to define whether the early use of HFOV will lead to improved survival with lower morbidity rates.

In this study, we present our experience with HFOV as a rescue therapy in 35 paediatric patients with respiratory failure. Depending on the underlying cause we employed 3 different strategies: the *"high-volume"* strategy designed to rapidly recruit and maintain optimal lung volume by the use of high CDP in patients with DAD and pulmonary haemorrhage; *the "low-volume"* strategy in patients with airleak where we accepted higher FIO_2 and lower saturation looking for the lowest CDP to allow closure of the airleak; and the *"open- airway"* and low stretch strategy in small airway disease.

We noticed that in the first group aggressive lung volume recruitment by increasing CDP was the mainstay for a successful transition. The major challenge in the transition was to

avoid under inflation rather than hyperinflation. Initially the team felt uncomfortable with the necessary high mean airway pressures. However, in normovolaemic patients circulatory effects of lung volume recruitment were minimal. Hypovolaemic patients sometimes failed to improve oxygenation, especially during transition. Adequate fluid administration improved haemodynamics as well as oxygenation.

In the patients with small airway disease, CDP was used to open up and “stent” the airways. To our knowledge the latter group has never been included in a study of HFOV before. HFOV was considered a contraindication in treating patients with a pulmonary pathology characterised by prolonged expiratory time constants.[7,8] However, preliminary results in our unit showed that HFOV can successfully be used in these patients, provided certain conditions are met.[23,24] The critical hallmark in ventilating these patients is the use of a device with an active expiratory phase and with the possibility to set the expiratory time longer than the inspiratory time. This can be done with the SensorMedics 3100. The opened and more stable airway diameter leads to a stable time constant during exhalation, which enables ventilatory oscillations to move freely in and out of the alveoli. However, there is only a small margin for the ”best CDP” because once the airways have been opened, the normal compliant alveolus is suddenly faced with a high CDP. Careful attention must be paid to pulmonary overdistention by chest X-ray and by monitoring haemodynamics.

As the data demonstrate, our approach produces an improvement in oxygenation in all survivors of the 3 groups, comparable to the results of previous studies.[5,8] Due to the high-volume strategy using high mean airway pressures to open up the lung, the OI rises during transition. In 4 patients additional administration of NO was tried during HFOV treatment because of ongoing hypoxemia or pulmonary hypertension. A discussion of the use of inhaled NO in improving oxygenation or decreasing pulmonary hypertension, is beyond the scope of this paper.[23,25,26]

In the study of Arnold et al.,[8] an increasing OI over time significantly predicted adverse outcome compared with a decreasing OI over time. In the study of Fort,[5] the pre-treatment OI was the most significant variable that distinguished survivors from non-survivors. These data suggest that the OI, representing the pressure and oxygen cost for oxygenation, might be a potentially accurate tool to assess pulmonary insufficiency and mortality in respiratory failure. Our data support this hypothesis (Fig. 2.2). However most of our patients died from non-respiratory causes.

Although the open-lung and open-airway strategy with the use of high mean airway pressures may feel uncomfortably aggressive to the treatment team, there are now convincing data that peak inspiratory pressures and phasic pressure changes in the alveoli

remain lower than during CMV.[27] Small phasic changes may be critical in preventing further lung injury.[28] Both repetitive overdistention and ongoing atelectasis contribute to progressive lung injury.[18] Nowadays, also CMV strategies are directed to avoid baro-and volutrauma, by using pressure limited techniques with permissive hypercapnia, prone position, inverse ratio ventilation and PEEP levels set a few cm above the inflection point on the inflation limb of the pressure volume loop. Amato et al. demonstrated that pursuit for an open lung approach with CMV does have an impact on outcome.[1,4] Prone positioning and permissive hypercapnia can be useful options with HFOV as well. During HFOV, the application of permissive hypercapnia will not affect lung inflation, because the lung can be fully recruited (CDP) and yet the stretch of the alveoli limited (deltaP). Permissive hypercapnia with conventional ventilators can give rise to reabsorption atelectasis: if not enough pressure is applied during inspiration, to open up the alveoli, they might collapse, especially when high oxygen concentrations are used which facilitates reabsorption.

In contrast to most other studies, we allowed our patients to breathe spontaneously during HFOV, unless permissive hypercapnia is used to reduce pressure swings as much as possible. Only the patients with small airway disease are always paralysed to avoid additional airtrapping.

An initial setting of HFOV requires medical expertise with the technique and a thorough understanding of the pathophysiology of the diseased lung. Once initiated, HFOV can easily be managed and nursing HFOV patients is not particularly complicated. Ventilation of patients is possible in various positions, giving the opportunity to profit from the beneficial effects of prone position.[29] HFOV is also feasible in tracheotomy patients.

We conclude that if managed properly, HFOV is effective and safe with very few side effects. It may be used as a primary ventilatory mode in paediatric patients with respiratory failure now. Recent experiences in the literature also offer perspectives for the application of HFOV in adult patients.

REFERENCES

1. Amato MB, Barbas CS, Medeiros DM, Magaldi RB, Schettino GP, Lorenzi-Filho G, Kairalla RA, Deheinzelin D, Munoz C, Oliveira R, Takagaki TY, Carvalho CR. Effect of a protective-ventilation strategy on mortality acute respiratory distress syndrome. *N Engl J Med* 1998; 338: 347 - 354.

2. Weg JG, Anzueto A, Balk RA, Wiedemann HP, Pattishal EN, Schork MA. The relation of pneumothorax and other air leaks to mortality in the acute respiratory distress syndrome. *N Engl J Med* 1998; 338: 341 - 346.

3. Stewart RJ, Meade MO, Cook DJ, Granton JT, Hodder RV, Lapinsky SE. Evaluation of a ventilation strategy to prevent barotrauma in patients at high risk for acute respiratory distress syndrome. *N Engl J Med* 1998; 338: 355 - 361.

4. Amato MB, Barbas CS, Medeiros DM, Schettino GP, Lorenzi FG, Kairalla RA, Deheinzelin D, Morais C, Fernandes EO, Takagaki TY. Beneficial effects of the "open lung approach" with low distending pressures in acute respiratory distress syndrome. *Am J Respir Crit Care Med* 1995; 152: 1835 - 1846.

5. Fort P, Farmer C, Westerman J, Johannigman J, Beninati W, Dolan S, Derdak S. High-frequency oscillatory ventilation for adult respiratory distress syndrome -a pilot study. *Crit Care Med* 1997; 25: 937 - 947.

6. Clark RH, Gerstmann DR, Null DM, deLemos RA. Prospective randomised comparison of high-frequency oscillatory and conventional ventilation in respiratory distress syndrome. *Paediatrics* 1992; 89: 5 - 12.

7. Kinsella JP, Clark RH. High-frequency oscillatory ventilation in paediatric critical care. *Crit Care Med* 1993; 21: 174 - 175.

8. Arnold JH, Hanson JH, Toro-Figuero LO, Gutierrez J, Berrens RJ, Anglin DL. Prospective, randomised comparison of high-frequency oscillatory ventilation and conventional mechanical ventilation in paediatric respiratory failure. *Crit Care Med* 1994; 22: 1530 - 1539.

9. Arnold JH, Truog RD, Thompson JE, Fackler JC. High-frequency oscillatory ventilation in paediatric respiratory failure. *Crit Care Med* 1993; 21: 272 - 278.

10. HiFO Study Group. Randomised study of high-frequency oscillatory ventilation in infants with severe respiratory distress syndrome. *J Pediatr* 1993; 122: 609 - 619.

11. Clark RH, Yoder BA, Sell MS. Prospective, randomised comparison of high-frequency oscillation and conventional ventilation in candidates for extracorporeal membrane oxygenation. *J Pediatr* 1994; 124: 447 - 454.

12. Bohn DJ, Miyasaka K, Marchak BE, Thompson WK, Froese AB, Bryan AC. Ventilation by high-frequency oscillation. *J Appl Physiol* 1980; 48: 710 - 716.

13. Butler WJ, Bohn DJ, Bryan AC, Froese AB. Ventilation by high-frequency oscillation in humans. *Anesth Analg* 1980; 59: 577 - 584.

14. Clark RH. High-frequency ventilation. *J Pediatr* 1994; 124: 661 - 669.

15. Chang HK. Mechanisms of gas transport during ventilation by high-frequency oscillation. *J Appl Physiol* 1984; 56: 553 - 563.

16. The HIFI Study Group. High-frequency oscillatory ventilation compared with conventional mechanical ventilation in the treatment of respiratory failure in preterm infants. *N Engl J Med* 1989; 320: 88 - 93.

17. Bryan AC. Reflections on the HIFI trial. *Paediatrics* 1991; 87: 565 - 567.

18. Froese AB. High-frequency oscillatory ventilation for adult respiratory distress syndrome: let's get it right this time! *Crit Care Med* 1997; 25: 906 - 908.

19. Gerstmann DR, Minton SD, Stoddard RA, Meredith KS, Monaco F, Bertrand JM, Battisti O, Langhendries JP, Francois A, Clark RH. The Provo multicenter high-frequency oscillatory ventilation trial: improved pulmonary and clinical outcome in respiratory distress syndrome. *Paediatrics* 1996; 98: 1044 - 1057.

20. Markhorst DG, Leenhoven T, van Genderingen HR, Uiterwijk JW, van Vught AJ. Bench test assessment of dosage accuracy and measurement inaccuracy in nitric oxide inhalational therapy during high frequency oscillatory ventilation. *J Clin Monit* 1997; 13: 349 - 355.

21. Carter JM, Gerstmann DR, Clark RH, Snyder G, Cornish JD, Null DM, Jr., deLemos RA. High-frequency oscillatory ventilation and extracorporeal membrane oxygenation for the treatment of acute neonatal respiratory failure. *Paediatrics* 1990; 85: 159 - 164.

22. Schwendeman CA, Clark RH, Yoder BA. Frequency of chronic lung disease in infants with high-frequency ventilation and/or extracorporeal membrane oxygenation. *Crit Care Med* 1992; 20: 372 - 377.

23. Duval ELIM, Leroy PLJM, Gemke RJBJ, van Vught AJ. High-frequency oscillatory ventilation in RSV-bronchiolitis patients. *Respir Med* 1999; 93: 435 - 440.

24. Duval ELIM, van Vught AJ. Status asthmaticus treated by high-frequency oscillatory ventilation. *Ped Pulm,* 2000; 30: 350 - 353.

25. Craig J, Mullins D. Nitric oxide inhalation in infants and children: physiologic and clinical implications. Am *J Crit Care* 1995; 443 - 450.

26. Abman SH. Inhaled nitric oxide therapy in neonatal and paediatric cardiorespiratory disease. In : Tibboel D, van der Voort E, eds. Intensive Care in Childhood; a Challenge to the Future. Berlin: Springer Verlag, 1996; 322 - 336.

27. Gerstmann DR, Fouke JM, Winter DC, Taylor AF, deLemos RA. Proximal, tracheal, and alveolar pressures during High-Frequency Oscillatory Ventilation in a normal rabbit model. *Pediatr Res* 1990; 28: 367 - 373.

28. Froese AB, Bryan AC. High-frequency ventilation. *Am Rev Respir Dis* 1987; 15: 1363 - 1374.

29. Langer M, Mascheroni D, Marcolin R, Gattinoni L. The prone position in ARDS. *Chest* 1988; 94: 103 - 107.

Chapter 3

A system for integrated measurement of ventilator settings, lung volume change and blood gases during high-frequency oscillatory ventilation

DG Markhorst, HR van Genderingen, T Leenhoven, AJ van Vught

Journal of Medical Engineering and Technology 2003; 27: 128 - 132

SUMMARY

Primary objective: To describe and validate a system for integrated measurement of ventilator settings and dependent physiological variables during high-frequency oscillatory ventilation (HFOV).

Methods: A custom interface was built for data acquisition. Lung volume change was determined by respiratory inductive plethysmography (RIP), modified to sampling rates of 140 Hz. Blood gas analysis was obtained using a continuous intra-arterial blood gas monitoring system. FIO_2 was measured by means of an electrochemical sensor. Pressure at the airway opening and trachea (microtip transducer) were sampled. Acquired data were sent to a laptop computer for analysis, display and storage. The system was tested during a lung recruitment procedure in an animal model of respiratory distress. Linearity of the RIP was checked by gas volume injection using a supersyringe.

Main outcomes and results: The system operated successfully. Agreement between RIP-measured volume with injected volume was excellent; bias was 5 ml; limits of agreement were 1 - 9 ml. Graphs were obtained, showing the relationship between imposed mean airway pressure and lung volume change, and oxygenation.

Conclusions: The integration of ventilator settings and dependent physiological variables may provide useful information for clinical, instructional and research applications.

INTRODUCTION

High-frequency oscillatory ventilation (HFOV) is a mode of mechanical ventilation in which lung volume is adjusted and maintained by a continuous distending pressure (CDP).[1] Superimposed small oscillations of airflow provide gas exchange with tidal volumes close to or lower than the anatomical deadspace at frequencies typically between 5 - 10 .sec^{-1}. It has been suggested that CDP levels that are too low can adversely affect outcome,[2] while excessive levels of CDP can lead to alveolar overdistention and barotrauma.[3] Therefore, it is important to find the safe window of CDP in each individual patient, in each stage of the patient's disease, to obtain an optimal lung volume. Currently, there is no clinical method for measurement of lung volume during HFOV, other than indirect methods such as chest X-ray and measurement of blood oxygenation. Recently, a number of methods have been experimentally investigated that are of potential clinical use. Brazelton et al. showed that lung volume changes can be monitored during HFOV by respiratory inductive plethysmography (RIP).[4] Van Genderingen et al. showed that the tracheal pressure swings contain information on respiratory system compliance,[5] which is related to optimal lung volume.[6] Previously, we proposed use of the oxygenation index to identify the optimal lung volume.[7] To clinically test these methods, there is a need for a safe and easy-to-use device for data acquisition and processing. We developed such a system and tested it in an animal model of acute lung injury.

METHODS AND MATERIALS

The measurement system

The measuring system consists of a custom-built data acquisition system (High-frequency Oscillation Acquisition and Data Logging system: HOADL), connected to a laptop computer with software for data analysis, display and storage (Fig. 3.1). Electrical power was supplied by a safety transformer approved for medical use (Powersupply 14.5 volt 0.3 mA pn 763355, SensorMedics, Yorba Linda, CA).

The HOADL hardware interface. The HOADL contains a number of interfaces to measurement devices and performs some measurements by itself.

Lung volume changes. Lung volume changes were derived from respiratory inductive plethysmography (RIP).[8] RIP measurement is based on the notion that the respiratory system is a two-compartment system comprising a rib cage and abdominal compartment.

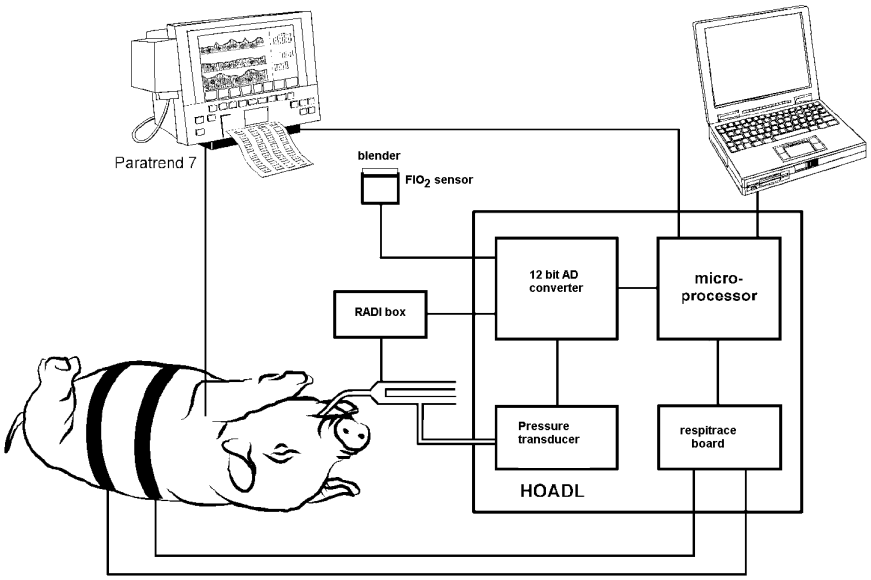

Fig. 3.1: Schematic setup of the system during the test. Respiratory inductive plethysmography (RIP) was applied by using a rib cage and abdominal band. Fractional inspired oxygen concentration was measured at the gas exit of the blender. Tracheal pressure (Radi microtip transducer) and airway opening pressure were measured. Invasive blood gases (Paratrend) were continuously determined. All data were acquired by the HOADL custom interface and sent to the laptop computer.

With plethysmographic measurement of both compartments, lung volume (change) can be derived. RIP uses thoracic and abdominal belts fitted with zigzag-shaped wires, which are placed in a resonator circuit. Inductance varies with extension of the bands, which in turn modulates the frequency of the resonator circuit. Resonator frequency is determined using a gated pulse counter. We integrated a commercially available Respitrace system circuit (Respitrace pn771727 (modified), SensorMedics, Yorba Linda, CA) in the HOADL. The standard Respitrace runs at 25 Hz, which is too low to detect dynamic changes during HFOV. We modified the circuit to increase sampling rate to 140 Hz with unaltered resolution.

Pressure at the airway opening. Pressure at the airway opening (Pao) was measured at the Y-piece of the ventilator (143PC05D differential pressure transducer, Honeywell, Freeport Ill). The pressure signal was low-pass filtered (Butterworth 35 Hz) and sampled by a 12-bit analog to digital converter (ADC) at a rate of 140 Hz.

Tracheal airway pressure. Tracheal airway pressure (Ptrach) was measured with a microtip pressure transducer (PressureWire sensor, RADI Medical Systems AB, Uppsala, Sweden) inserted through the endotracheal tube. Pressure was converted to an analog voltage that was subsequently sampled by the ADC at a rate of 140 Hz. The internal low pass filter of the RADI system was set at 500 Hz.

Fractional inspired oxygen concentration. Fractional inspired oxygen concentration (FIO_2) was measured by means of an electrochemical sensor (galvanic oxygen sensor, Bird, Palm Springs, CA) placed at the air-oxygen blender. The ADC sampled the analog voltage generated by this sensor at 140 Hz.

Blood gases. Blood gases (arterial oxygen tension PaO_2, carbon dioxide tension $PaCO_2$ and pH) were determined continuously by a commercial intra-arterial blood gas monitoring system (Paratrend 7, Philips Medical Systems, Boblingen, Germany). Data was sampled by the HOADL using a RS232 protocol.

The sampled abdominal (RIPabd) and rib cage (RIPrc) counts, airway pressures, FIO_2 and blood gas values were collected by a microcomputer (Basic Stamp 2sx microcontroller, Parallax Inc, Rocklin, CA) and sent to a laptop computer using a RS232 protocol.

The HOADL software.

The software was implemented in Delphi 5 (Borland, Scotts Valley, CA).

Data acquisition: Blood gases were sampled at a rate of 0.1 Hz, all other data at 140 Hz. All data were collected into a dataset along with sampling time.

Data calibration: A two point (at FIO_2 0.21 and FIO_2 1.0) calibration of the oxygen sensor was part of the system. To calibrate RIP to volume change (ΔV) relative to functional residual capacity (FRC), the qualitative diagnostic calibration (QDC) procedure was performed, as previously described by Sackner et al.[8] The method uses the equation $\Delta V = M * (K * \Delta RIPrc + \Delta RIPab)$, in which $\Delta RIPrc$ and $\Delta RIPab$ are the rib cage and abdominal RIP changes relative to the values at FRC, respectively. *K* is a calibration factor, indicating the relative contribution of both compartments to volume, and *M* scales the sum to volume and is expressed in ml. In the QDC method, a number of undisturbed breaths are collected during 5 minutes uninterrupted mechanical ventilation. Breaths with similar tidal volume are selected, based on the uncalibrated sum signal (RIPrc+RIPab), including only breaths within one standard deviation of the mean. Then, the standard deviations of RIPrc

and RIPab are determined over the selected breaths. Calibration factor *K* is estimated by SD(RIPab) / SD(RIPrc). *M* is determined by injection of a known volume, e.g. tidal volume. Alternatively, a "standard ratio" *K* to weight relative gains of the rib cage and abdominal signals could be entered.[9] With *M* and *K* known, every pair of RIPab and RIPrc was converted to a calibrated volume.

Data processing and reduction: Mean and amplitude of proximal and tracheal pressure and RIP signals were calculated for each breath, followed by a median determination to obtain values each 10 s.

Manual data entry: Remarks could be entered during the sampling process.

Data processing: Calculations were performed, such as peak-to-peak detection to determine amplitudes. Derived quantities were determined such as the oxygenation index OI, defined as $OI=CDP*FIO_2*100/PaO_2$ [7], the PaO_2/FiO_2 ratio, and the oscillatory pressure ratio OPR, defined as $OPR=\Delta Ptrach/\Delta Pao$,[5] with ΔPtrach and ΔPao the pressure amplitudes measured at the airway opening and in the trachea, respectively.

Data display: The screen display could be chosen: (a) Snapshots of raw data with fixed time axis; (b) trend graphs of mean airway pressure, lung volume and PaO_2, e.g. over the last 15 minutes; (c) X-Y plots: mean airway pressure against lung volume or PaO_2.
Data storage: Every 10 s, a 1 s epoch of raw data was stored in a file. Processed data such as mean and amplitudes of each signal, in combination with the values of PaO_2, $PaCO_2$ and pH and remarks were stored in a second file.

System test

Animal preparation. The system was tested during a routine training session with use of an animal model of acute lung injury to teach application of HFOV to clinicians. A 20 kg pig was sedated intravenously (midazolam 0.2 $mg.kg^{-1}.h^{-1}$ and sufentanyl 0.2 $microg.kg^{-1}.h^{-1}$). After oral intubation, the animal received conventional mechanical ventilation (Siemens Servo 900, Siemens Elema, Solna, Sweden) with ventilator settings of FIO_2 0.21, positive end-expiratory pressure (PEEP) 2 cm H_2O, respiratory minute volume 3300 ml, and frequency 16 breaths per min. The animal was placed in supine position on a thermo-controlled operation table to maintain body temperature at 38^oC. A catheter was inserted via the left femoral artery for continuous blood gas measurement. A catheter, inserted through the right jugular

vein was used for drug infusions. After surgery, the animal received vecuronium (0.2 mg.kg^{-1}.h^{-1}) for muscle relaxation. The RIP bands were placed 5 cm cranial to the xiphoid (rib cage band) and halfway xiphoid and umbilicus (abdominal band) and secured.
After the study, the animal was sacrificed using high dose pentobarbital. All procedures and protocols were reviewed and approved by the Animal Care and Use Committee at the University of Utrecht. Handling of the animal was in accord with local animal care guidelines.

Protocol

20 minutes after surgery, a 5 minute baseline recording was obtained during conventional mechanical ventilation. Calibration factor *K* (relative gain for the rib cage and abdominal signals) for RIP calibration was calculated from these data, using the QDC method. Then, the animal was disconnected from the ventilator and connected to a supersyringe (Model Series 5540; Hans Rudolph). RIP scaling factor *M*, was determined by injection of 500 ml ambient air. Next, the lungs were insufflated in randomised steps from 100 to 500 ml. Between each volume injection the animal was ventilated to assure return of end-expiratory lung volume to baseline.

FIO_2 was set to 1.0 and repeated lung lavage was applied with 35 ml.kg^{-1} warm saline until PaO_2 was below 80 mm Hg,[10] to obtain an animal model of acute respiratory distress. Then, high-frequency oscillatory ventilation (3100 A, SensorMedics, Yorba Linda CA) was initiated at an oscillation frequency of 8 Hz, initial mean airway pressure (CDP) 25 cm H_2O, and relative inspiration time of 33% of the respiratory cycle. All lung volumes were related to lung volume at this initial CDP. Pressure amplitude was increased until vibrations were visible in the lower abdomen. CDP was increased in steps of 2-5 cm H_2O to a maximum of 45 cm H_2O, and thereafter decreased to 16 cm H_2O. After each step the animal was allowed to stabilise for 5-15 minutes. At a CDP of 45 cm H_2O, FIO_2 was lowered from 1.0 to 0.5, and maintained at this level.

Next, the animal was switched back to conventional ventilation, and the volume injection procedure was repeated with 100, 200, 400 and 500 ml injections.

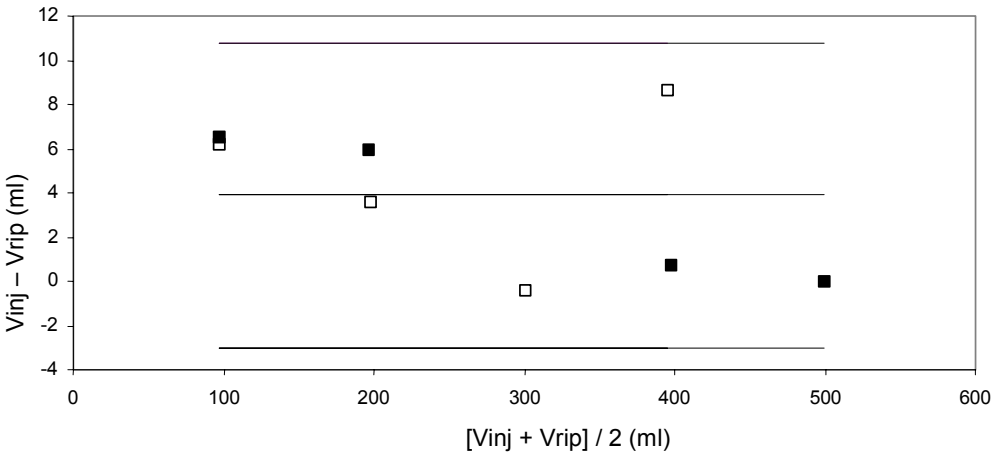

Fig. 3.2: Agreement between supersyringe-injected (V_{inj}) and RIP-measured volume (V_{RIP}). Bias (centre line), defined as the mean difference, was 5 ml. Lower and upper limits of agreement (upper and lower lines), defined as bias $\pm$ 2 x standard deviation, were 1 and 9 ml.

Statistical analysis

Comparisons between supersyringe-imposed and RIP-measured lung volume change were analysed using a Bland-Altman analysis.[11]

RESULTS

Validation of RIP

QDC procedure yielded calibration values *K* =0.66 and *M*=1.19. Linear regression of supersyringe-imposed versus RIP-measured lung volume changes demonstrated an excellent fit (r^2=0.99). The average between-method bias was 5 ml; the 95% confidence limits of agreement were 1 - 9 ml (Fig. 3.2).

Mean pressure-volume and mean pressure-oxygenation curves

Pressure-volume curves were obtained by plotting mean airway pressure (CDP) versus mean lung volume change in respect to lung volume at the onset of HFOV (Fig. 3.3(a)). Relation between CDP and oxygenation was assessed from a CDP versus PaO_2 plot (Fig. 3.3(b)) and CDP versus OI plot (Fig. 3.3(c)). Lung volume increased with increasing CDP. With decrease of CDP, lung volume initially increased, followed by a gradual decrease.

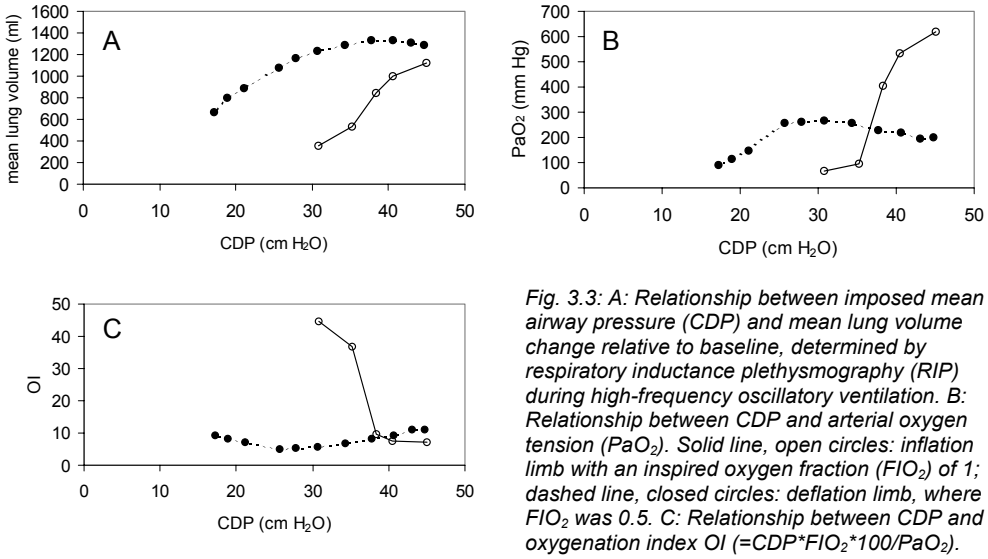

Fig. 3.3: A: Relationship between imposed mean airway pressure (CDP) and mean lung volume change relative to baseline, determined by respiratory inductance plethysmography (RIP) during high-frequency oscillatory ventilation. B: Relationship between CDP and arterial oxygen tension (PaO_2). Solid line, open circles: inflation limb with an inspired oxygen fraction (FIO_2) of 1; dashed line, closed circles: deflation limb, where FIO_2 was 0.5. C: Relationship between CDP and oxygenation index OI (=CDPFIO_2*100/PaO_2).*

There was a marked volume hysteresis. PaO_2 increased with increasing CDP, characteristic for lung recruitment. Prior to reduction of CDP, FIO_2 was reduced to 0.5 with a subsequent fall in oxygenation. With decrease of CDP, PaO_2 initially increased further, despite of the decreasing lung volume. With further decrease of CDP, oxygenation rapidly decreased.

Dynamic measurements

During HFOV with 8 Hz, dynamic variations of the rib cage and abdominal compartments were detected (Fig. 3.4). Asynchrony between the compartments was observed. Tracheal pressure measurements were obtained and OPR was calculated for the deflation limb of the pressure volume loop only (Fig. 3.5). OPR reaches a nadir around 25 cm H_2O.

DISCUSSION

The tested system functioned well in acquiring mean lung volume changes and oxygenation in response to changes in mean airway pressure and oxygen concentration during HFOV. The obtained quasi-static mean airway pressure-volume curve showed marked hysteresis. Clinically, this may be relevant information, as a similar lung volume and oxygenation level can be obtained at much lower CDP on the deflation limb, after a lung recruitment

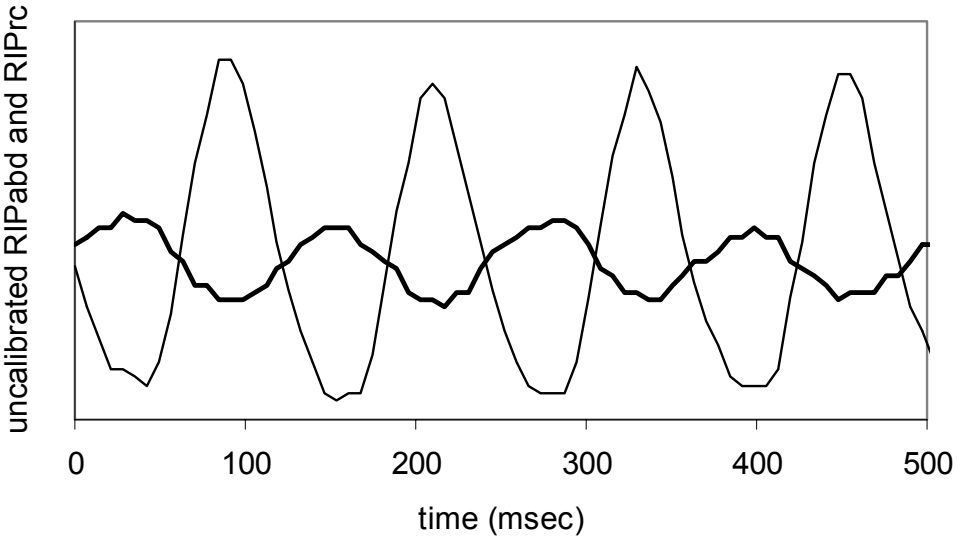

Fig. 3.4: Tracing of rib cage (RIPrc; thin line) and abdominal (RIPab; thick line) motions using respiratory inductance plethysmography during high-frequency ventilation with 8 Hz. Tracings show the asynchrony between the two compartments.

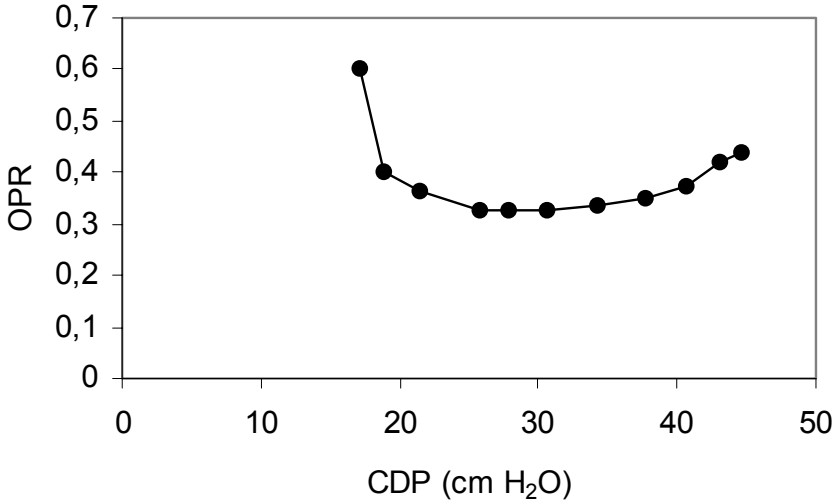

Fig. 3.5: Ratio of distal and proximal airway pressure amplitudes (OPR), during decreasing mean airway pressure (CDP) and following complete recruitment of lung volume. OPR reaches a nadir around 25 cm H_2O.

manoeuvre, as compared to the inflation limb. This may have a lung-protective effect, and minimise ventilator associated lung injury.[2]

We confirmed the linear behaviour of respiratory inductance plethysmography for the estimation of lung volume change imposed by the supersyringe, although this was limited to one subject. Linearity between supersyringe insufflated volumes and RIP measurements has been demonstrated previously by others.[9,12,13] By modifying the Respitrace circuit to higher sampling rates, we were able to record rib cage and abdominal motions during HFOV at 8 Hz. The (a-)synchrony of movement may be studied in future investigations to further clarify the dynamics of high-frequency ventilation.

We conclude that the system operated successfully to integrate ventilator settings and dependent physiological variables, and may prove to be a useful clinical, instructional and research tool.

REFERENCES

1. Arnold JH, Hanson JH, Toro-Figuero LO, Gutierrez J, Berens RJ, Anglin DL. Prospective, randomized comparison of high-frequency oscillatory ventilation and conventional mechanical ventilation in pediatric respiratory failure. *Crit Care Med* 1994; 22: 1530 - 1539.

2. Bryan AC, Froese AB. Reflections on the HIFI trial. *Pediatrics* 1991; 87: 565 - 567.

3. Froese AB. High-frequency oscillatory ventilation for adult respiratory distress syndrome: let's get it right this time! *Crit Care Med* 1997; 25: 906 - 908

4. Brazelton III TB, Watson KF, Murphy M, Al Khadra E, Thompson JE, Arnold JH. Identification of optimal lung volume during high-frequency oscillatory ventilation using respiratory inductive plethysmography. *Crit Care Med* 2001; 29: 2349 - 2359.

5. van Genderingen HR, Versprille A, Leenhoven T, Markhorst DG, van Vught AJ, Heethaar RM. Reduction of oscillatory pressure along the endotracheal tube is indicative for maximal respiratory compliance during high-frequency oscillatory ventilation: a mathematical model study. *Pediatr Pulmonol* 2001; 31: 458 - 463.

6. van Genderingen HR, van Vught AJ, Duval ELIM, Markhorst DG, Jansen JR. Attenuation of pressure swings along the endotracheal tube is indicative of optimal distending pressure during high-frequency oscillatory ventilation in a model of acute lung injury. *Pediatr Pulmonol* 2002; 33: 429 - 436.

7. van Genderingen HR, van Vught AJ, Jansen JR, Duval ELIM, Markhorst DG, Versprille A. Oxygenation index, an indicator of optimal distending pressure during high-frequency oscillatory ventilation? *Intensive Care Med* 2002; 28:1151-1156.

8. Sackner MA, Watson H, Belsito AS, Feinerman D, Suarez M, Gonzalez G, Bizousky F, Krieger B. Calibration of respiratory inductive plethysmography during natural breathing. *J Appl Physiol* 1989; 66: 410 - 420.

9. Weber K, Courtney SE, Pyon KH, Chang GY, Pandit PB, Habib RH. Detecting lung overdistention in newborns treated with high-frequency oscillatory ventilation. *J Appl Physiol* 2001; 89: 364 - 372.

10. Lachmann B, Robertson B, Vogel J. In vivo lung lavage as an experimental model of the respiratory distress syndrome. *Acta Anaesthesiol Scand* 1980; 24: 231 - 236.

11. Bland, J. M., Altman D. G. Statistical methods for assessing agreement between two methods of clinical measurement. *Lancet* 1986; 1: 307 - 310.

12. De Groote A, Paiva M, Verbandt Y. Mathematical assessment of qualitative diagnostic calibration for respiratory inductive plethysmography. *J Appl Physiol* 2001; 90: 1025 - 1030.

13. Gothberg S, Parker TA, Griebel J, Abman SH, Kinsella JP. Lung volume recruitment in lambs during high-frequency oscillatory ventilation using respiratory inductive plethysmography. *Pediatr Res* 2001; 49: 38 - 44.

Chapter 4

Accuracy of respiratory inductive plethysmography at varying PEEP levels during different degrees of acute lung injury

DG Markhorst, JPMD van Gestel, HR van Genderingen, J Haitsma, B Lachmann, AJ van Vught

submitted

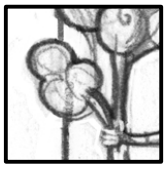

SUMMARY

Background: This study was performed to assess the accuracy of respiratory inductive plethysmographic (RIP) estimated lung volume changes at varying positive end-expiratory pressures (PEEP) during different degrees of acute respiratory failure.

Methods: RIP measurements of inspiratory tidal volume (V_{Ti}) were validated in eight piglets during constant V_{Ti} ventilation at incremental and decremental PEEP levels and with increasing severity of pulmonary injury. RIP accuracy was assessed using Qualitative Diagnostic Calibration (QDC) derived calibration from the healthy state, from the disease state as the measurement error was assessed, and at various PEEP levels. Additionally, the influence of fixed calibration factors on RIP accuracy was assessed.

Results: Best results (bias 3%, precision 7%) were obtained in healthy animals. RIP accuracy decreased with progressing degrees of acute respiratory failure and was PEEP dependent, unless RIP was calibrated again. When QDC was performed in the disease state as the measurement error was assessed, bias was reduced but precision not improved (bias -2%, precision 9%). In healthy animals, fixed calibration factors could be used without reducing accuracy, whereas accuracy decreased with progressing pulmonary injury.

Conclusions: RIP accuracy is within the accuracy range found in monitoring devices currently in clinical use. Most reliable results with RIP are obtained when measurements are preceded by calibration in pulmonary conditions that are comparable to the measurement period. When RIP calibration is not possible, fixed weighting of the RIP signals with species and subject size adequate factors is an alternative. Measurement errors should be taken into account with interpretation of small volume changes.

INTRODUCTION

Mechanical ventilation may lead to ventilator-associated lung injury as a result of alveolar overdistention as well as cyclic reexpansion of alveoli collapsed during expiration.[1-4] Both experimental and clinical data suggest that mechanical ventilation which optimises lung volume can diminish the deleterious effects of mechanical ventilation.[5,6]

A serious deficiency in current routine monitoring of patients receiving mechanical ventilation is the lack of simple, reliable and practical methods that can be used to measure mean lung volume (changes) during ventilation. Respiratory inductive plethysmography (RIP) is a non-invasive monitoring technique, which is able to monitor and measure lung volume changes. RIP is based on the principle that the chest wall has two compartments, the rib cage and abdomen. Each compartment is associated with a single motion variable that can be measured with external sensors, and the sum of both variables can be calibrated against a known volume change to provide volumetric measurements. RIP generates dimensionless counts that can be calibrated to volume using the Qualitative Diagnostic Calibration (QDC) algorithm or the Least Mean Squares technique.[7,8] RIP can be used to monitor tidal volume (V_T) [9] and changes in end-expiratory lung volume (ΔEELV).[10] RIP has also been used to assess mean lung volume induced by the mean airway pressure during high-frequency oscillatory ventilation (HFOV) and may provide a clinical useful tool, provided its accuracy with changing airway pressures can be established.[11]

Linearity of RIP with insufflated volume has been validated [10,12-14], although some have reported a limited precision of the method.[15]

We studied the accuracy of RIP during conventional mechanical ventilation (CMV) to assess whether this accuracy depended on PEEP level or disease.

MATERIALS AND METHODS

Animal preparation

The experiments were performed at the department of anesthesiology, Erasmus MC-Faculty Rotterdam; the study was approved by the local Animal Committee of the Erasmus University Rotterdam.

Anesthesia was induced in 8 female Yorkshire pigs (weight 20 ± 1 kg) with 10 mg/kg ketamine (Ketalin 100 mg/ml, Apharmo, Arnhem, the Netherlands) and 0.5 mg/kg midazolam (Dormicum 5.0 mg/ml, Roche Ned., Mijdrecht, the Netherlands) intramuscularly. After obtaining intravenous access a loading dose of 35 μg/kg fentanyl (0.05 mg/ml, B. Braun Melsungen AG, Melsungen,

Germany) was given and continuous infusion of fentanyl (35 μg/kg/h) and midazolam (9 μg/kg/min) was started. After placing a 8-mm endotracheal tube via a tracheotomy, the animals were ventilated (AVEA, Viasys Healthcare, Palm Springs, CA) in volume controlled mode (VC) with the following settings: frequency 20/min, positive end-expiratory pressure (PEEP) 5 cm H_2O, inspiratory time 0.8 sec (25%), inspiratory pause time 0.3 sec (10%) and 100% oxygen. Minute ventilation was set to deliver an inspiratory tidal volume (V_{T_i}) of 10 ml/kg. Inspiratory gas was humidified with a hygrophobe heat and moisture exchanger ("Sterivent S" Mallinckrodt, Mirandola, Italy). Muscle relaxation was achieved by continuous infusion of 2.5 μg/kg/min pancuronium bromide (Pavulon; Organon Technika, Boxtel, The Netherlands).
Subsequently, the carotid artery was cannulated to obtain arterial blood pressures. A blood gas-monitoring sensor (Paratrend 7+/Trendcare, Diametrics Medical Ltd, High Wycombe, UK) was inserted into the right femoral artery to continuously analyse blood gases and pH. The right internal jugular vein was cannulated and a 5 Fr pulmonary artery catheter was introduced (TD catheter 4 lumen; Arrow Holland medical products, Houten, The Netherlands). The bladder was catheterised through the abdominal wall. Temperature was kept in the normal range by a heating pad.
On completion of the experiments, the animals were killed with an overdose of pentobarbital.

Measurements

Hemodynamic and respiratory baseline measurements were performed prior to lung lavage and following stabilisation after surgery (*prelavage measurements*). Respiratory system compliance was derived according to $Crs = V_{T_i}/(P_{plat} – PEEP)$, with V_{T_i} being inspiratory tidal volume and P_{plat} the plateau pressure.
A system for integrated measurement of ventilator settings and dependent physiological variables as described in detail previously was used.[16] In short, pressure at the airway opening was measured at the Y-piece of the ventilator (143PC05D differential pressure transducer, Honeywell, Freeport Ill). Inspiratory and expiratory flow were measured continuously at the airway opening using a flow probe (AVEA, Viasys Healthcare, Palm Springs, CA) and integrated to a volume signal (Vvent).[17] Lung volume changes were derived from RIP. The thoracic belt was placed 4 cm above the xiphoid processus, the abdominal belt 4 cm above the umbilicus. Both belts were then secured by stitches and the position of the belts was checked at the end of experiments. The dimensionless counts of the abdominal (RIPabd) and ribcage (RIPrc) belts, airway pressure and Vvent were sampled at 140 Hz and stored for offline analysis.[16]

Experimental procedure

Reference measurements

Following stabilisation after instrumentation, respiratory variables (Paw, Vvent, RIPabd and RIPrc) were recorded during a 5-minute period of uninterrupted mechanical ventilation (*HEALTHYQDC*). These signals were used for calibration of the RIP, using the QDC algorithm.

Then, the animals were ventilated with constant V_{Ti} and PEEP increasing from 5 to 20 cm

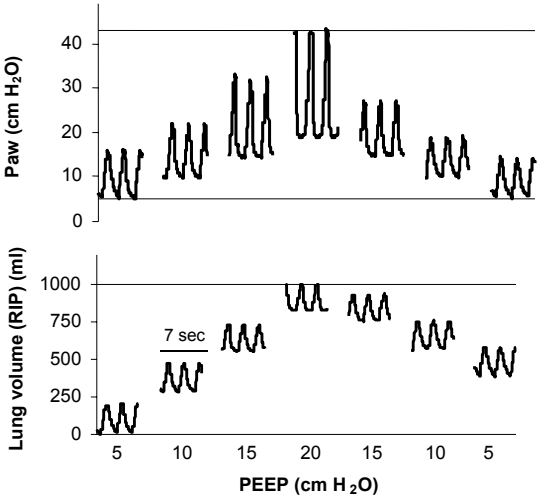

Fig. 4.1: Representative data record showing physiologic data (Paw and calibrated RIP volume signal) during a PEEP sequence in a healthy piglet. Signals are presented as 7 second snapshots per step and plotted as a function of time, with each PEEP step labeled on the horizontal axis.

H_2O, with 5 cm H_2O increments. This was followed by PEEP decrements of 5 cm H_2O down to 5 cm H_2O (*HEALTHY*) (Fig. 4.1). Time between PEEP changes was 5 minutes. Prior to PEEP change, physiologic variables were noted.

Subsequently, moderate lung injury was induced with a single lung lavage with 50 ml/kg warmed saline.[18] To avoid development of respiratory acidosis, V_{Ti} was temporarily increased to maintain $PaCO_2$ below 65 mmHg. Following a 30-minute stabilisation period, physiologic variables were noted (*LAV1*), and incremental and decremental PEEP steps were applied again at the initial V_{Ti} setting.

Acute lung injury (*ALI*) was induced by repeated lung lavages with 50 ml/kg warmed saline until PaO_2 was persistently below 80 mm Hg at 5 cm H_2O PEEP, FiO_2 of 1.0 and a tidal volume of 10 ml/kg.[18] After the last lavage, the ventilator settings remained unchanged for

one hour. If PaO_2 increased to values above 100 mmHg, lavages were repeated and stabilisation time reset. Thereafter, the lungs are assumed to be injured and atelectatic.[18] Following stabilisation at lavage target, measurements were repeated (*lavage target measurements*). Subsequently, PEEP was increased stepwise until P_{plat} reached 50 cm H_2O and stepwise decreased to baseline.
Ventilator-induced lung injury (VILI) was induced by ventilation with zero PEEP and V_{T_i} set to obtain P_{plat} of 50 cm H_2O.[19] These settings were maintained for 60 minutes. Physiologic measurements and incremental and decremental PEEP steps were repeated (*VILI*).
At the end of the experiment, PEEP was reduced to 5 cm H_2O and physiologic variables were recorded after a stabilisation period (*end experiment*).

Data processing

Determination of VT

V_{T_i} delivered by the ventilator ($V_{T_{i,VENT}}$) was determined from the Vvent signal as the difference between end-inspiratory and the preceding end-expiratory value. The same algorithm was used to determine inspiratory amplitudes of RIPabd, RIPrc and the summed RIP signals.

Calibration of RIP signals

To calibrate RIP to volume (ΔV) above functional residual capacity (FRC), the QDC procedure was performed as described by Sackner et al.[7] The method uses the equation $\Delta V = M * (K * \Delta RIPrc + \Delta RIPab)$, in which $\Delta RIPrc$ and $\Delta RIPab$ are the rib cage and abdominal RIP changes relative to the values at end-expiratory lung volume, respectively. *K* is a calibration factor, indicating the relative contribution of both compartments to volume, and *M* scales the sum to volume and is expressed in ml. To perform the QDC, a number of undisturbed breaths were collected during 5 minutes of ventilation. Breaths with similar tidal volume were selected, based on the uncalibrated sum signal (RIPrc+RIPab), including only breaths within one standard deviation (SD) of the mean. Then, the SDs of RIPrc and RIPab were determined over the selected breaths. Calibration factor *K* was estimated by SD(RIPab) / SD(RIPrc). *M* was calculated by using mean $V_{T_{i,VENT}}$. With *M* and *K* known, every pair of RIPab and RIPrc was converted to a calibrated volume.

To assess the validity of RIP at various end-expiratory lung volumes and in various disease states, RIP was calibrated using QDC on the *HEALTHYQDC* signals. Inspiratory tidal volume measured with RIP ($V_{T_{i,RIP}}$) per PEEP step was calculated, using the obtained QDC

calibration factor. To assess the influence of factor *K*, we also used *K* = 0 (abdominal band only), *K* = 1 (weighing ribcage and abdominal band equally) and *K* infinite (ribcage band only), as well as values that have been used in other studies of 0.5 and 2.0.[20,21] These values were compared with concomitant $V_{T_{i,VENT}}$. This procedure was performed for each disease state (*HEALTHY, LAV1, ALI, VILI*) and for each PEEP step.
Next, to investigate the influence of end-expiratory lung volume on the validity of QDC, RIP was calibrated at each PEEP step in *HEALTHY*. $V_{T_{i,RIP}}$ was compared with concomitant $V_{T_{i,VENT}}$ for each PEEP step (excluding values used for calibration). To investigate QDC validity in different disease states, $V_{T_{i,RIP}}$ was calculated for each PEEP step, with QDC calibration factors *M* and *K* obtained at PEEP of 10 (incremental PEEP), 20 and 10 (decremental PEEP) cm H_2O. This procedure was performed for each disease state (*HEALTHY, LAV1, ALI, VILI*).

Statistical analysis

Contiuous data of normal distribution are represented as mean ± standard deviation (SD). Intragroup comparisons were computed using the paired T-test with Bonferroni's correction. $V_{T_{i,RIP}}$ was compared with $V_{T_{i,VENT}}$ by means of Bland – Altman analysis.[22] Bias is expressed as the mean of differences between both measurements ($V_{T_{i,VENT}}$, minus $V_{T_{i,RIP}}$), precision is expressed 2 standard deviations (2SD) of the relative differences. Root mean square error (RMSE) was used as a measure of accuracy. A p-value less than 0.05 was considered significant.

RESULTS

Data could be obtained in eight piglets in disease states state *HEALTHY, LAV1* and *ALI.* During infliction of VILI one animal died and two developed a pneumothorax. In one animal oxygenation did not significantly decrease during the induction of VILI (PaO_2 286 mmHg after 60 minutes). The results of these four animals were excluded from analysis of *VILI* and end experiment data. Induction of VILI had to be terminated in the four remaining animals before 60 minutes as a result of decreasing PaO_2 of 39 ± 15 mmHg at zero PEEP. Analysis of *VILI* measurements is based on measurements in these four animals.
Physiologic variables describing each disease state at baseline measurements are given in Table 4.1. Crs decreased significantly as a result of lavages. Following the first lavage, PaO_2/FiO_2 was below 400 mmHg and significantly decreased with further lavages. At *VILI*, PaO_2/FiO_2 was lower than the values at *ALI*.

Table 4.1.Ventilatory and blood gas values at baseline (PEEP = 5 cm H_2O), except at VILI where measurements were obtained at the lowest PEEP with target PaO2 of 50 mm Hg.

	Prelavage (healthy) (n=8)	Following 1 lavage (n=8)	At lavage target (n=8)	At VILI target (n=4)	End experiment (n=4)
V_{Ti} (ml/kg)	10 ± 1	12 ± 1 [a]	12 ± 1 [a]	12 ± 1	13 ± 1
Crs (ml/cm H_2O/kg)	0.75 ± 0.14	0.58 ± 0.13[a]	0.4 ± 0.08 [a,b]	0.35 ± 0.07 [a,b]	0.39 ± 0.06 [a,b]
PaO_2 (mm Hg)	532 ± 51	321 ± 101 [a]	61 ± 12 [a,b]	40 ± 9 [a,b,c]	43 ± 5 [a,b,c]
$PaCO_2$ (mm Hg)	52 ± 6	61 ± 3 [a]	61 ± 5 [a]	47 ± 7 [c]	64 ± 6 [a]

a: p<0.05 compared with healthy, b: p<0.05 compared with one lavage, c: p<0.05 compared with lavage target

Figure 4.1 shows a representative example of the PEEP sequence. With subsequent PEEP steps, $V_{Ti,VENT}$ remained constant. At high PEEP levels in the healthy animal pressure amplitude (P_{plat} – PEEP) increased. Grouped data from a PEEP sequence in healthy animals are shown in Figure 2; incremental PEEP steps are shown in the left panels, decremental PEEP steps in the right panels. Hysteresis of end-expiratory lung volume is shown in Fig. 4.2; at identical PEEP levels, RIP estimated end-expiratory volume is lower during incremental PEEP steps (Fig. 4.2(a)) compared to decremental PEEP (Fig. 4.2(b)). Amplitudes of uncalibrated RIPrc (Fig. 4.2(c) and (d)) and RIPabd signals (Fig. 4.2(e) and (f)) and tidal volumes (Fig. 4.2(i) and (j)) measured from the calibrated RIP signals changed with changing PEEP. RIPrc amplitudes were lower during decremental PEEP than during incremental PEEP ($p < 0.05$), RIPabd amplitudes at 10 and 15 cm H_2O decremental PEEP were higher than they were at equivalent values incremental ($p < 0.05$). RIP amplitude change also displayed hysteresis. There was no relation between RIP amplitude change of either band and summed end-expiratory uncalibrated RIP counts or respiratory system compliance (Crs) (Fig. 4.2(g) and (h)). The relative RIP measurement error, expressed as $[V_{Ti,vent} – V_{Ti,RIP}]/ V_{Ti,vent}$ was not related to PEEP, but measurement standard deviation increased with increasing PEEP.

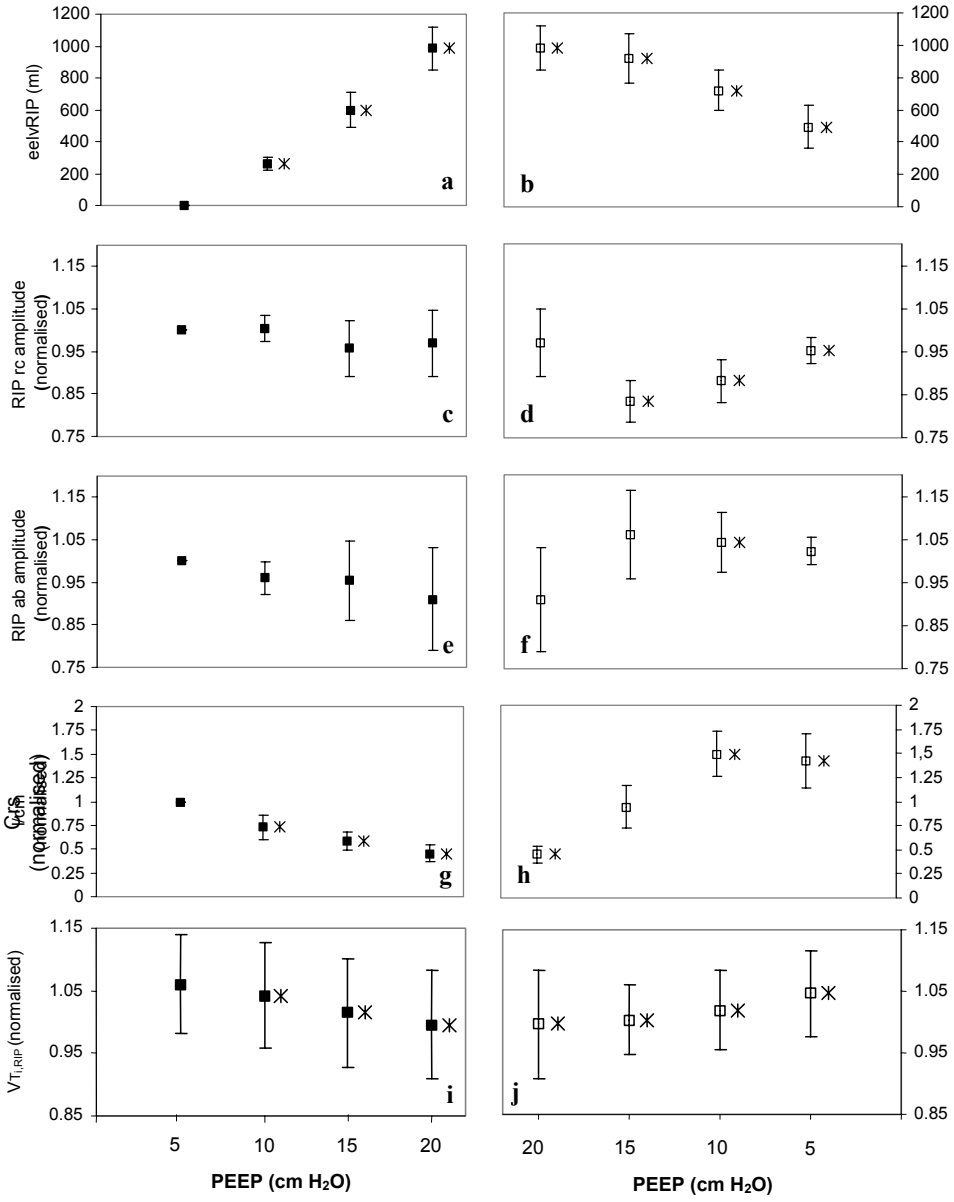

*Fig. 4. 2: Grouped data from a PEEP sequence in healthy animals. Values are normalized to the initial value at PEEP = 5 cm H_2O (incremental). Decremental PEEP steps are plotted in reverse order. *: Significant difference from value obtained at 5 cm H_2O incremental PEEP, $p<0.05$.*

Table 4.2. Measurement error as quantified by the bias (precision) of Respiratory Inductive Plethysmographic inspiratory tidal volume measurement, at various PEEP levels levels and in multiple disease states. Calibration using HEALTHYQDC signals. K = 0: chest wall belt changes ignored, K = 1: weighing ribcage and abdominal belt equally, K = infinite: abdominal belt changes ignored.

	QDC	*K* = 0	*K* = 0.5	*K* = 1	*K* = 2	*K* = infinite
Healthy	3 (7)	0 (18)	2 (11)	3 (7)	3 (10)	4 (15)
Following 1 lavage	5 (10) [a]	-2 (23) [b]	2 (14) [b]	5 (10) [a]	7 (13) [a,b]	11 (24) [a,b]
At lavage target	8 (11) [a]	0 (25) [b]	4 (14) [b]	8 (12) [a]	10 (16) [a]	13 (30) [a,b]
VILI (n=4)	11 (11) [a]	0 (16) [b]	9 (10) [a,b]	10 (10) [a]	14 (13) [a,b]	18 (18) [a,b]
Overall	6 (12)	0 (21) [b]	4 (14) [b]	6 (11)	8 (15) [a,b]	11 (25) [b]

a: significant difference when compared to values derived during health, using identical calibration (P <0.05). b: significant difference when compared to QDC derived values (P <0.05).

Table 4.2 lists the RIP measurement errors after QDC calibration in the healthy animal. The best results, bias and precision (defined as 2SD interval) <10% were obtained in the healthy animal, whereas the error increased with progressing disease severity.

The use of *K* = 1 did not influence the measurement error compared to the use of calibration factors obtained with QDC in the healthy state. With *K* = 0 bias was reduced but precision increased. *K* = infinite resulted in both increased bias and precision (Table 4.2).

When QDC was performed in the same disease state as the measurement error was

Table 4.3 Measurement error as quantified by the bias (precision) of Respiratory Inductive Plethysmograpic inspiratory tidal volume measurement, at various PEEP levels and in multiple disease states. QDC calibration at PEEP of 10 (incremental PEEP), 20 and 10 (decremental PEEP) cm H_2O, respectively. Data used for calibration were excluded from analysis of precision and accuracy.

	QDC on PEEP 10 (incremental) Bias (2SD) %	QDC on PEEP 20 (decremental) Bias (2SD) %	QDC on PEEP 10 (decremental) Bias (2SD) %
Healthy	2 (8)	-4 (9) [a]	-3 (8) [a]
Following 1 lavage	2 (9) [a]	0 (9) [a]	-1 (9) [a]
At lavage target	1 (11) [a]	-1 (10) [a]	1 (14) [a]
VILI (n=4)	3 (11) [a]	-2 (8) [a]	-3 (13) [a]
Overall	2 (10) [a]	-2 (9) [a]	-1 (12) [a]

a: significant difference when compared to HEALTHYQDC derived QDC values (P <0.05).

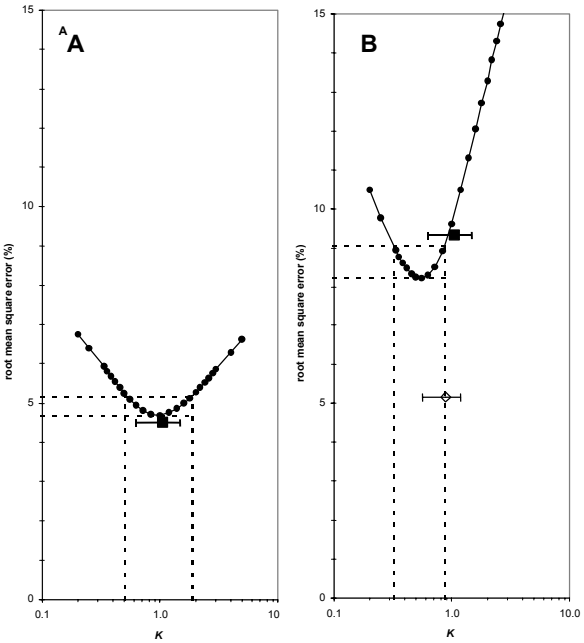

Fig. 4.3: Measurement error (dots), expressed as root mean square error, with changing weight factor K in healthy animals (A) and animals at lavage target (B). Solid squares represent error obtained with calibration factors obtained from individual calibration in healthy animals (HEALTHYQDC), open diamond represents error obtained with calibration factors from individual calibration at PEEP = 20 cm H_2O in lavaged animals. Dotted lines represent boundaries of minimal error ± 10%. Note logarithmic scale on horizontal axis.

assessed (Table 4.3), we found a reduction in bias but not in precision. Figure 4.3 illustrates the dependence of accuracy on *K.* In the *HEALTHY* animals (Fig. 4.3(a)) maximal accuracy with fixed *K* was found with K = 1. Accuracy was slightly higher when individual QDC calibration was performed in the healthy state. Accuracy remained within 10% of maximal accuracy with fixed *K* between 0.5 and 1.8. In the *ALI* animals RIP accuracy with fixed *K* was significantly reduced (Fig. 4.3(b)). Here, accuracy remained within 10% of maximal accuracy with fixed *K* between 0.3 and 0.9. In this range of fixed *K*, accuracy was higher than with *K* derived from individual QDC calibration performed in the healthy state. QDC calibration performed in the same disease state as the measurement error was assessed, yielded higher accuracy than could be reached with fixed *K*.

K and *M*, obtained during QDC at different levels of PEEP, were not PEEP dependent (Table 4.4).

Table 4.4. Values for K and M obtained with QDC in healthy animals, at various PEEP steps
.

	K mean (sd)	M mean (sd) (ml)
Healthy PEEP 5 (incremental PEEP)	1.03 (0.45)	1.74 (0.31)
Healthy PEEP 10 (incremental PEEP)	0.97 (0.41)	1.83 (0.44)
Healthy PEEP 15 (incremental PEEP)	0.93 (0.19)	1.88 (0.41)
Healthy PEEP 20 (maximal PEEP)	1.15 (0.70)	1.75 (0.47)
Healthy PEEP 15 (decremental PEEP)	1.09 (0.38)	1.85 (0.47)
Healthy PEEP 10 (decremental PEEP)	1.09 (0.17)	1.75 (0.31)
Healthy PEEP 5 (decremental PEEP)	1.15 (0.69)	1.75 (0.47)

All differences NS

DISCUSSION

This study assessed the validity of estimation of lung volume changes by respiratory inductive plethysmography during conventional mechanical ventilation at changing PEEP levels and at progressive degrees of acute respiratory failure in animals. A major finding of the present study was a decreasing accuracy of RIP-estimated lung volume changes with progressing degrees of acute respiratory failure, unless RIP was calibrated again. Best accuracy was obtained when calibration weight factor *K* was determined using QDC. The obtained results were in line with other studies,[12,23] but we obtained better precision than earlier investigators did using older versions of the RIP hardware.[15,24]
Optimal results (minimal bias) of RIP-estimated volume changes were obtained when calibration was performed in a representative pulmonary condition, e.g. the disease state the animal was in, and above the minimal end-expiratory lung volume. As a consequence, RIP accuracy decreases when pulmonary conditions change significantly, e.g. with deterioration or improvement of the disease. Thus, RIP should not be used to monitor long-term changes. When these conditions can be met, measurement error is within a range of about $\pm$10%. For purposes of clinical monitoring during relatively short procedures, such as lung volume recruitment and subsequent titrating of volume or compliance targeted ventilation, this may be acceptable (even though the accuracy is limited) given the ease of use of RIP, the fact that measurement does not interfere with treatment, and the ability to measure tidal

Table 4.5. Measurement errors of other measurement devices. RIP accuracy obtained with QDC performed at 10 cm H_2O incremental PEEP and in the same disease state as the measurements were performed is given (Table 4.3).

Device	Bias (%)	2 SD (%)	measures	reference
Siemens Servo 300	18	12	VT	[32]
Respiratory Inductive Plethysmograpy	-2	9	VT/relative EELV changes	Present study
Hot wire anemometer (Florian)	6.3	5	VT	[33]
Babylog 8000	-5.5	3	VT	[34]

volumes as well as end-expiratory lung volume changes. RIP accuracy is within the accuracy range found in monitoring devices currently in clinical use (Table 4.5), and its use provides additional information. PEEP induced lung volume recruitment and compliance change in a surfactant-depleted piglet is shown in Fig. 4.4 as an example. This could possibly alleviate the need for partitioning respiratory mechanics to differentiate between acute respiratory distress syndrome caused by pulmonary and extrapulmonary disease.[25] Omitting QDC and assuming a fixed weight factor *K* would facilitate clinical RIP application, especially during none conventional ventilation modes such as HFOV, where measurement of lung volume is cumbersome. Weighing both signals equally did not influence bias or precision compared with the use of calibration factors obtained in healthy animals. This

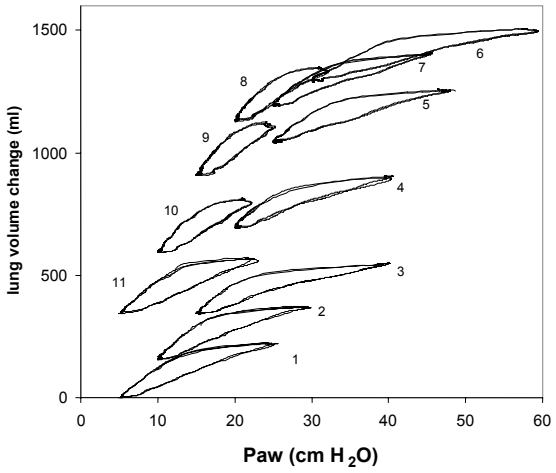

Fig 4.4: Lung volume change (calibrated RIP signal) with each PEEP step in one piglet at lavage target, relative to lung volume at initial PEEP of 5 cm H_2O. Numbers indicate successive changes in PEEP. Step 1 to 6: incremental PEEP changes from 5 to 30 cm H_2O, step 6 to 11: decremental PEEP changes from 30 to 5 cm H_2O. Each dynamic pressure volume curve is constructed of 2 subsequent breaths following 5 minutes of undisturbed mechanical ventilation. Respiratory Inductive Plethysmograph calibrated at 20 cm H_2O decremental PEEP.

suggests that QDC is valid during mechanical ventilation, but is not mandatory. Calibration of the dimensionless RIP counts to a known volume is, however, still needed to obtain a calibrated volume. Equal weighing of the signals was adequate, as was found by others using RIP in piglets.[11] In other species this may not be the case, due to anatomic or physiologic differences. In spontaneous breathing healthy infants a *K* of 0.5 – 1.0 has been found adequate [12,20] whereas in healthy adults a *K* of 2.0 was found.[21] If knowledge of relative rather than absolute changes in lung volume is of interest, the use of uncalibrated summed RIP signals may be sufficient.[11,26] However, we have shown that RIP accuracy is *K* dependent and in our experiments optimal *K* decreased with increasing lung injury (Fig. 4.3). Underestimation of $V_{T_{i,VENT}}$ by $V_{T_{i,RIP}}$ may in part be explained by the volume reduction when gas is compressed; isovolumetric pressure change of the lung, sometimes referred to as compressible volume of the lung. When a given volume is inflated in a container with infinite compliance and zero volume, the volume change of the container will be the inflated volume. At the other extreme, when the same volume is injected into a container with infinite pressure and low compliance, the volume change will be negligible. We did not measure functional residual capacity (FRC). Using FRC measured by others in piglets following pulmonary lavage [27] we calculated a compressible volume of 7% in a *lavage target* animal at PEEP 5 cm H_2O up to 30% at a PEEP of 25 cm H_2O. This would account for a difference of about 25% of externally measured volume changes in these animals with RIP calibrated at PEEP 5 cm H_2O (incremental) and comparing $V_{T_{i,VENT}}$ and $V_{T_{i,RIP}}$ at PEEP 5 and 25 cm H_2O. A further explanation for the varying precision may be found in interindividual changes in thoracic shape with changing PEEP. With increasing lung volume, the shape of the thorax changes; in the upper portion of the ribcage lateral displacement is minimal with inspiration ('pump handle' motion) whereas ventral displacement is minimal in the lower portion of the rib cage ('bucket handle' motion).[28] We placed the thoracic belt at the caudal part of the chest. In humans, in this region chest expansion with inspiration is mainly in the frontal plane rather than in the transversal plane, leading to a change in cross-sectional shape. It has been shown that inductive sensors are sensitive to both cross-sectional perimeter and area variations, and that (depending on the deformation) these sensors measure either perimeter or area.[29] Watson et al. have demonstrated a linear relationship between RIP output and cross-sectional area.[30] However, the relation between self-inductance of the RIP coils and cross-sectional area varies with ellipticity or shape of the cross-section.[31]

CONCLUSION

Our results suggest that when RIP is used during mechanical ventilation, most reliable results are obtained when measurements are preceded by a calibration in comparable pulmonary conditions to the measurement period. In practice, this may not always be feasible and practical. When RIP calibration is omitted, a fixed weight factor *K* may be used which may, however, result in less accuracy. Our study demonstrated an unpredictable dependence of PEEP. Despite this limitation, RIP is a measurement method comparable to other techniques of lung volume change measurement. Measurement errors should be taken into account with interpretation of small volume changes.

When lung conditions change, RIP partially loses its accuracy; during mechanical ventilation RIP should not be used as a device to monitor lung volume changes during a prolonged period of time. The potential advantage of the technique is its use during relatively short procedures, such as lung volume recruitment and subsequent decrease in airway pressures.[11] A device that provides clinicians with integrated information on ventilator settings and dependent physiologic variables may prove to be a valuable asset,[16] but this remains to be demonstrated in clinical tests.

REFERENCES

1. Dreyfuss D, Saumon G. Ventilator-induced lung injury: lessons from experimental studies. *Am J Respir Crit Care Med* 1998; 157: 294 - 323.

2. Dreyfuss D, Soler P, Basset G, Saumon G: High inflation pressure pulmonary edema. Respective effects of high airway pressure, high tidal volume, and positive end-expiratory pressure. *Am Rev Respir Dis* 1988; 137: 1159 - 1164.

3. Taskar V, John J, Evander E, Robertson B, Jonson B. Surfactant dysfunction makes lungs vulnerable to repetitive collapse and reexpansion. *Am J Respir Crit Care Med* 1997; 155: 313 - 320

4. McCulloch PR, Forkert PG, Froese AB: Lung volume maintenance prevents lung injury during high frequency oscillatory ventilation in surfactant-deficient rabbits. *Am Rev Respir Dis* 1988; 137: 1185 - 1192.

5. Amato MB, Barbas CS, Medeiros DM, Magaldi RB, Schettino GP, Lorenzi-Filho G, Kairalla RA, Deheinzelin D, Munoz C, Oliveira R, Takagaki TY, Carvalho CR. Effect of a protective-ventilation strategy on mortality in the acute respiratory distress syndrome. *N Engl J Med* 1998; 338: 347 - 354.

6. Rimensberger PC, Pache JC, McKerlie C, Frndova H, Cox PN. Lung recruitment and lung volume maintenance: a strategy for improving oxygenation and preventing lung injury during both conventional mechanical ventilation and high-frequency oscillation. *Intensive Care Med* 2000; 26: 745 - 755.

7. Sackner MA, Watson H., Belsito AS, Feinerman D, Suarez M, Gonzalez G, Bizousky F, Krieger B. Calibration of respiratory inductive plethysmograph during natural breathing**.** *J Appl Physiol* 1989; 66: 410 - 420.

8. Stromberg NO, Dahlback GO, Gustafsson PM. Evaluation of various models for respiratory inductance plethysmography calibration *J Appl Physiol* 1993; 74: 1206 - 1211.

9. Adams JA, Zabaleta IA, Stroh D, Johnson P, Sackner MA. Tidal volume measurements in newborns uing respiratory inductive plethysmography. *Am Rev Respir Dis* 1993; 148: 585 - 588.

10. Valta P, Takala J, Foster R, Weissman C, Kinney JM. Evaluation of respiratory inductive plethysmography in the measurement of breathing pattern and PEEP-induced changes in lung volume. *Chest* 1992; 102: 234 - 238.

11. Brazelton III TB, Watson KF, Murphy M, Al Khadra E, Thompson JE, Arnold JH. Identification of optimal lung volume during high-frequency oscillatory ventilation using respiratory inductive plethysmography. *Crit Care Med* 2001; 29: 2349 - 2359.

12. Weber K, Courtney SE, Pyon KH, Chang GY, Pandit PB, Habib RH. Detecting lung overdistention in newborns treated with high-frequency oscillatory ventilation. *J Appl Physiol* 2000; 89: 364 - 372.

13. Gothberg S, Parker TA, Griebel J, Abman SH, Kinsella JP. Lung volume recruitment in lambs during high-frequency oscillatory ventilation using respiratory inductive plethysmography. *Pediatr Res* 2001; 49: 38 - 44.

14. Leino K, Nunes S, Valta P, Takala J. Validation of a new respiratory inductive plethysmograph. *Acta Anaesthesiol Scand* 2001; 45: 104 - 111.

15. Neumann P, Zinserling J, Haase C, Sydow M, Burchardi H. Evaluation of respiratory inductive plethysmography in controlled ventilation: measurement of tidal volume and PEEP-induced changes of end-expiratory lung volume. *Chest* 1998; 113: 443 - 451.

16. Markhorst DG, Genderingen HR, Leenhoven T, van Vught AJ. A system for integrated measurement of ventilator settings, lung volume change and blood gases during high-frequency oscillatory ventilation. *J Med Eng Technol* 2003; 27: 128 - 132.

17. Cannon ML, Cornell JACK, Tripp-Hamel DS, Gentile MA, Hubble CL, Meliones JN, Cheifetz IM. Tidal Volumes For Ventilated Infants Should Be Determined with a Pneumotachometer Placed at the Endotracheal Tube. *Am J Respir Crit Care Med* 2000; 162: 2109 - 2112.

18. Lachmann B, Robertson B, Vogel J. In vivo lung lavage as an experimental model of the respiratory distress syndrome. *Acta Anaesthesiol Scand* 1980; 24: 231 - 236.

19. Vazquez de Anda GF, Lachmann RA, Gommers D, Verbrugge SJ, Haitsma J, Lachmann B. Treatment of ventilation-induced lung injury with exogenous surfactant. *Intensive Care Med* 2001; 27: 559 - 565.

20. Poole KA, Thompson JR, Hallinan HM, Beardsmore CS. Respiratory inductance plethysmography in healthy infants: a comparison of three calibration methods. *Eur Respir J* 2000; 16: 1084-1090.

21. Banzett RB, Mahan ST, Garner DM, Brughera A, Loring SH. A simple and reliable method to calibrate respiratory magnetometers and Respitrace. *J Appl Physiol* 1995; 79: 2169 - 2176.

22. Bland J, Altman DG: Statistical methods for assessing agreement between two methods of clinical measurement. *Lancet* 1986; 1: 307 - 310.

23. Albaiceta GM, Piacentini E, Villagra A, Lopez-Aguilar J, Taboada F, Blanch L. Application of continuous positive airway pressure to trace static pressure-volume curves of the respiratory system. *Crit Care Med* 2003; 31: 2514 - 2519.

24. Werchowski JL, Sanders MH, Costantino JP, Sciurba FC, Rogers RM. Inductance plethysmography measurement of CPAP-induced changes in end-expiratory lung volume. *J Appl Physiol* 1990; 68: 1732 - 1738.

25. Gattinoni L, Pelosi P, Suter PM, Pedoto A, Vercesi P, Lissoni A. Acute respiratory distress syndrome caused by pulmonary and extrapulmonary disease. Different syndromes? *Am J Respir Crit Care Med* 1998; 158: 3 - 11.

26. Manczur T, Greenough A, Hooper R, Allen K, Latham S, Price JF, Rafferty GF. Tidal breathing parameters in young children: comparison of measurement by respiratory inductance plethysmography to a facemask pneumotachograph system. *Pediatr Pulmonol* 1999; 28: 436 - 441.

27. Grotjohan HP, van der Heijde RMJL. Experimental models of the respiratory distress syndrome. Lavage and oleic acid. PhD thesis Erasmus University, Rotterdam, The Netherlands. 1992, 87-112.

28. Troyer AD. The respiratory muscles. In: The lung: scientific foundations. 2nd ed. Edited by Crystal RG, West JB. Philadelphia, Lippincott-Raven Publishers, 1997, 1203 - 1216.

29. de Groote A, Verbandt Y, Paiva M, Mathys P. Measurement of thoracoabdominal asynchrony: importance of sensor sensitivity to cross section deformations. *J Appl Physiol* 2000; 88: 1295 - 1302.

30. Watson HL, Poole DA, Sackner MA. Accuracy of respiratory inductive plethysmographic cross-sectional areas. *J Appl Physiol* 1988; 65: 306 - 308.

31. Martinot-Lagarde P, Sartene R, Mathieu M, Durand G. What does inductance plethysmography really measure? *J Appl Physiol* 1988; 64: 1749 - 1756.

32. Castle RA, Dunne CJ, Mok Q, Wade AM, Stocks J. Accuracy of displayed values of tidal volume in the pediatric intensive care unit. *Crit Care Med* 2002; 30: 2566 - 2574.

33. Scalfaro P, Pillow JJ, Sly PD, Cotting J. Reliable tidal volume estimates at the airway opening with an infant monitor during high-frequency oscillatory ventilation. *Crit Care Med* 2001; 29: 1925 - 1930.

34. Roske K, Foitzik B, Wauer RR, Schmalisch G. Accuracy of volume measurements in mechanically ventilated newborns: a comparative study of commercial devices. *J Clin Monit Comput* 1998; 14: 413 - 420.

Chapter 5

Static pressure-volume curve characteristics are moderate estimators of optimal airway pressures in a mathematical model of (primary/pulmonary) ARDS

DG Markhorst, HR van Genderingen, AJ van Vught

Intensive Care Medicine, in press

SUMMARY

Objective: To study the value of objective pressure-volume characteristics to predict optimal airway pressures and the development of atelectasis and overstretching during a structured lung volume recruitment procedure with subsequent reduction of airway pressures.
Methods: We used a mathematical model of a lung with adjustable characteristics of acute respiratory distress syndrome (ARDS) characteristics. Simulations were performed in 5 grades of ARDS in the presence of pure alveolar or combined alveolar-small airway closure as well complete or incomplete lung volume recruitability. For each simulation, optimal end-expiratory pressure was determined. A static pressure-volume curve was constructed and objective characteristics of this curve calculated. The predictive value of these characteristics for end-expiratory atelectasis, overstretching and optimal end-expiratory pressure was assessed.
Results: Simultaneous alveolar recruitment and overstretching during inflation were more pronounced than alveolar derecruitment and overstretching during deflation. End-expiratory pressure needed to prevent significant alveolar collapse in severe ARDS resulted in maximal safe tidal volumes that may be insufficient for adequate ventilation using conventional mechanical ventilatory modes. Plateau pressures well below the 'upper corner point' (airway pressure where compliance decreases) resulted in significant alveolar overstretching.
Conclusions: A recruitment manoeuvre followed by subsequent reduction of airway pressure limits end-expiratory atelectasis, overstretching and pressure. None of the objective characteristics of the pressure-volume curve were predictive for end-expiratory atelectasis, overstretching or optimal airway pressure.

DEFINITIONS AND ABBREVIATIONS

Transmural pressure (Ptm)	pressure difference over the alveolar wall resulting from alveolar recoil
Chest wall pressure (Pcw)	elastic recoil pressure exerted by the chest wall
Superimposed pressure (Ps)	gravitationally determined, superimposed pressure on the alveoli in a lung compartment
Airway pressure (Paw)	alveolar and airway pressure during no-flow conditions with Paw=Ptm+Ps+Pcw
Transpulmonary pressure (Plungs)	Pressure difference over the lung compartment, originating from alveolar recoil and superimposed pressure, defined by Plungs=Ptm+Ps=Paw-Pcw for aerated alveoli
Threshold closing pressure (TCP)	the transmural pressure at which an alveolus or small airway closes
Threshold opening pressure (TOP)	the transmural pressure that must be exceeded for a closed alveolus to open

INTRODUCTION

The administration of positive end-expiratory pressure (PEEP) is aimed at preventing the end-expiratory collapse of diseased pulmonary areas in order to reverse severe hypoxemia resulting from pulmonary shunting, a hallmark of acute respiratory distress syndrome (ARDS). In patients with ARDS, alveolar and systemic inflammatory responses can be attenuated by minimising overinflation and cyclic recruitment/derecruitment of the lung, via a reduction of tidal volume and an increase in PEEP.[1] The pressure-volume curve (P-V curve) of the respiratory system has long been used as an orientation for setting the optimal PEEP in patients with acute lung injury and ARDS.[2-4]

Generally, analysis of the P-V curve has been done by eye; a method that has been shown to be affected by inter- and intra-observer variability.[5] Further confusion has arisen due to the lack of rigorous definitions of terms such as (upper and lower) inflection point. This makes it difficult to compare the results of different studies. Since the inflection of a curve is a mathematical term that refers to the point of a function where concavity changes direction, the use of uniform, objective and reproducible parameters to describe a P-V curve has been advocated (Fig. 5.1).[6]

The objective of this study was to gain insight into the physiological implication of the P-V curve, using a mathematical model. We hypothesised that objective and reproducible parameters to describe a P-V curve could be used to define optimal airway pressure during mechanical ventilation.

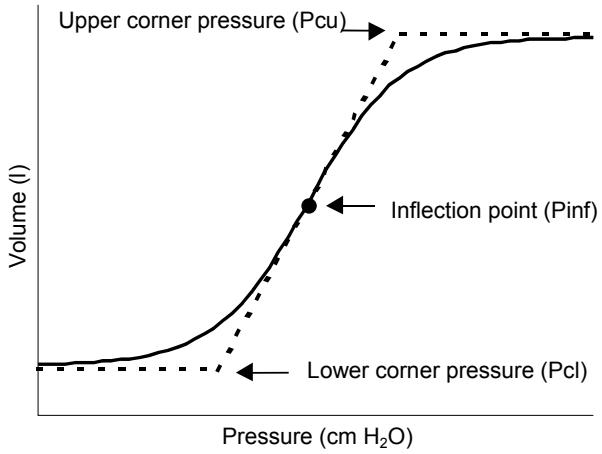

Fig. 5.1: Example of pressure-volume loop characteristics, adapted from [6].

METHODS

The model

We used the mathematical ARDS lung model as described by Hickling,[7] which we modified to include air trapping, degree of alveolar recruitability, degree of ARDS severity and chest wall characteristics. The lungs of a supine patient (15 cm ventro-dorsal diameter) were modelled as multiple lung units or 'alveoli', each with an exponential pressure-volume relation, resulting in a progressively decreasing lung compliance with increasing lung volume.[8] The model consisted of 30 compartments, representing 'horizontal slices' of lung. Each compartment consisted of 9000 lung units, which encountered a gravitational superimposed pressure (Ps) from 0 in the ventral compartment (non dependent zone) to a maximal value in the dorsal compartment (dependent zone). Each lung unit was assigned an individual threshold closing pressure (TCP), to simulate either alveolar or small airway collapse, and a threshold opening pressure (TOP), to simulate reopening. A transmural pressure (Ptm) below TCP led to the total loss of volume in the case of alveolar collapse, and led to volume maintenance (air trapping) in the case of small airway collapse. We performed simulations with alveolar closure only, as well as with 25% of airway closure and 75% of alveolar closure. Small airway volume was ignored. The mechanical characteristics of the chest wall were included in the model, by calculation of chest wall recoil pressure (Pcw) at the instantaneous total lung volume (V), assuming chest wall characteristics adopted from Grassino et al.[9] Airway pressure was computed (under no-flow conditions) as

$$Paw = Ptm + Ps + Pcw \qquad (1)$$

The extent of atelectasis (%atelectasis) and overstretching (%overstretching) was determined at each static lung condition. %Atelectasis was determined from the proportion of closed units to total recruitable units. An alveolus was assumed to be overstretched when its volume exceeded 98% of its volume at infinite pressure (achieved at a transmural pressure of 23.3 cm H_2O). The sequential steps of each simulation were: Ptm was fed into the computer model; the status (open/closed) was determined per alveolus; individual alveolar volume was computed and summed to total lung volume; Pcw and subsequently Paw were determined. Finally, the degree of atelectasis and overstretching was computed.

Table 5.1. Threshold opening (TOP) and threshold closing (TCP) pressures used in the model

ARDS grade	TOP mean (sd) (cm H_2O)	TCP mean (sd) (cm H_2O)
0	4.5 (2)	2 (2)
25	10 (2.9)	2.5 (2.4)
50	14.5 (3.8)	4.5 (2.9)
75	20 (3.8)	8 (3.4)
100	24.5 (4.8)	13 (3.8)

Simulation of ARDS severity

The degree of ARDS severity was simulated, on a linear scale from 0 (healthy lungs) to 100 (severe ARDS). Ps increased linearly with ARDS severity, ranging from 0.23 cm H_2O per cm height in healthy lungs to 0.69 cm H_2O/cm in the most severe ARDS.[10] In the simulation of healthy lungs, this led to a superimposed pressure ranging from 0 cm H_2O in the non dependent lung zones to a maximum of 3.3 cm H_2O in the most dependent lung zones. In the most severe ARDS, superimposed pressure ranged from 0 cm H_2O to a maximum of 10 cm H_2O in the most dependent regions of the lung. The TOP and TCP had a Gaussian distribution, with their mean and standard deviation depending on ARDS severity (Table 5.1). Values for TOP and TCP were adopted from Crotti et al.[11] Negative values for TOP and TCP were eliminated, and TCP could not exceed TOP in all lung units. In addition, the degree of lung volume recruitability ranged from 100% in healthy lungs to 60% in ARDS grade 100. A non-recruitable lung unit remained closed at all time. A linear vertical gradient was chosen for the distribution of non-recruitable lung units, with the largest number in the lowermost part of the lungs.

Static pressure-volume curve

Starting with all recruitable lung units open, zero end-expiratory pressure (ZEEP) was applied. Then, Paw was increased in steps of 0.5 cm H_2O to 50, and decreased to ZEEP, in steps, to determine the static pressure-volume (P-V) relation of the model lung. Functional residual capacity (FRC) was determined. The P-V curve shape was characterised by fitting the P-V curve to a predefined sigmoid equation and secondly by using this equation to extract the following characteristic points for both inflation and deflation limbs : the lower corner pressure (Pcl), where compliance increased significantly; the pressure at the

inflection point (Pinf), where the curve changes from convex to concave; and the upper corner pressure (Pcu), where compliance substantially decreased (Fig. 5.1). Percentage atelectasis and overstretching were determined at each lung condition.

Sustained inflation and tidal inflation

Safe airway pressures were determined atelectasis and overstretching were limited: starting with all recruitable lung units open, ZEEP was applied. Paw was increased to the sustained inflation pressure (Psi) when the lungs were deemed adequately recruited (%atelectasis less than 2.5%). From Psi, the minimal safe end-expiratory pressure (PEEPmin: %atelectasis less than 5%) was determined. A tidal inflation was then simulated, increasing Paw to the maximal safe plateau pressure, (Pplat,max) during tidal ventilation, defined as the Paw where overstretching was maximal 5% or where more than 50% of the atelectatic lung units at PEEPmin had been recruited. The volume increase between PEEPmin and Pplat,max was the maximal acceptable tidal volume ($V_T$max).

Prediction of safe airway pressures

The predictive value of the P-V characteristics obtained from the inflation (I) and deflation (D) limbs as potential determinants of safe airway pressures was investigated in accordance to the atelectasis and overstretching criteria. The inflation characteristics were compared to the obtained sustained inflation pressure Psi. Both inflation and deflation P-V characteristics were compared to the safe minimal (PEEPmin) and maximal (Pplat,max) pressures for tidal ventilation.

Data analysis

Data are presented as means $\pm$ standard deviation, or as median [interquartile range] when data were not normally distributed. Wilcoxon signed rank test was used to compare means, Pearson bivariate correlation test was used to assess the relation between variables. $P<0.05$ was considered to be significant. Precision and bias of P-V characteristics as estimators of several airway pressures (e.g. PEEPmin) were calculated according to Bland and Altman.[12]

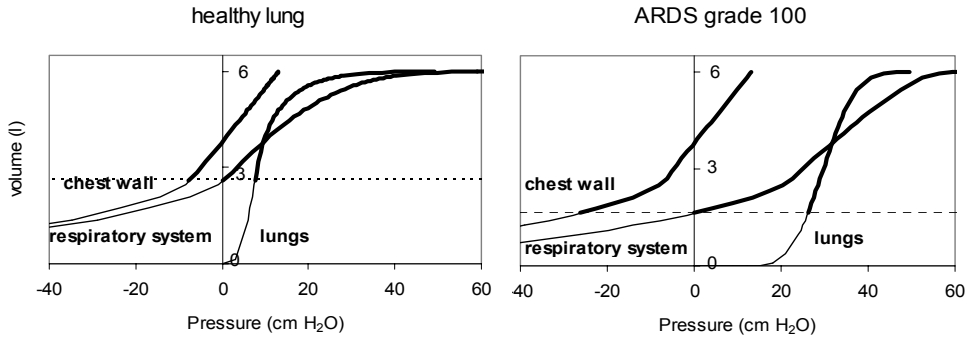

Fig. 5.2: Examples of pressure-volume relationships of the components of the simulated respiratory system for the simulated healthy lung (left panel) and severe ARDS (right panel). Dotted line indicates FRC. Thick solid line indicates volume above FRC. Pressure for the respiratory system is equivalent to airway pressure, pressure for the modelled lungs is equivalent to transpulmonary pressure and pressure for the modelled chest wall is equivalent to pleural pressure.

RESULTS

Static P-V curve

Figure 5.2 displays the pressure-volume relationship of the chest wall and lungs in the case of healthy and severely injured lungs. In severe ARDS, FRC is markedly reduced; the pulmonary P-V curve (Plungs-V) is shifted to the right, due to increased TOP and Ps. The chest wall curve (Pcw-V) had a biphasic shape: exponential at low lung volumes and linear at higher lung volumes. In the healthy lungs, Pcw-V is linear above FRC, and the non-linear shape of the total P-V curve (Paw–V) is mainly determined by the lungs component. In severe ARDS, the Paw-V curve shape has changed, firstly, by the non-linear Pcw-V relation at low airway pressures on account of the lower FRC, and secondly, by the right-shifted Plungs-V curve. Interestingly, the total P-V curve shows a lower corner point around 20 cm H_2O, whereas there is no clear inflection nor a lower corner point in the transpulmonary curve above FRC.

For all 20 simulations, a static P-V curve with an inflation and deflation limb was obtained, and the P-V characteristics calculated (examples in Fig. 5.3). FRC decreased from 2688 $\pm$ 8 ml in the healthy lungs to 1977 $\pm$ 71 ml in ARDS grade 100 (p<0.01, r=-0.98). Average values for Pcl, Pinf and Pcu for both inflation and deflation limbs are presented in Table 5.2. These characteristics were found at significantly (p<0.05) lower values on the deflation limb than on the inflation limb, showing the hysteresis of the modelled lungs. There was a

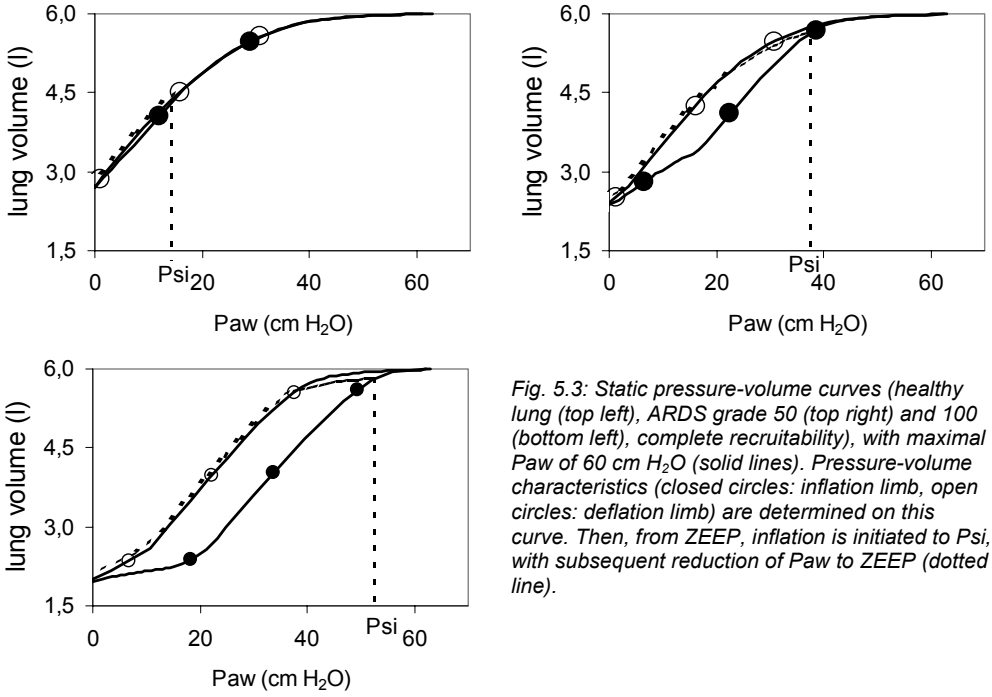

Fig. 5.3: Static pressure-volume curves (healthy lung (top left), ARDS grade 50 (top right) and 100 (bottom left), complete recruitability), with maximal Paw of 60 cm H_2O (solid lines). Pressure-volume characteristics (closed circles: inflation limb, open circles: deflation limb) are determined on this curve. Then, from ZEEP, inflation is initiated to Psi, with subsequent reduction of Paw to ZEEP (dotted line).

positive correlation with ARDS grade for most variables: Pcl,I increased from 0 in grade 0 to 17 in grade 100 (r=0.97); Pinf,I from 15 to 30 (r=0.93); Pcu,I from 29 to 43 (r=0.79); Pcl,D from 1 to 6 (r=0.84). Degree of recruitability changed some of the characteristic pressures: with decreasing recruitability, Pcu,D and Pinf,D decreased (r=0.52 and 0.84 respectively), while Pcl,I increased (r= -0.46). Airway closure did not significantly influence the P-V characteristics included in our analysis, although it influenced P-V slope. In small airway closure, FRC was significantly higher compared to alveolar closure alone (2407 $\pm$ 254 ml vs 2363 $\pm$ 273 ml, p< 0.01). Pressure-volume characteristics were also assessed for the transpulmonary pressure (Plungs) – volume curve, where Plungs = Ptm+Ps = Paw-Pcw. Pinf,I for the Plungs-V curve was not different from the Paw-V curve while Pcl,I was slightly higher (1 $\pm$ 1 cm H_2O). All other Plungs-V characteristics were at slightly lower Paw (2 $\pm$ 2 cm H_2O) (and volume) than their Paw-V counterparts (p<0.05, Table 5.2).
With decreasing recruitability, Pcl,D decreased (p < 0.05, r = 0.85).

*Table 5.2. Static P-V characteristics for the Paw-V (A) and Plungs-V curve (B) and optimal airway pressure (PEEPmin). Airway pressure, and percentage atelectasis and overstretching found at the characteristic points in the static P-V curve and at PEEPmin. Values are presented as means (SD) or median [range]. Bias: mean difference between PEEPmin and static P-V characteristic (positive value: above PEEPmin), limits of agreement: 2 * standard deviation of differences between PEEPmin and static P-V characteristic.*

A

Characteristics Paw-V curve	Paw mean (sd) in cm H_2O	%atelectasis	%overstretching	Correlation with PEEPmin, R (Pearson)	Difference withPEEPmin in cm H_2O bias (limits of agreement)
Inflation					
Upper corner point,inflation	8 (7)*	24 [10 – 75]	0 [0 – 37]	0.89	-5 (-13 to 3)
Inflection point, inflation	22 (6)*	16 [1 – 39]	4 [0 – 71]	0.98	9 (3 to 14)
Lower corner point, inflation	36 (7)*	1 [0 – 6]	64 [25 – 98]	0.96	23 (17 to 28)
Deflation					
Upper corner point,deflation	30 (4)	0 [0 – 3]	9 [0 – 57]	0.39	17 [1 to 33)
Inflection point, deflation	16 (3)*	3 [0 – 27]	0 [0 – 9]	0.71	3 (-11 to 17)
Lower corner point, deflation	3 (3)*	17 [6 – 54]	0 [0 – 1]	0.83	-10 (-23 to 3)
PEEPmin	13 (8)	5 [5 – 17]	0 [0 – 17]	--	--

B

Characteristics Plungs-V curve	Paw mean (sd) in cm H_2O	%atelectasis	%overstretching	Correlation with PEEPmin, R (Pearson)	Difference withPEEPmin in cm H_2O bias (limits of agreement)
Inflation					
Upper corner point,inflation	9 (7) *,#	24 [10 – 75]	0 [0 – 37]	0.94	-4 (-10 to 2)
Inflection point, inflation	21 (7) *	17 [1 – 40]	0 [0 – 71]	0.98	7 (4 to 13)
Lower corner point, inflation	34 (6) *,#	2 [0 – 12]	62 [0 – 98]	0.96	21 (15 to 27)
Deflation					
Upper corner point,deflation	28 (4) #	1 [0 – 41]	0 [0 – 57]	0.38	15 (-1 to 31)
Inflection point, deflation	14 (3) *,#	11 [0 – 50]	0 [0 – 9]	0.78	1 (-13 to 14)
Lower corner point, deflation	1 (3)#	32 [6 – 59]	0 [0 – 1]	0.18	-12 (-29 to 5)

**: Statistically significant correlation with PEEPmin (p<0.05, Pearson bivariate correlation). #: Difference between Paw-V curve characteristics and equivalent Plungs-V curve characteristic (P<0.05, Wilcoxon signed rank test).*

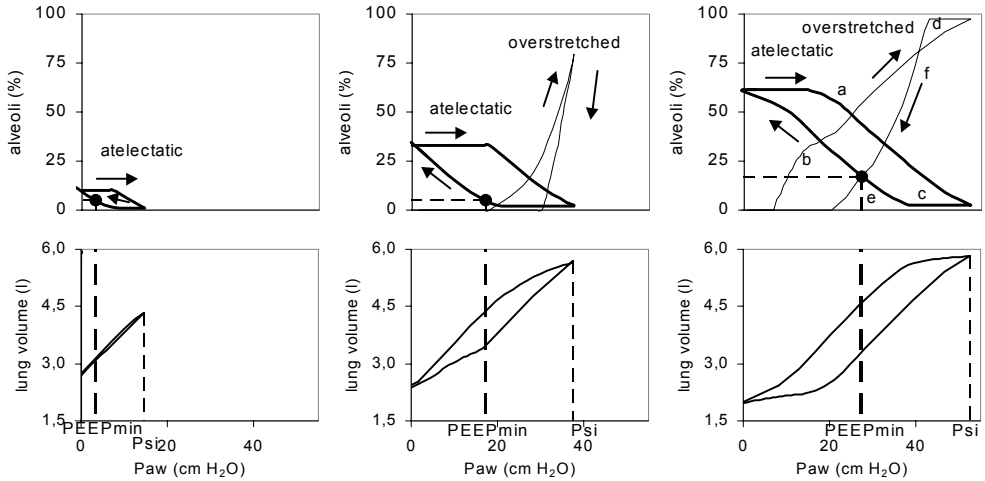

Fig. 5.4: Static pressure-volume curves (healthy lung (left), ARDS grade 50 (center) and 100 (right), complete recruitability) (lower panel) and development of atelectasis and overstretching (upper panel) during increase of airway pressure from zero to Psi, followed by a reduction of airway pressure to zero. Arrows indicate direction of pressure change. Closed circles indicate PEEPmin, where %atelectasis is 5%. In severe ARDS (right) this could not be achieved without marked overstretching; here PEEPmin was defined as the Paw where %atelectasis equalled %overstretching. With Paw increasing from zeep to Psi, lung volume initially increases as the result of volume increase in alveoli that were open at ZEEP (FRC). With further increase in Paw, increase in lung volume results of a combination of opening of collapsed alveoli and elastic volume increase in open alveoli, at the cost of developing significant overstretching. With decreasing Paw from Psi, initially overstretching is reduced, with further decreasing Paw atelectasis reoccurs. In the example of severe ARDS (right) with increasing Paw during inflation, atelectasis is reduced (A), the volume of reopened lung units abruptly increases toward overstretching (B). When Paw is then decreased, initially alveolar opening is maintained (C) with concomitant overstretching (D). With further Paw reduction some of the lung units collapse (E), while other units reduce their volume but remain open, giving rise to a steep reduction of %overstretching (F).

Sustained inflation and tidal inflation

Figure 5.4 shows the amount of atelectasis and overstretching in three simulations (upper panels), and the course of lung volume (lower panels), during a Paw increase from ZEEP up to Psi, and subsequent decrease towards ZEEP. With increasing Paw, lung volume increased and atelectasis progressively decreased. When atelectasis reached the 2.5% criterion, the amount of overstretched alveoli was already substantial (12 [2–28]%). Decrease of Paw initially reduced the amount of overstretching, and finally increased atelectasis. Both the volume and atelectasis patterns show the hysteresis of the model lung. Psi (mean Psi=31 $\pm$ 12 cm H_2O) increased with ARDS grade (p<0.01, r=0.89).

The 5% atelectasis criterion was not achieved without marked overstretching in the most severe ARDS grades. In these cases, PEEPmin was defined as the Paw where %atelectasis equalled %overstretched. This led to an average PEEPmin = 13 ± 8 cm H_2O, and a median %overstretching 0 [0-17]%. PEEPmin increased with ARDS severity (Fig. 5.5, left panel) ($p<0.01$, $r=0.85$). Pplat,max initially increased with ARDS severity and subsequently decreased (Fig. 5.5, left panel) (NS). The maximal safe tidal volume ($V_T$max) decreased with ARDS severity (Fig. 5.5, right panel) ($p<0.01$, $r=-0.85$). In ARDS grades 0 and 25, reopening of endexpiratory collapsed alveoli (maximum 2.5%) was the limiting factor for Pplat,max, whereas in higher ARDS grades, Pplat,max was determined by the threshold of overstretching (maximum 5%).

Prediction of safe airway pressures

The Paw needed to reduce %atelectasis to 2.5% (Psi) increased with ARDS severity from 13 to 44 cm H_2O. At Psi in severe ARDS 77 ± 23% of alveoli were overstretched. Pcl, Pinf or Pcu of the inflation P-V limb did not correlate well with Psi. Psi varied from 2 ± 0.2 cm H_2O below Pinf for the healthy lungs to 1 ± 2 cm above Pcu in the severest ARDS grades. %Atelectasis and %overstretching found at PEEPmin and various characteristic pressures of the P-V curve are given in Table 5.2. With exception of Pcu,D, there was a significant relation between PEEPmin and each P-V curve characteristic, although the agreement was poor evidenced by the bias and wide limits of agreement (Table 5.2).
If, on the P-V deflation limb, Paw was reduced to a level equivalent to the inflection point on the inflation limb of the Paw-V curve, this resulted in %atelectasis of 0 [0 – 8]% and %overstretching of 0 [0 – 52]%, indicating that this pressure was sufficient to prevent significant atelectasis but may not be the lowest pressure possible to obtain this goal.

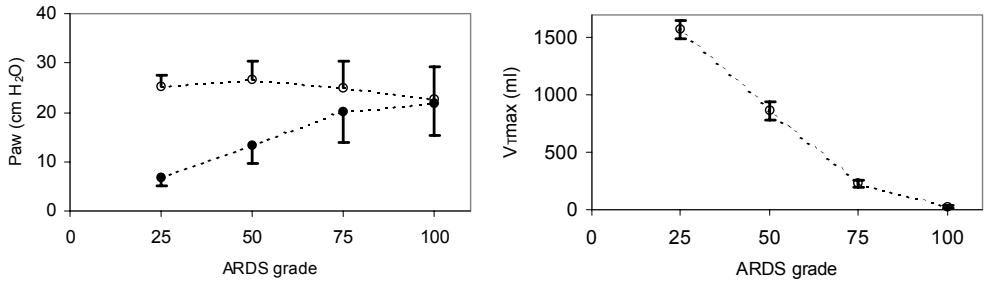

Fig. 5.5: Right panel: Calculated PEEPmin (closed circles) and Pplat,opt (open circles) plotted against simulated ARDS severity. Left panel: Calculated $V_T$max decrease with increasing simulated ARDS severity.

Paw, atelectasis and overstretching were lower at *deflation* limb Pcl, Pinf and Pcu than on equivalent *inflation* limb characteristics ($p<0.05$).
Correlation between P-V characteristics and Pplat,max was weak; maximal correlation was found for Pcu of the inflation limb of the Paw-V curve (R=0.65, bias of 13, limits of agreement between 2 and 24 cm H_2O) and Pcu of the inflation limb of the Plungs-V curve (R=0.65, bias of 11, limits of agreement between 1 and 22 cm H_2O). The difference between limits of agreement was lowest for the upper corner point of the inflation limb of the Plungs-V curve. Pcl, Pinf and Pcu neither correlated or agreed well with Pplat,max.

DISCUSSION

The main finding from this study was that analysis of the static pressure-volume curve did not yield robust predictors for either Psi, PEEPmin or Pplat,max.
The pressure needed to recruit a significant number of previously collapsed alveoli (Psi) increased with increasing severity of ARDS, the minimal PEEP needed to avoid significant atelectasis (PEEPmin) increased, while the maximal safe plateau pressure (Pplat,max) tended to decrease. As a result, the maximal safe tidal volume ($V_T$max) decreased to levels that may be insufficient for adequate ventilation using conventional mechanical ventilatory modes.

The model

The model used was previously described by Hickling.[7,13] We modified this model, in that we added variability of ARDS severity with threshold opening and closing pressures as well as vertical hydrostatic pressure gradients adapted from the literature.[10,11] In Hickling's papers, the lungs were completely collapsed at ZEEP (in fact transmural pressure) and chest wall influences were neglected. To be able to inflate the lung from ZEEP, airway pressure – rather than transmural ZEEP- and to relate volume changes to changes in airway pressures, a simulated chest wall with fixed characteristics was added to the model. Impairment of chest wall elastic properties may vary with the underlying disease responsible for ARDS.[14] Chest wall compliance may be normal in ARDS caused by pulmonary disease, but is markedly decreased in ARDS secondary to an extrapulmonary cause.[15] A decreased chest wall compliance would lead to an increase of pleural pressure and therefore airway pressure at a given transmural pressure or lung volume. As a result, Psi, PEEPmin, lower and upper corner points and inflection point would have been found at higher values. The shape of the Plungs-V curve is not influenced by changes in chest wall properties. The exact shape of the

Paw-V curve however cannot be determined without sufficient data on the low lung volume Pcw-Volume curve. Since data on low lung volume chest wall mechanics in humans is lacking, variable chest wall mechanics were not incorporated into the model.

It has been suggested that in ARDS, not only alveolar but also small airway collapse may play a role.[16] This was incorporated in our model and simulations with alveolar closure only and with 75% alveolar and 25% small airway closure were performed. These percentages could not be based on the literature and were chosen arbitrarily.

Although in early ARDS it is claimed to be possible to recruit lung volume to a point were there is little or no atelectasis and optimal gas exchange,[17] this may be impossible in ARDS that has existed for a longer period with associated ventilator induced lung injury. In the fibroproliferative phase of ARDS, deposition of elastic system fibres takes place and this may contribute to alveolar mechanical dysfunction and remodelling that occur in acute lung disease.[18] Also, when the prevalent pathology is lung tissue consolidation such as in pneumonia, application of pressure should induce only a moderate lung volume recruitment and possible alveolar overdistention. We modelled the altered alveolar function as non-recruitability, with a vertical distribution gradient towards the dependent lung zones. Simulations were performed with lungs that could either be completely recruited (as a model of early ARDS) as well as with lungs with part of their alveoli not recruitable even at infinite airway pressure as a model of damaged or partly fibrotic lungs. In our model, the extent of this simulated damage was linearly related to ARDS severity.

Current knowledge of micromechanics of the injured lung is limited. In order to construct a mathematical model, some assumptions (e.g. distribution of alveolar and small airway closure, the acceptable amounts of atelectasis, reexpansion of collapsed alveoli and overstretching) had to be made.

In vivo, both recruitment and derecruitment show some time dependence,[19] and this was not incorporated in our model. Time dependence of recruitment and derecruitment could limit the amount of recruitment occurring during a tidal inflation in ARDS. A study of pulmonary injury in pigs showed that most of the recruitment during inspiration and derecruitment during expiration occurred within 1.4 second,[20] a finding supported by others.[21] We studied the influence of pressure at static end inspiration and expiration in the static P-V manoeuvre and tidal ventilation at no flow conditions and assuming extremely long inspiration and expiration. At low frequencies, stress relaxation in the viscoelastic elements is essentially completed at end inspiration and inertive contribution to respiratory mechanics is negligible.[22,23] Resistive contribution to respiratory mechanics is most evident at low frequencies.[24] Since at no-flow the influence of resistance is eliminated, and assuming

viscoelastic time constants of approximately 1.5 second we believe that our model is realistic for mechanical ventilation at low rates (e.g. below 10 breaths.minute^{-1}) and can be used to generate hypotheses that could be tested clinically. Although methodologically superior, incorporation of frequency dependent viscoelastic properties into our model would have significantly complicated the model used. With extrapolation of our findings to higher ventilatory frequency ranges therefore, the increase of inertia and decrease of viscoelastic effects should be taken into account.

Static pressure-volume curve

As is illustrated by figure 5.2, changes of slope of the Plungs-V curve (which may be seen as the lower corner point and inflection point) were found at lung volumes at or below FRC, at negative airway pressures. Since the Paw-V curve does show a clear lower corner point around 20 cm H_2O, this means that the lower corner point of the Paw-V curve may represent a chest wall property rather than a characteristic of the lung. At low lung volumes, chest wall compliance is minimal, pleural pressures are negative and Pcw-V relationship is exponential. At higher lung volumes in the range of vital capacity, the Pcw-V relation is more linear. This results in a biphasic Pcw-V curve with a change in curvature at low lung volumes, as can be seen in figure 5.2. Our model was not exposed to negative airway pressures and only P-V curves at volumes at or above FRC were analysed. The Plungs-V curves did not display a symmetrical biphasic shape, whereas the used fit method assumed such a pattern. Quantification of the effect of this on the accuracy of the fit is beyond the scope of this study, but has been addressed by Harris et al.;[6] the calculation of Pinf is not affected, yet Pcl and Pcu may be affected and calculated values that fall outside the range of available data should be disregarded. In all calculations we performed, Pcl for the Plungs-V curve was found outside the range of available data and below FRC. This warrants care in the use of Pcl for the Plungs-V curve.

With increasing Paw from ZEEP, volume initially increased while atelectasis was more or less constant as is illustrated by figure 5.4. Initial volume increase was the result of elastic alveolar volume increase rather than volume increase due to opening of previously collapsed alveoli. In general, the lower corner point has been regarded as the opening pressure of noncompliant, dependent alveoli.[2] This is not supported by our results. The lower corner point or ‘lower inflection point’ is influenced by a number of factors, including chest wall elastic properties.[14] In our model, most alveolar recruitment occurred around the inflection point of the P-V inflation limb. In severe ARDS, significant recruitment of collapsed alveoli may take place above Pcu,I. The upper corner point is thought to be the point at

which parts of the lungs become overdistended. In our model, alveolar overstretching was present throughout the inflation limb of the P-V curve –depending on the severity of disease- and became substantial in all simulations, except the simulation of the healthy lung, between Pinf and Pcu. Alveolar volume and overstretching is related to absolute Plungs. With increasing ARDS severity Pinf and Pcu will shift to higher values and thus do not relate to the development of alveolar overstretching. The phenomenon where alveolar recruitment and lung overinflation can be observed simultaneously in different parts of the lung parenchyma after PEEP administration has been demonstrated by CT findings.[25] A decreasing rate of recruitment during inflation can create an 'upper inflection point' which is unrelated to overdistention.[7] Our results show that the inflation characteristics of the Paw-V curve are not uniquely related to alveolar recruitment and overdistention.
Following complete alveolar recruitment, decreasing Paw resulted in reduction of lung volume, initially with a decrease of alveolar overstretching while alveoli remained open. In other words, the pressure-volume relationship, but also pressure-atelectasis and pressure-overstretching display hysteresis. As a consequence, a procedure aimed at opening collapsed alveoli may facilitate subsequent reduction of Paw with avoidance of atelectasis, overstretching and high Paw.
Between the upper corner point and inflection point of the deflation limb, significant overstretching decreased, while significant atelectasis reappeared in the pressure range between Pinf and Pcl.

Sustained inflation and safe tidal volume

We defined Psi as the inflation pressure needed to obtain less than 2.5% (recruitable) atelectasis and PEEPmin as the end-expiratory pressure where at most 5% recruitable alveoli were collapsed. These criteria were chosen arbitrarily. It is believed that significant end-expiratory atelectasis plays a role in the development of ventilator induced lung injury[26,27] and there is evidence that sufficient PEEP should be applied to 'keep the lung open' and to prevent tidal recruitment.[4,17,28,29] It is not known however, which threshold of atelectasis may be considered acceptable or safe. Healthy subjects, following induction of anaesthesia, develop 5% atelectasis or more. In our simulations we arbitrarily regarded 5% end-expiratory atelectasis as the upper limit for defining PEEPmin, having previously simulated a sustained inflation to recruit all but 2.5% of recruitable alveoli. There was no benefit in increasing recruitment pressure above this point, since alveoli with high opening pressures also had high closing pressures and thus collapsed during tidal deflation, unless very high PEEP was applied.

In severe ARDS, with high closing pressures, high PEEP was needed to prevent significant alveolar collapse. When recruited, the increase in alveolar volume was immediate to a value appropriate for that transalveolar pressure, and when pressure was subsequently reduced below the threshold closing pressure, the alveolus abruptly collapsed.[8,13,30] As a result, in situations with high threshold closing pressures, an open alveolus will have a high volume; alveoli with excessive threshold closing pressures were either collapsed or overstretched. When end-expiratory collapse and tidal overstretching were to be avoided, in severe ARDS, high PEEP was needed, while the safe maximal plateau pressure seems to be related to the hyperinflation pressure that is relatively constant. In our model, with increasing severity of disease, PEEPmin increased, Pplat,max remained constant, and as a result the maximal safe tidal volume decreased (Fig. 5.5) to a level at which CO_2 removal with conventional mechanical ventilation may not be adequate. If the assumptions in our model are correct, this finding suggests that a ventilation mode with smaller tidal volumes may be of benefit, such as high-frequency oscillatory ventilation, especially in severe ARDS. Clinical trials are needed to clarify whether this hypothesis is correct.

Prediction of safe airway pressures

It has been proposed to use the pressure-volume curve as a guide for optimal ventilatory settings at bedside, with the goal of limiting lung damage related to mechanical ventilation.[2,4] Several variables can be identified. The shape of this curve is described, in ARDS, as having three main segments; a segment with minimal compliance, an intermediate segment of maximal compliance, and a final segment where compliance is reduced again.[3] We analysed the limits of each of these segments (Pcl and Pcu) and a point on the segment with maximal compliance (Pinf) on their value as a guide to adjust ventilator settings.
A pressure 2 cm H_2O above the lower corner point of the inspiratory limb has been advocated as a predictor of minimal required PEEP,[2,4] whereas others found this point to be a poor predictor of alveolar closure.[31] In our experiments, we found median PEEPmin 5 cm above Pcl, with limits of agreement between 3 cm H_2O below Pcl and 13 cm H_2O above Pcl, depending mainly on the severity of ARDS. In general, correcting for the bias (difference between actual and measured value) can enhance precision of a measurement method or indicator, but accuracy (the limits of agreement) can not be enhanced by numerical correction since it represents a non-systematic error. Intuitively, it seems that PEEPmin should be related to *maintenance* of alveolar volume and hence threshold closing pressures. We therefore expected that the deflation limb characteristics would be more related to PEEPmin than would inflation limb characteristics, as is supported in the literature.[3,13] The

good correlation between inflation characteristics and PEEP min reflects the fact that the range of TOP, Ps and TCP were related to ARDS severity. The inflation characteristics are mainly determined by TOP, and PEEPmin by TCP and Ps. Alterations of the relationship between TOP and TCP and Ps in the model would have altered the relationship between inflation characteristics and PEEPmin.

Since optimal PEEP and tidal volume, especially in severe ARDS, are compromises between atelectasis and overstretching, and pulmonary and cardiovascular function, one single value of best PEEP probably does not exist but rather is represented by a range of pressures. Our findings support the finding that neither the 'lower' nor the 'upper' inflection point' provides reliable information to determine safe ventilator settings in the acute respiratory distress syndrome. Recruitment probably continues throughout the inflation pressure-volume curve and studies of the deflation pressure-volume curve, reinflations after partial deflation, or decremental PEEP trials after a recruitment manoeuvre are needed to determine optimal open-lung positive PEEP.[32] Other than measuring lung volume, variables like cardiac output, shunt, arterial oxygenation, blood pressure or lung compliance [33] may yield superior indicators of optimal airway pressures during mechanical ventilation. Systems that can be used at the bedside and that integrate measurement of respiratory system mechanics and cardiovascular effects of ventilation may aid in the determination of optimal ventilator settings.[34,35]

In conclusion, static pressure-volume characteristics in our model proved to be moderate estimators of Psi, PEEPmin and Pplat,max. This may mainly be caused by the fact that the effects of alveolar recruitment and collapse, elastic volume changes and alveolar overstretching mutually influence the shape of the P-V curve, and the individual contribution is lost in the shape of these curves. In contrast to our findings, in clinical studies static P-V curve characteristics was considered to reflect optimal PEEP . This may be caused by the fact that these studies were performed on patients suffering from severe ARDS and hence comparable threshold opening and closing pressures. Our study demonstrated that the relation between PEEPmin and static P-V curve characteristics however is not fixed and depends mainly on severity of ARDS.

REFERENCES

1. Ranieri VM, Suter PM, Tortorella C, De Tullio R, Dayer JM, Brienza A, Bruno F, Slutsky AS. Effect of mechanical ventilation on inflammatory mediators in patients with acute respiratory distress syndrome: a randomized controlled trial. *JAMA* 1999; 282: 54 - 61.

2. Matamis D, Lemaire F, Harf A, Brun-Buisson C, Ansquer JC, Atlan G. Total respiratory pressure-volume curves in the adult respiratory distress syndrome. *Chest* 1984; 86: 58 - 66.

3. Holzapfel L, Robert D, Perrin F, Blanc PL, Palmier B, Guerin C. Static pressure-volume curves and effect of positive end-expiratory pressure on gas exchange in adult respiratory distress syndrome. *Crit Care Med* 1983; 11: 591 - 597.

4. Amato MB, Barbas CS, Medeiros DM, Schettino GP, Lorenzi FG, Kairalla RA, Deheinzelin D, Morais C, Fernandes EO, Takagaki TY, Carvalho CR. Beneficial effects of the "open lung approach" with low distending pressures in acute respiratory distress syndrome. A prospective randomized study on mechanical ventilation. *Am J Respir Crit Care Med* 1995; 152: 1835 - 1846.

5. Venegas JG, Harris RS, Simon BA. A comprehensive equation for the pulmonary pressure-volume curve. *J Appl Physiol* 1998; 84: 389 - 395.

6. Harris RS, Hess DR, Venegas JG. An objective analysis of the pressure-volume curve in the acute respiratory distress syndrome. *Am J Respir Crit Care Med* 2000; 161: 432 - 439.

7. Hickling KG. The pressure-volume curve is greatly modified by recruitment. A mathematical model of ARDS lungs. *Am J Respir Crit Care Med* 1998; 158: 194 - 202.

8. Salazar E, Knowles JH. An analysis of pressure-volume relationships in the lung. *J Appl Physiol* 1964; 19: 97 - 104.

9. Grassino AE, Roussos C, Macklem PT. Static Properties of the Chest Wall. In: The lung: scientific foundations 2nd edition. Edited by Crystal RG, West JB. Philadelphia, Lippincott-Raven Publisher, 1997, 855 – 867.

10. Pelosi P, D'Andrea L, Vitale G, Pesenti A, Gattinoni L. Vertical gradient of regional lung inflation in adult respiratory distress syndrome. *Am J Respir Crit Care Med* 1994; 149: 8 - 13.

11. Crotti S, Mascheroni D, Caironi P, Pelosi P, Ronzoni G, Mondino M, Marini JJ, Gattinoni L. Recruitment and derecruitment during acute respiratory failure: a clinical study. *Am J Respir Crit Care Med* 2001; 164: 131 - 140.

12. Bland JM, Altman DG. Statistical methods for assessing agreement between two methods of clinical measurement. *Lancet* 1986; 1: 307 - 310.

13. Hickling KG. Best compliance during a decremental, but not incremental, positive end-expiratory pressure trial is related to open-lung positive end- expiratory pressure: a mathematical model of acute respiratory distress syndrome lungs. *Am J Respir Crit Care Med* 2001; 163: 69 - 78.

14. Ranieri VM, Brienza N, Santostasi S, Puntillo F, Mascia L, Vitale N, Giuliani R, Memeo V, Bruno F, Fiore T, Brienza A, Slutsky AS. Impairment of lung and chest wall mechanics in patients with acute respiratory distress syndrome: role of abdominal distension. *Am J Respir Crit Care Med* 1997; 156: 1082 - 1091.

15. Gattinoni L, Pelosi P, Suter PM, Pedoto A, Vercesi P, Lissoni A. Acute respiratory distress syndrome caused by pulmonary and extrapulmonary disease. Different syndromes? *Am J Respir Crit Care Med* 1998; 158: 3 - 11.

16. Koutsoukou A, Armaganidis A, Stavrakaki-Kallergi C, Vassilakopoulos T, Lymberis A, Roussos C, Milic-Emili J. Expiratory flow limitation and intrinsic positive end-expiratory pressure at zero

positive end-expiratory pressure in patients with adult respiratory distress syndrome. *Am J Respir Crit Care Med* 2000; 161: 1590 - 1596.

17. Lachmann B. Open up the lung and keep the lung open. *Intensive Care Med* 1992; 18: 319 - 321.

18. Negri EM, Montes GS, Saldiva PH, Capelozzi VL. Architectural remodelling in acute and chronic interstitial lung disease: fibrosis or fibroelastosis? *Histopathology* 2000; 37: 393 - 401.

19. Bates JHT, Irvin CG. Time dependence of recruitment and derecruitment in the lung: a theoretical model. *J Appl Physiol* 2002; 93: 705 - 713.

20. Neumann P, Berglund JE, Mondejar EF, Magnussom A, Hedenstierna G. Effect of Different Pressure Levels on the Dynamics of Lung Collapse and Recruitment in Oleic-Acid-induced Lung Injury. *Am J Respir Crit Care Med* 1998; 158: 1636 - 1643.

21. Markstaller K, Eberle B, Kauczor HU, Scholz A, Bink A, Thelen M, Heinrichs W, Weiler N. Temporal dynamics of lung aeration determined by dynamic CT in a porcine model of ARDS. *Br J Anaesth* 2001; 87: 459 - 468.

22. D'Angelo E, Prandi E, Tavola M, Robatto FM. Assessment of respiratory system viscoelasticity in spontaneously breathing rabbits. *Respir Physiol* 1998; 114: 257 - 267.

23. Stamenovic D, Glass GM, Barnas GM, Fredberg JJ. Viscoplasticity of respiratory tissues. *J Appl Physiol* 1990; 69: 973 - 988.

24. Hantos Z, Daroczy B, Suki B, Galgoczy G, Csendes T. Forced oscillatory impedance of the respiratory system at low frequencies. *J Appl Physiol* 1986; 60: 123 - 132.

25. Puybasset L, Gusman P, Muller JC, Cluzel P, Coriat P, Rouby JJ. Regional distribution of gas and tissue in acute respiratory distress syndrome. III. Consequences for the effects of positive end-expiratory pressure. CT Scan ARDS Study Group. Adult Respiratory Distress Syndrome. *Intensive Care Med* 2000; 26: 1215 - 1227.

26. Sugiura M, McCulloch PR, Wren S, Dawson RH, Froese AB. Ventilator pattern influences neutrophil influx and activation in atelectasis-prone rabbit lung. *J Appl Physiol* 1994; 77: 1355 - 1365.

27. McCulloch PR, Forkert PG, Froese AB. Lung volume maintenance prevents lung injury during high frequency oscillatory ventilation in surfactant-deficient rabbits. *Am Rev Respir Dis* 1988; 137: 1185 - 1192.

28. Gattinoni L, D'Andrea L, Pelosi P, Vitale G, Pesenti A, Fumagalli R. Regional effects and mechanism of positive end-expiratory pressure in early adult respiratory distress syndrome. *JAMA* 1993; 269: 2122 - 2127.

29. Gattinoni L, Pelosi P, Crotti S, Valenza F. Effects of positive end-expiratory pressure on regional distribution of tidal volume and recruitment in adult respiratory distress syndrome. *Am J Respir Crit Care Med* 1995; 151: 1807 - 1814.

30. Staub N, Nagano H, Pearce M.L. Pulmonary edema in dogs, especially the sequence of fluid accumulation in lungs. *J Appl Physiol* 1967; 22: 227 - 240.

31. Maggiore SM, Jonson B, Richard JC, Jaber S, Lemaire F, Brochard L. Alveolar Derecruitment at Decremental Positive End-Expiratory Pressure Levels in Acute Lung Injury. Comparison with the lower inflection point, oxygenation, and compliance. *Am J Respir Crit Care Med* 2001; 164: 795 - 801.

32. Hickling KG. Reinterpreting the pressure-volume curve in patients with acute respiratory distress syndrome. *Curr Opin Crit Care* 2002; 8: 32 - 38.

33. Ward NS, Lin DY, Nelson DL, Houtchens J, Schwartz WA, Klinger JR, Hill NS, Levy MM. Successful determination of lower inflection point and maximal compliance in a population of patients with acute respiratory distress syndrome. *Crit Care Med* 2002; 30: 963 - 968.

34. Karason S, Sondergaard S, Lundin S, Stenqvist O. Continuous on-line measurements of respiratory system, lung and chest wall mechanics during mechanic ventilation. *Intensive Care Med* 2001; 27: 1328 - 1339.

35. Markhorst DG, Genderingen HR, Leenhoven T, van Vught AJ. A system for integrated measurement of ventilator settings, lung volume change and blood gases during high-frequency oscillatory ventilation. *J Med Eng Technol* 2003; 27: 128 – 132.

Chapter 6

Breath to breath analysis of abdominal and rib cage motion in surfactant depleted piglets during high frequency oscillatory ventilation

DG Markhorst, JRC Jansen, AJ van Vught, HR van Genderingen

Intensive Care Medicine, in press

SUMMARY

Objective: To evaluate abdominal and rib cage breath-to-breath displacement during a stepwise decrease of mean airway pressure (mean Paw) following a lung volume recruitment procedure in surfactant-depleted piglets during high-frequency oscillatory ventilation (HFOV).

Design and setting: Prospective, observational study in a university research laboratory.

Animals: Eight piglets weighing 12.0 ± 0.5 kg, surfactant depleted by lung lavage.

Interventions: In each piglet, a quasi-static pressure volume loop was constructed and compliance of the respiratory system calculated. After initiation of HFOV, lung volume was recruited by slowly increasing Paw to 40 cm H_2O. Then, mean Paw was decreased in steps until PaO_2/FiO_2 was below 100 mm Hg. Proximal pressure amplitude remained constant.

Measurements and main results: At each setting, arterial blood gases were obtained and physiological shunt fraction calculated. Abdominal ($V_{T,A}$) and rib cage ($V_{T,R}$) tidal displacement was determined using respiratory inductive plethysmography (RIP). During HFOV, there was maximum in tidal volume (V_T, determined by calibrated RIP) in seven of eight piglets. At maximal mean Paw, $V_{T,A}$ and $V_{T,R}$ were in phase. Phase difference between $V_{T,A}$ and $V_{T,R}$ increased to a maximum of 178 $\pm$ 28 degrees at minimum mean Paw. $V_{T,A}$ remained relatively small (0.71 $\pm$ 0.17 ml/kg). $V_{T,R}$ increased from 1.6 $\pm$ 0.4 ml/kg to 3.3 $\pm$ 1.1 ml/kg. A minimum in $V_{T,A}$ and a maximum of V_T was found near the optimal mean Paw, defined as the lowest mean Paw where shunt fraction is below 0.1.

Conclusions: During HFOV, rib cage and abdominal motion displayed a significant airway pressure dependent asynchrony. Maximal V_T and minimal $V_{T,A}$ coincided with optimal respiratory system compliance, oxygenation and ventilation, suggesting a potential clinical relevance of monitoring V_T and abdominal displacement during HFOV.

INTRODUCTION

Lung injury may be augmented by mechanical ventilation of patients with acute respiratory distress syndrome when large tidal volumes are used (volutrauma) or at low end-expiratory lung volume (atelectrauma).[1-6] High-frequency oscillatory ventilation (HFOV) is a ventilatory mode in which a small tidal volume (1-2 ml/kg) is administered at a high frequency (5-15 Hz, 300-900 breaths/min). The mean airway pressure, referred to as continuous distending pressure (CDP) mainly determines lung volume and oxygenation. Ventilation is provided by the oscillations. The level of CDP applied is a major determinant of patient outcome.[7,8] Today there is no clinical monitoring tool to determine the optimal level of applied CDP, other than via indirect parameters, i.e. blood oxygenation and arterial blood pressure. Previously, we have described the use of the oxygenation index, physiologic shunt fraction, electrical impedance tomography and tracheal pressure amplitude measurements as estimators of optimal CDP during HFOV.[9-12] Electrical impedance tomography is not yet available as a clinical tool. Measurement of tracheal pressure requires introduction of a pressure transducer into the endotracheal tube and pressure measurement in the trachea is sensitive to mucus and fluid accumulation on the sensor. Calculation of the oxygenation index is clinically available, but the results may not be available instantaneous at the bedside. In search of an easy applicable method that may give instantaneous measurements at the bedside we assessed the use of respiratory inductive plethysmography (RIP) during HFOV.

Respiratory system compliance (C_{rs}), the ratio of tidal volume and pressure amplitude, was proposed as an indicator to adjust conventional mechanical ventilation (CMV) at safe airway pressures.[13-,15] Maximal C_{rs} coincides with the occurrence of minimal atelectasis and minimal overdistention. During HFOV there is no clinically acceptable method to determine the tidal volume. Tidal volume displacement of the lung leads to displacement of two compartments; the rib cage and abdomen. RIP is a non-invasive technique to measure lung volume changes. RIP is based on the principle that the chest wall has two compartments, the rib cage and abdomen. Each compartment is associated with a single motion variable that can be measured with external sensors (RIP), and the sum of both variables can be calibrated against a known volume change to provide volumetric measurements.[16] This method has been used to estimate mean lung volume changes during HFOV.[17,18] We hypothesised that monitoring of rib cage and abdominal displacement may also be used for breath-to-breath analysis during HFOV and that maximal tidal motion of the respiratory system components would reflect maximal respiratory system compliance when a constant

pressure amplitude is administered to the airway opening. If this is valid the monitoring of rib cage and abdominal motion using RIP during HFOV may aid in adjusting ventilator settings during HFOV.

MATERIAL AND METHODS

Animal preparation

All animal experiments were performed according to the Guide for the Care and Use of Laboratory Animals, published by the National Institutes of Health (NIH publication 85-23, revised 1985) and approved by the Animal Care Committee of Erasmus University Rotterdam, The Netherlands.

Eight Yorkshire piglets (12.0 $\pm$ 0.5 kg body weight) were anaesthetised with a sodium pentobarbital (30 $mg.kg^{-1}$) bolus followed by a continuous infusion (8.5 $mg.kg^{-1}.h^{-1}$). The piglets were ventilated through a tracheal cannula in a volume controlled mode using a ventilator allowing for lung volume estimation by the open helium washin method.[19] Frequency was 10 breaths per minute, F_{IO2} 1 and PEEP 5 cm H_2O. I:E ratio was 1:1, with an inspiratory pause of 0.6 s. V_T was adjusted to achieve normocarbia (P_aCO_2 38-45 mm Hg). An arterial line was inserted in the aorta for measuring aortic blood pressure (P_{ao}). A four-lumen catheter was inserted into the superior vena cava to measure central venous pressure (P_{cv}) and to infuse fluids (5 $ml.kg^{-1}.h^{-1}$ saline) and anaesthetics. All pressure catheters were flushed (3 $ml.h^{-1}$) with normal saline containing 10 I.U. ml^{-1} heparin. The bladder was catheterised to retain urinary output. After the surgical procedures pancuronium bromide (0.3 $mg.kg^{-1}.h^{-1}$) was given to suppress spontaneous breathing. Repeated lung lavages were applied with 35 $ml.kg^{-1}$ saline until P_aO_2 was below 80 mm Hg.[20] PEEP was set at 2 cm H_2O.

Respiratory inductive plethysmograph

Respiratory inductance plethysmography was applied to assess rib cage and abdominal motion. Before lung lavage, a thoracic gauge was placed 4 cm above the xiphoid processus, an abdominal gauge 4 cm above the umbilicus. Both gauges were then secured by stitches and the position of the gauges was checked at the end of experiments. The distension of the abdominal (RIPabd) and ribcage (RIPrc) gauges, and airway pressure were sampled at 200 Hz and stored for offline analysis. RIP was calibrated to lung volume using the Qualitative Diagnostic Calibration (QDC) method. V_T was estimated by means of calibrated RIP.

Measurements and lavage procedure

Baseline measurements were performed during conventional ventilation (CMV) after lavage (*postlavage measurements*). Arterial blood gas samples were analysed with ABL3 and OSM2 hemoximeters (Radiometer, Copenhagen, Denmark). Respiratory system compliance was derived according to $C_{rs} = V_T/(P_{plat} – PEEP)$ with P_{plat} the plateau pressure. In addition, the functional residual capacity (FRC) of the lungs was estimated using an open helium washin method. A pressure-volume manoeuvre was performed to construct a quasi-static PV curve of the respiratory system. Following exposure to ambient pressure, the lungs were manually inflated in steps of about 3.5 $ml.kg^{-1}$ air with 3-4 s. pauses up to an airway pressure of 40 cm H_2O, followed by deflation in similar steps. Airway pressure was measured at the airway opening (Viggo-Spectramed DT-NN, Oxnard, CA). After insertion of an endotracheal tube, HFOV (SensorMedics 3100A, Yorba Linda, CA, USA) was initiated with a frequency of 8 Hz, an inspiratory time of 33% and bias flow of 20 L/min. These settings were kept constant during the experiment. Initial CDP was set 3 cm H_2O higher than the mean airway pressure during CMV. Proximal pressure amplitude was set at 54 $\pm$ 6 cm H_2O, and kept constant during the experiment.
After the experiment the tube was removed and CMV was resumed at the initial settings. After a 30 minutes stabilisation period the postlavage measurements were repeated (*end experiment measurements*) to check stability of the model.

Experimental procedure

CDP was increased in 3 cm H_2O steps to 40 cm H_2O to obtain total lung recruitment. CDP at P_aO_2 of 450 mm Hg was defined as CDP_{open}. Next, CDP was lowered to CDP_{open} and then lowered in 3 cm H_2O steps until P_{aO2} was below 100 mm Hg. At each CDP, RIPabd and RIPrc, blood gases, and blood pressures were measured after a 10 minute stabilisation period.

Data analysis

To mathematically describe the *deflation* quasi-static PV curves, the individual curves were fitted to a sigmoid equation as described by Venegas and Harris.[21,22] Mean curves were determined by averaging the fit parameters. Amplitudes were determined from the rib cage, abdominal and total RIP signal, calibrated with QDC. The phase difference between the proximal airway pressure, rib cage and abdominal signal were determined, by application of the maximal linear correlation method to the first harmonic of the signals.[23] Data are

Table 6.1: Physiological variables during conventional mechanical ventilation. Values at end experiment were tested against postlavage. Data are represented as mean (SD).

	Prelavage	*Postlavage*	*End experiment*
P_{aO2}/F_{IO2} (mm Hg)	490 (48)	60 (11)	96 (61)
Q'_S/Q'_T	0.01 (0.02)	0.46 (0.08)	0.39 (0.14)
P_{aCO2} (mm Hg)	42 (2)	52 (5)	60 (8) *
C_{rs} (ml.cm H_2O^{-1}.kg^{-1})	1.20 (0.16)	0.54 (0.06)	0.55 (0.07)
Q'_T (ml.s^{-1}.kg^{-1})	1.9 (0.3)	1.9 (0.4)	1.9 (0.5)
P_{ao} (mm Hg)	90 (9)	85 (12)	83 (18)
P_{pa} (mm Hg)	16 (2)	26 (5)	32 (6) *
P_{cv} (mm Hg)	4.3 (0.9)	4.2 (1.2)	3.7 (1.1)
heart rate (min^{-1})	171 (18)	119 (16)	154 (40) *

**: p<0.05.*

presented as means ± SD. Data with normal distribution were compared using Student's t-test. The CDP values were compared using the Wilcoxon signed rank test. $P < 0.05$ was accepted as statistically significant.

RESULTS

Lung lavage produced a large increase of Q'_S/Q'_T, and a decrease of C_{rs}. Comparison of the baseline measurements postlavage and end experiment revealed statistically significant increases in P_aCO_2, P_{pa} and heart rate (Table 6.1).

During the recruitment phase of HFOV, CDP_{open} was 29 ± 3 cm H_2O. CDP was decreased from 40 cm H_2O to CDP_{open} and then decreased in steps to 9 ± 1cm H_2O. In the first experiment oxygenation deteriorated rapidly when CDP was lowered from 10 to 7 cm H_2O; only part of the measurements could be completed before we increased CDP. In the following seven experiments we performed smaller CDP decrements (1-2 cm H_2O) at the end of the *deflation* phase.

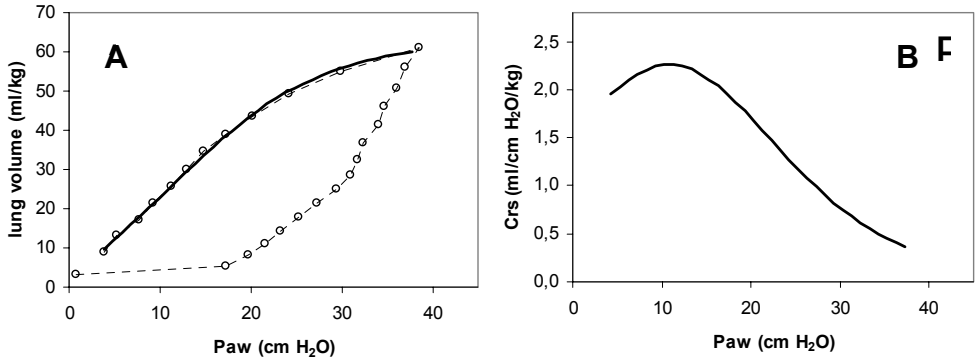

Fig. 6.1: Results in one subject. Quasi-static pressure volume curve of the respiratory system (A). Solid line represents fitted curve data as described by Venegas and Harris. Compliance curve (B) was constructed from the pressure volume curve.

Inflation phase: P_aO_2 increased substantially from 55 ± 12 to 525 ± 37 mm Hg. Q'_S/Q'_T decreased from 0.53 ± 0.10 at initial CDP of 17 ± 2 cm H_2O to 0.06 ± 0.03 at maximal CDP of 40 cm H_2O. Deflation phase: Oxygenation did not change significantly until CDP = 13 ± 4 mm Hg and then decreased to 90 ± 131 mm Hg. Q'_S/Q'_T increased 0.06 ± 0.03 to 0.61 ± 0.20. P_aCO_2 decreased from 82 ± 11 to 43 ± 5 mm Hg at CDP = 18 ± 2 cm H_2O, remained constant until CDP = 13 ± 4 mm Hg and in six animals increased again.

PV curve and RIP

An excellent fit was found between the sigmoid model and the PV curve (r^2 from 0.9987 to 0.9994) (example in Fig. 6.1A). C_{rs} was computed from the fitted PV curve (Fig. 6.1B). From the averaged fit parameters, a PV curve was constructed (Fig. 6.2A), and C_{rs} calculated from this curve (Fig. 6.2B). Maximal C_{rs} was 1.5 ± 0.4 ml/cm H_2O/kg and was found at 12.5 ± 1.9 cm H_2O. Typical patterns of the RIP signals at maximal and minimal CDP are shown in Fig. 6.3. The relative amplitude and phase of the rib cage and abdominal signal depend largely on the imposed CDP. The total RIP signal is CDP dependent as a consequence of the phase difference of the individual signals.
Rib cage motion was significantly larger than abdominal motion (Fig. 6.2 C and D). In addition, rib cage amplitude increased twofold with decreasing CDP. Abdominal amplitude was characterised by a nadir (0.35 ± 0.18 ml/kg) at a CDP of 13.8 ± 2.1 cm H_2O, and was significantly different from the initial value (0.71 ± 0.17 ml/kg).

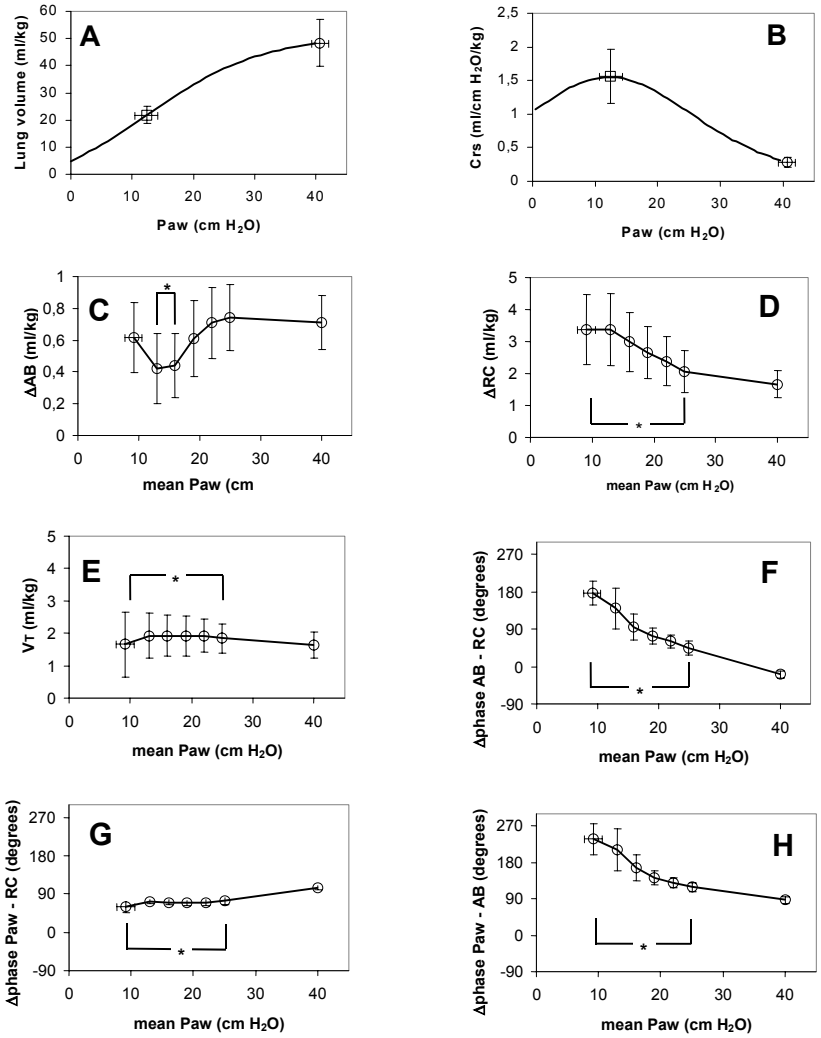

*Figure 6.2: Averaged quasi-static respiratory system pressure volume curve (A), following lung volume recruitment. The sigmoid curve was constructed by using the average curve fitting parameters for of the eight piglets for the deflation limb, according to the equation $V = a+b/(1+e^{-(P-c)/d})$ with V=volume, P=airway pressure and a, b,c and d the parameters obtained from the fitting procedure.[36] Symbols represent pressure and volume at pressure of maximal compliance (square) and at maximal airway pressure reached (circle) for individual PV curves. Average respiratory system compliance (C_{rs}; B) was calculated from the averaged quasi-static PV curve. Symbols represent pressure and compliance of each subject at maximal compliance (square) and maximal airway pressure reached (circle). Respiratory inductive plethysmograph estimated displacement of abdomen (ΔAB; C) and rib cage (ΔRC; D) and respiratory system displacements (V_T; E). Phase difference (Δphase); between abdominal (AB) and rib cage (RC) movement (F), between proximal airway pressure (Paw) and rib cage (G) and abdominal (H) movement. *: Significant difference with value at maximal CDP ($p < 0.05$).*

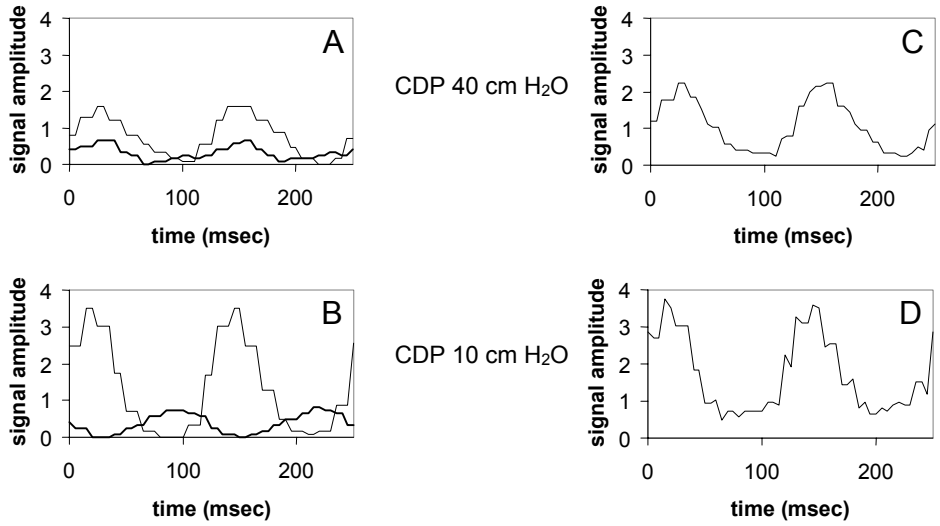

Figure 6.3: Signal amplitudes of Respiratory inductive plethysmograph (RIP) rib cage (thin line) and RIP abdominal (thick line) gauges at continuous distending pressure 40 (A) and 10 (B) cm H_2O in one subject. Summed RIP signal at CDP 40 (C) and 10 (D) cm H_2O. Note the reduction in amplitude of the summed signal resulting from the phase difference between rib cage and abdominal displacement. Signals are aligned to t=0 msec at maximal airway pressure.

Table 6.2: Tidal volume at start and end of deflation and at maximal VT in eight piglets.

	VT at max CDP (ml/kg)	max VT (ml/kg)	CDP at max Vt (cm H_2O)	VT end deflation (ml/kg)	CDP end deflation (cm H_2O)
piglet 1	2,1	3,0	10	3,0	10
piglet 2	1,0	1,3	22	0,6	9
piglet 3	1,6	2,4	25	1,4	8
piglet 4	1,5	1,7	13	1,4	7
piglet 5	1,9	2,3	13	2,2	9
piglet 6	1,8	2,6	13	2,6	9
piglet 7	1,1	1,2	25	0,4	12
piglet 8	2,0	2,2	22	2,1	9

In one of eight piglets, after initial increase of V_T with decreasing CDP no subsequent reduction in V_T was observed with further decreases of CDP. In the remaining seven piglets a clear maximum V_T was found (Table 6.2). In these seven piglets V_T increased significantly from 1.6 $\pm$ 0.4 ml/kg at a CDP of 40 cm H_2O to 2.0 $\pm$ 0.6 ml/kg ($p < 0.05$) at CDP 19 $\pm$ 6 cm H_2O. With further reduction of CDP to its final value of 9 $\pm$ 1 cm H_2O, V_T significantly decreased again to 1.5 $\pm$ 0.8 ml/kg ($p < 0.05$). Maximal C_{rs}, obtained during a PV manoeuvre, of 1.46 $\pm$ 0.30 ml/kg was found at an airway pressure of 12 $\pm$ 3 cm H_2O, which is lower than the CDP coinciding with maximal V_T ($P < 0.05$).
At CDP of 40 cm H_2O rib cage and abdominal motion were in phase, and became increasingly out-of-phase to about 180 degrees with decreasing CDP. This phase shift was mostly attributed to the abdominal pattern, depicted in the phase lag between Paw and both RIP signals (Fig. 6.2F, G and H).
To assess optimal ventilatory conditions, we determined best CDP, where oxygenation was still adequate and CDP was as low as possible to avoid adverse circulatory effects. This criterion was previously defined as the lowest CDP where physiologic shunt fraction was just below 0.1. With this criterion, best CDP was 14 $\pm$ 2 cm H_2O (Table 6.3). Abdominal amplitude nadir was the best estimator of best CDP. $PaCO_2$ was minimal around this CDP (Table 6.3). CDP at maximal V_T tended to be higher than best CDP and CDP at maximal C_{rs} tended to be lower than best CDP, but the differences did not reach statistical significance.

DISCUSSION

The main results of this study are that CDP at maximal V_T is a good estimator of best CDP, optimal ventilatory conditions coincide with a *minimum* in abdominal motion, maximal V_T during HFOV does not reflect respiratory system compliance as determined from a PV manoeuvre and relative amplitude and phase of the rib cage and abdominal motion are strongly dependent on imposed mean airway pressure.
We imposed constant proximal airway pressure amplitudes and therefore changes in abdominal and rib cage motion reflect changes in respiratory system impedance. Peslin et al. have suggested that the human abdomen and rib cage can be modelled as two parallel pathways, with elastic, viscous and inertive characteristics.[24] The rib cage is a low compliance, low inertance, underdamped system with a high resonant frequency, whereas the abdomen is a high compliance, high inertance, overdamped system with a low resonant frequency.[25]

Table 6.3: Physiologic variables during decremental CDP steps, at maximal CDP, CDP where tidal volume was maximal, abdominal tidal displacement was minimal and best CDP where $Q'_S/Q'_T < 0.1$ and at end deflation. Additionally values at CDP equivalent to airway pressure at maximal respiratory system compliance obtained during a PV manoeuvre are included. Data are presented as means (SD). CDP continuous distending pressure, V_T tidal volume, C_{rs} respiratory system compliance, Q'_S/Q'_T physiologic shunt fraction, PaO_2 partial arterial oxygen pressure, $PaCO_2$ partial arterial pressure of carbon dioxide.

	at maximal CDP	At maximal V_T	At minimal abdominal tidal displacement	At best CDP	At maximal Crs	at minimal CDP
Airway pressure (cm H_2O)	41 (1)*	18 (6)	14 (2)	14 (2)	12 (3)	9 (1)*
Abdominal amplitude (ml/kg)	0.71 (0.17)*	0.60 (0.34) *	0.35 (0.18)	0.42 (0.18)	0.54 (0.24)	0.62 (0.21)
Q'_S/Q'_T	0.06 (0.03)	0.08 (0.03)	0.10 (0.09)	0.07 (0.02)	0.20 (0.23)*	0.55 (0.3)*
PaO_2 (mm Hg)	525 (37)	501 (61)	472 (143)	509 (40)	354 (201)*	91 (132)*
$PaCO_2$ (mm Hg)	82 (11) *	50 (8)	43 (6)	43 (5)	46 (3)	50 (6)*

*Values displayed are means (SD. * differences statistically significant (P<0.05) in comparison to values at best CDP.*

With decreasing CDP, pulmonary compliance initially increases and impedance decreases as a result of release of alveolar overdistention. As a result, the summed displacement of abdominal and rib cage would increase. We assume that rib cage compliance also increases leading to a decrease in rib cage impedance. Abdominal impedance, dominated by its inertance, remains relatively constant. This accounts for the more pronounced changes in rib cage displacement and relatively stable abdominal displacement. At optimal rib cage compliance, its resonance frequency may approach ventilator frequency applied, giving rise to an additional redistribution of chest wall displacement from the abdomen towards the ribcage. This would account for the observed decrease in abdominal displacement. Our results did however not show coinciding increases in rib cage displacement. RIP assumes that ventilation is confined to two compartments, a rib cage and abdominal, that can be assessed by two gauges measuring their lateral displacement. However, the compartments may also exhibit a cranial displacement,[26] indicating a third degree of freedom that is not measured using RIP. With increasing mean lung volume, outward rib displacement may decrease significantly in favour of cranial displacement, which would lead to an underestimation of rib cage displacement at higher lung volumes using RIP. This in part may account for the fact that the decrease in abdominal displacement is not reflected in a significant increase in RIP estimated rib cage displacement. Furthermore, the changes in abdominal displacement were relatively small in comparison to the absolute rib cage displacements. The observed decrease and subsequent increase of abdominal displacement may thus reflect maximal chest wall compliance**.**

The pressure-volume curve (PV curve) of the respiratory system has been described as an orientation for setting optimal PEEP in patients with acute lung injury and ARDS.[27-29] We hypothesised that maximal V_T would coincide with maximal respiratory system compliance. On the basis of the results, we had to reject the hypothesis, since the airway pressures at which both variables are maximal differ significantly. The airway pressure at which respiratory system compliance was maximal was not statistically different from best CDP, but Q'_S/Q'_T at this pressure had risen significantly to unacceptable high values, precluding its use as a clinical estimator of best CDP.
We used the pressure volume relationship, obtained during a quasi-static PV manoeuvre as an estimate for the PV relation during HFOV. It has been suggested that best PEEP can be determined from maximal compliance of the PV curve. Recently, it was shown that steady-state end-expiratory lung volume is not well predicted by the quasi-static P–V curve.[30] The

consequence is that respiratory system compliance may differ between the quasi-steady state and HFOV condition.

Recently V_T measurement using a hot-wire flowmeter was validated for use during HFOV. [31-33] At the time these experiments were conducted, this was not available in our laboratory. This technique may be used in future research to measure V_T changes during HFOV. In contrast to RIP however, it does not measure mean lung volume changes and the relative contribution of abdominal and rib cage displacement to respiratory system displacement.

Our study was limited to surfactant depleted paralysed animals. The value of decreasing abdominal displacement as an estimator of optimal airway pressure is influenced by the relative contribution of lung, rib cage, and abdominal and diaphragmatic impedance. These contributions may differ between species as a result of different anatomy. Furthermore, increased chest wall impedance itself may be the cause of respiratory insufficiency.[34,35] Further research is needed to assess the biomedical and clinical value of monitoring abdominal tidal displacement.

In summary, we demonstrated in seven of eight surfactant depleted piglets the presence of a maximum tidal chest wall displacement during HFOV with decremental airway pressure. This maximum coincided fairly well with the optimal airway pressure. In addition we have shown that, in surfactant depleted piglets, abdominal tidal motion decreases in the pressure range where respiratory system compliance, oxygenation and ventilation are optimal. We therefore consider monitoring of tidal volume and abdominal tidal displacement during HFOV, as potential clinically applicable methods, that may be used bedside, but further research is needed to clarify the biomedical and clinical relevance.

REFERENCES

1. Parker JC, Hernandez LA, Peevy KJ. Mechanisms of ventilator-induced lung injury. *Crit Care Med* 1993; 21: 131 - 143.
2. Dreyfuss D, Soler P, Basset G, Saumon G. High inflation pressure pulmonary edema. Respective effects of high airway pressure, high tidal volume, and positive end-expiratory pressure. *Am Rev Respir Dis* 1988; 137: 1159 - 1164.
3. Dreyfuss D, Saumon G. Barotrauma is volutrauma, but which volume is the one responsible? *Intensive Care Med* 1992; 18: 139 - 141.
4. Dreyfuss D, Saumon G. From ventilator-induced lung injury to multiple organ dysfunction? *Intensive Care Med* 1998; 24: 102 - 104.
5. Ricard JD, Dreyfuss D, Saumon G. Ventilator-induced lung injury. Eur Respir J Suppl 2003; 42: 2s - 9s.
6. Slutsky AS. Lung injury caused by mechanical ventilation. *Chest* 1999; 116: 9S - 15S.
7. Gerstmann DR, Minton SD, Stoddard RA, Meredith KS, Monaco F, Bertrand JM, Battisti O, Langhendries JP, Francois A, Clark RH. The Provo multicenter early high-frequency oscillatory ventilation trial: improved pulmonary and clinical outcome in respiratory distress syndrome. *Pediatrics* 1996; 98: 1044 - 1057.
8. Bryan AC, Froese AB. Reflections on the HIFI trial. Pediatrics 1991; 87: 565 - 567.
9. van Genderingen HR, Versprille A, Leenhoven T, Markhorst DG, van Vught AJ, Heethaar RM. Reduction of oscillatory pressure along the endotracheal tube is indicative for maximal respiratory compliance during high-frequency oscillatory ventilation: a mathematical model study. *Pediatr Pulmonol* 2001; 31: 458 - 463.
10. van Genderingen HR, van Vught JA, Jansen JR, Duval EL, Markhorst DG, Versprille A. Oxygenation index, an indicator of optimal distending pressure during high-frequency oscillatory ventilation? Intensive Care Med 2002; 28: 1151 - 1156.
11. van Genderingen HR, van Vught AJ, Duval EL, Markhorst DG, Jansen JR. Attenuation of pressure swings along the endotracheal tube is indicative of optimal distending pressure during high-frequency oscillatory ventilation in a model of acute lung injury. Pediatr Pulmonol 2002; 33: 429 - 436.
12. van Genderingen HR, van Vught AJ, Jansen JR. Regional lung volume during high-frequency oscillatory ventilation by electrical impedance tomography. Crit Care Med 2004; 32: 787 - 794.
13. Suter PM, Fairley B, Isenberg MD. Optimum end-expiratory airway pressure in patients with acute pulmonary failure. *N Engl J Med* 1975; 292: 284 - 289.
14. Hickling KG. The pressure-volume curve is greatly modified by recruitment. A mathematical model of ARDS lungs. *Am J Respir Crit Care Med* 1998; 158: 194 - 202.
15. Hickling KG. Best compliance during a decremental, but not incremental, positive end-expiratory pressure trial is related to open-lung positive end-expiratory pressure: a mathematical model of acute respiratory distress syndrome lungs. *Am J Respir Crit Care Med* 2001; 163: 69 - 78.
16. Sackner MA, Watson H., Belsito A.S., Feinerman D, Suarez M, Gonzalez G, Bizousky F, Krieger B. Calibration of respiratory inductive plethysmograph during natural breathing**.** *J Appl Physiol* 1989; 66: 410 - 420.
17. Gothberg S, Parker TA, Griebel J, Abman SH, Kinsella JP. Lung volume recruitment in lambs during high-frequency oscillatory ventilation using respiratory inductive plethysmography. *Pediatr Res* 2001; 49: 38 - 44.

18. Brazelton III TB, Watson KF, Murphy M, Al Khadra E, Thompson JE, Arnold JH. Identification of optimal lung volume during high-frequency oscillatory ventilation using respiratory inductive plethysmography. *Crit Care Med* 2001; 29: 2349 - 2359.

19. Jansen JR, Hoorn E, Van Goudoever J, Versprille A. A computerized respiratory system including test functions of lung and circulation. *J Appl Physiol* 1989; 67: 1687 - 1691.

20. Grotjohan, H. P. and van der Heijde, R. M. J. L. Experimental models of the respiratory distress syndrome. Lavage and oleic acid. PhD thesis, Erasmus University Rotterdam, The Netherlands 1992, pp 87 - 112.

21. Harris RS, Hess DR, Venegas JG. An objective analysis of the pressure-volume curve in the acute respiratory distress syndrome. *Am J Respir Crit Care Med* 2000; 161: 432 - 439.

22. Venegas JG, Harris RS, Simon BA. A comprehensive equation for the pulmonary pressure-volume curve. *J Appl Physiol* 1998; 84: 389 - 395.

23. Prisk GK, Hammer J, Newth CJ. Techniques for measurement of thoracoabdominal asynchrony. *Pediatr Pulmono*l 2002; 34: 462 - 472.

24. Peslin R, Duvivier C, Gallina C. Total respiratory input and transfer impedances in humans. *J Appl Physiol* 1985; 59: 492 - 501.

25. Boynton BR, Fredberg JJ, Buckley BG, Frantz ID, III. Rib cage versus abdominal displacement in rabbits during forced oscillations to 30 Hz. *J Appl Physiol* 1987; 63: 309 - 314.

26. De Troyer A, Leduc D. Effects of inflation on the coupling between the ribs and the lung in dogs. *J Physiol* 2004; 555: 481 - 488.

27. Matamis D, Lemaire F, Harf A, Brun-Buisson C, Ansquer JC, Atlan G. Total respiratory pressure-volume curves in the adult respiratory distress syndrome. *Chest* 1984; 86: 58 - 66.

28. Holzapfel L, Robert D, Perrin F, Blanc PL, Palmier B, Guerin C. Static pressure-volume curves and effect of positive end-expiratory pressure on gas exchange in adult respiratory distress syndrome. *Crit Care Med* 1983; 11: 591 - 597.

29. Amato MB, Barbas CS, Medeiros DM, Schettino GP, Lorenzi FG, Kairalla RA, Deheinzelin D, Morais C, Fernandes EO, Takagaki TY,. Beneficial effects of the "open lung approach" with low distending pressures in acute respiratory distress syndrome. A prospective randomized study on mechanical ventilation. *Am J Respir Crit Care Med* 1995; 152: 1835 - 1846.

30. Luecke T, Meinhardt JP, Herrmann P, Weisser G, Pelosi P, Quintel M. Setting mean airway pressure during high-frequency oscillatory ventilation according to the static pressure--volume curve in surfactant-deficient lung injury: a computed tomography study. *Anesthesiology* 2003; 99: 1313 - 1322.

31. High-frequency oscillatory ventilation compared with conventional mechanical ventilation in the treatment of respiratory failure in preterm infants. The HIFI Study Group. *N Engl J Med* 1989; 320: 88 - 93.

32. Scalfaro P, Pillow JJ, Sly PD, Cotting J. Reliable tidal volume estimates at the airway opening with an infant monitor during high-frequency oscillatory ventilation. *Crit Care Med* 2001; 29: 1925 - 1930.

33. Sedeek KA, Takeuchi M, Suchodolski K, Kacmarek RM. Determinants of tidal volume during high-frequency oscillation. Crit Care Med 2003; 31: 227 - 231.

34. Gattinoni L, Pelosi P, Suter PM, Pedoto A, Vercesi P, Lissoni A. Acute respiratory distress syndrome caused by pulmonary and extrapulmonary disease. Different syndromes? *Am J Respir Crit Care Med* 1998; 158: 3 - 11.

35. Pelosi P, D'Onofrio D, Chiumello D, Paolo S, Chiara G, Capelozzi VL, Barbas CS, Chiaranda M, Gattinoni L. Pulmonary and extrapulmonary acute respiratory distress syndrome are different. *Eur Respir J Suppl* 2003; 42: 48s - 56s.

36. Albaiceta GM, Taboada F, Parra D, Blanco A, Escudero D, Otero J. Differences in the deflation limb of the pressure-volume curves in acute respiratory distress syndrome from pulmonary and extrapulmonary origin. *Intensive Care Med* 2003; 29: 1943 - 1949.

Chapter 7

Bench test assessment of dosage accuracy and measurement inaccuracy in nitric oxide inhalational therapy during high-frequency oscillatory ventilation

DG Markhorst, T Leenhoven, HR van Genderingen, JW Uiterwijk,
AJ van Vught

Journal of Clinical Monitoring 1997; 13: 349 - 355

SUMMARY

Objective: The objective of this study is to determine the accuracy and precision of chemiluminescence and electrochemical nitric oxide (NO) measurements and accuracy of NO dosage with electronic mass flow controllers (MFC) versus rotameters during NO inhalational therapy.

Methods: NO flow was delivered to a high-frequency oscillator and mixed with ventilator flow. NO and NO_2 concentrations were measured simultaneously with a standard chemiluminescence analyser and a modified electrochemical analyser. Dosage accuracy was assessed with gas flows adjusted with either MFC's or rotameters. Accuracy of both analysers was validated with both NO and ventilator flow regulated with a MFC.

Results: In dry air, without pulsatile pressure, MFC controlled NO and ventilator flow resulted in an accuracy expressed as the ratio of calculated concentration to measured concentration (RCM) of 0.995 (CI: 0.983-0.988) when measured with chemiluminescence. When the ventilator rotameter was used instead of a MFC, RCM was 0.856 (95% confindence interval (CI): 0.835-0.877). With a rotameter for both NO and ventilator flow, RCM increased to 1.175 (CI: 0.793-1.740) with an increase of confidence interval limits. Chemiluminescence was sensitive to humidification of the ventilatory gases ($p < 0.05$), slightly sensitive to the addition of oxygen and to pulsatile pressure (not significant). RCM obtained with the modified electrochemical analyser was in close agreement with chemilurninescence RCM, although 95% CI were wider with electrochernical analysis.

Conclusions: During high-frequency oscillatory ventilation (HFOV), standard rotameter flow control of both NO and ventilator flow results in unpredictable NO concentrations that would be clinically unacceptable. When one MFC was used for NO flow control, with ventilator flow controlled with a rotameter, this resulted in moderate dosage accuracy. To achieve a still higher accuracy, MFC flow control for both NO and ventilator flow is indicated. During HFOV, standard chemiluminescence analysers cannot be considered to be the gold standard for determination of the NO concentration delivered. Measurement of NO concentration may not be mandatory for determination of inhaled NO dose during HFOV, but may be used to monitor for unsafe or unwanted events.

INTRODUCTION

Inhalation of nitric oxide (NO) reduces pulmonary artery pressure and increases arterial oxygenation by improving ventilation-perfusion matching, without producing systemic vasodilatation in newborns with severe persistent pulmonary hypertension of the newborn (PPHN),[1-3] in children with pulmonary hypertension [4] and in patients with severe adult respiratory distress syndrome (ARDS).[5] It has been suggested that NO inhalational therapy may be less successful without optimal lung volume management and that some patients benefit from combined treatment of inhaled NO and high-frequency oscillatory ventilation.[3,6] Inhalation of gas mixtures containing high concentrations of NO and NO_2 can be rapidly lethal in humans,[7] and long term effects of NO exposure are unknown. Therefore, accurate monitoring of NO and NO_2 concentrations is considered to be important. Three measurement methods are currently in use in intensive care practice: chemiluminescence analysis, infrared monitoring and systems based on electrochemical cells. This last method has the advantage of relative modest costs. All of these methods may be sensitive to high oxygen concentrations, humidity and pressure. These limitations may not always be taken into consideration in every set up for NO inhalational therapy.
The aim of this study was to assess the accuracy of NO dosage with two types of flow controllers, as well as the accuracy of chemiluminescence and electrochemical analysis in measuring NO concentration during HFOV, in an effort to describe a system for NO inhalational therapy with optimal accuracy both for clinical and research purposes. This study has been performed as a bench test without involvement of human subjects, enabling assessment of the influence of various ventilator settings on the accuracy of NO dosage and measurement.

MATERIALS AND METHODS

Nitric oxide system set-up

NO was provided in tanks containing 800 parts per million (ppm) nominal value NO in nitrogen (N_2) (Linde AG, Düsseldorf, Germany). The certificate of analysis stated an analytical value of 796 ppm with a relative accuracy of $\pm$ 2%. Using the chemiluminescence analyser, we found a NO concentration of 798 ppm. The applied NO concentrations in the ventilatory circuit at each ventilator setting were 1, 2.5, 5, 10, 20 and 40 ppm. Dosage calculation was based on the measured concentration of 798 ppm, using formula (3) (appendix).

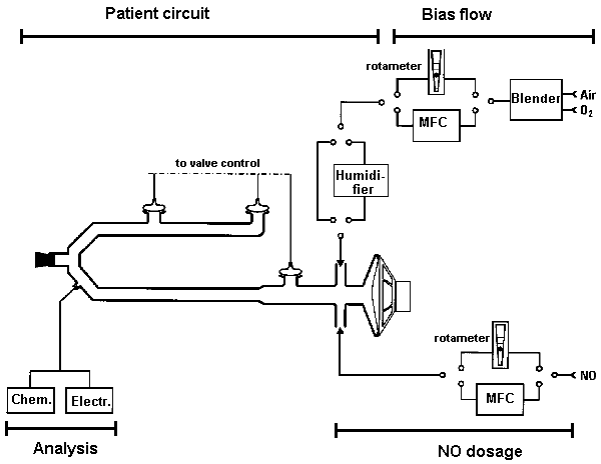

Fig. 7.1. Schematic drawing of the experimental setup. Chem = chemiluminescence analyser; electr = electrochemical monitor; MFC = electronic mass flow controller. The oscillator loudspeaker is drawn in the centre of the figure. See text for explanation.

NO flow was fed into the inspiratory limb of the patient circuit, just distally from the humidifier. Gas was sampled for NO and NO_x concentration measurement in the inspiratory limb just before the tube connection site (Fig. 7.1).

Ventilator

The ventilator used in this experiment was a 3100A HFOV ventilator (SensorMedics Corp., Yorba Linda, CA). Frequency and inspiratory fraction were set at respectively 10 Hz and 0.33 and were not altered. Mean airway pressure (MAP) setting was cycled through 10, 20, 30 and 40 cm H_2O, where ventilator flow was sufficient to obtain these values. Ventilator flow was set at 10, 15 or 20 l/min. Pulsatile pressure was set to either 0 or 40 cm H_2O. Oxygen was set to 21% or 100%. The measurements were performed in dry gas and repeated in humidified and heated gas (approximately 95% relative humidity at a temperature of 36 ^{o}C). Gas concentrations were simultaneously measured with chemiluminescence and electrochemical analysers. The tube connector of the ventilator circuit remained plugged during measurements.

Flow controllers

In NO inhalational therapy, both NO flow and flow of the air-oxygen mixture are regulated independently. In our experimental set-up, NO flow was regulated either with a 0-1 l/min electronic mass flow controller (MFC) (accuracy, measured at 21 ^{o}C room temperature and pressure of 101.4 kPa, -0.4% to 0.3% full scale (FS) (F-201C-FA, Bronkhorst Hi-Tec, Veenendaal, The Netherlands), or with a standard 0-1 l/min rotameter (accuracy $\pm$ 10% FS)

(SNL 41375 Ln/N2, Brooks, Veenendaal, The Netherlands). Ventilator flow could be regulated either by the 0-40 l/min ventilator rotameter (accuracy 2.5 l/min or 10% FS, whichever is greater, using air or oxygen at 21 ^{o}C and 103.4 kPa) or by a 0-30 l/min mass flow controller (accuracy -0.9 to 0.4% FS) (F-201AC-FA, Bronkhorst Hi-Tec, Veenendaal, The Netherlands), in which case the ventilator rotameter was bypassed (Fig. 7.1). Measurements were performed, comparing the use of a combination of 2 MFC's, the ventilator rotameter combined with a MFC for NO flow, and application of two rotameters.

Humidifier

A standard humidifier (MR 730, Fisher & Paykel, Auckland, New Zealand) was used in conjunction with heater wires in the ventilatory circuit. Temperature was set at 36 ^{o}C, heater wire delta temperature at -1 ^{o}C, resulting in a 1 ^{o}C increase in temperature of inspiratory gas. This humidifier was bypassed for dry gas measurements.

Chemiluminescence NO/NOx analyser

Chemiluminescence is the reference method for automatic measurement of nitrogen oxide concentrations in 21% oxygen at ambient pressure and in dry gas.[10] In the reactor, NO reacts with ozone, the release of photons being detected by a photomultiplier tube. NO_x measurement is obtained by reduction of the higher nitrogen oxides to NO in a heated (400 ^{o}C) molybdenum converter (3 NO_2 + Mo-→ 3 NO + MoO_3) prior to entrance into the reactor. Thus, NO_2 is not measured directly, but calculated as the difference between NO and NO_x measurements. The difference between NO_x and NO measurements can be considered as a specific NO_2 measurement.[8]
We measured NO and NO_2 concentrations using a standard chemiluminescence analyser (CLD 700 AL, Eco Physics, Diirnten, Switzerland) which was calibrated by means of a certified reference gas (802 ppm $\pm$ 2%, Messer Griesheim, Moerdijk, the Netherlands). Calibration was repeated prior to and after completion of the experiment, revealing no signs of drift (<0.1 ppm). The range of measurement is 0.001-100 ppm, 95% response time is 70 seconds.

Electrochemical NO/NO2 monitors

Simultaneous with chemiluminescence analysis, NO and NO_2 concentrations were measured with an electrochemical combined NO and NO_2 monitor (SensorNOx, Sensor Medics Europe, Bilthoven, the Netherlands). Ninety- percent response time is less than 30 seconds. The monitor uses active side stream sampling at a rate of 200 ml/min. Prior to the

experiment both NO and NO_2 analysers were calibrated against 100% nitrogen (zero values), at a NO concentration of 48 ppm and a NO_2 concentration of 5 ppm (gas calibration). Chemiluminescence validated gases were used to calibrate the electrochemical analyser. Calibration was repeated after completion of the experiment, revealing no signs of drift (< 0.1 ppm).

Protocol

Simultaneous chemiluminescence and electrochemical analysis of NO concentrations resulted in two measured NO concentrations or a measurement set. Calculated NO concentrations (derived from rotameter and/ or MFC flowrates) were compared to the measured concentrations (by chemiluminescence and/or electrochemistry).

Statistical analysis

We used the method described by Bland and Altman to evaluate the agreement between the calculated and the measured concentrations.[9] Individual differences between two methods (Di = Xi- Yi) were plotted, against their mean [(Xi + Yi)/2] and the distribution of these differences and their relation to the individual means were analysed. Since in this study the individual differences increased with their mean, a log transformation of the parameters was performed, resulting in a plot of $Di = \log(X_i) - \log(Y_i)$ against $\log((X_i + Y_i)/2)$. Bias was then calculated as the mean difference (*d*) and the standard deviation (*s*) of the differences. 95% confidence interval (CI) for the bias was calculated as $d \pm \sqrt{(s^2/n)}$, where n is the sample size and t the appropriate point of the t distribution at p = 0.05 with n -1 degrees of freedom. The results were related to the original scale of measurement in computing their anti-logs. This resulted in a dimensionless ratio, we refer to as the ratio of calculated to measured concentration (RCM). Values are expressed as mean, 95% CI limits are noted between brackets, unless otherwise noted. The mean RCM is an estimate of the systematic error of either calculation (flow) or measurement. The 95% CI width is an estimate of the precision of either calculated or measured concentration. Based on these calculations (Table 7.1), for each covariate (humidity, oxygen content, HFOV pulsatile pressure) the systematic error (Table 7.2) and precision (Table 7.3) of chemiluminescence and electrochemical analysis were compared using the Wilcoxon signed rank test. Probabilities of less than 0.05 were considered to be significant.

Table 7.1. Measurement results obtained with a standard chemiluminescence analyser and a NO monitor based on electrochemical cells

Series	Number of measure-ment sets (N)	Ventilator flow control	NO flow control	Humidi-fication	FIO_2	Pulsatile pressure	RCM chemoluminescence	RCM electrochemical
A	48	MFC	MFC	-	0.21	-	0.995 (0.983 – 0.998)	1.071 (1.030 –1.113)
B	30	Rotameter	MFC	-	0.21	-	0.856 (0.835 – 0.877)	Not measured
C	9	Rotameter	Rotameter	-	0.21	-	1.175 (0.793 – 1.740)	Not measured
D	30	MFC	MFC	-	1.0	-	0.997 (0.980 – 1.014)	1.027 (0.988 – 1.069)
E	24	MFC	MFC	-	0.21	+	0.971 (0.945 – 0.997)	1.024 (0.976 – 1.075)
F	12	MFC	MFC	-	1.0	+	1.018 (0.988 – 1.050)	1.079 (0.981 – 1.187)
G	48	MFC	MFC	+	0.21	-	1.126 (1.112 – 1.139)	1.118 (1.059 – 1.180)
H	18	MFC	MFC	+	0.21	+	1.144 (1.110 – 1.178)	1.192 (1.047 – 1.357)
I	30	MFC	MFC	+	1.0	-	1.138 (1.122 – 1.154)	1.117 (1.037 – 1.203)
J	12	MFC	MFC	+	1.0	+	1.166 (1.141 – 1.192)	1.129 (1.008 – 1.265)
K	108	MFC	MFC	+	0.21 – 1.0	$\pm$	1.136 (1.126 – 1.146)	1.131 (1.089 – 1.175)

N = number of measurement sets; MFC, mass flow controller; FIO_2, inspiratory fraction of oxygen; RCM, ratio of calculated to measured NO concentration; +, present, -, absent. 95% CI limits between brackets.

RESULTS

The results are presented in Table 7.1. 153 Measurement sets were obtained from dry gas mixtures (Table 7.1, series A-F), 108 sets from humidified gas mixtures (Table 7.1, series G-J).

With the use of a MFC both for NO and ventilator flow, a RCM was found of 0.995 indicating a mean overestimation by chemiluminescence of 0.5% of the calculated value (series A). When the ventilator flow meter was used instead of a MFC for ventilator flow control, a RCM of 0.856 was found (series B). When flows were regulated with two rotameters for NO flow and ventilator flow control, RCM increased to 1.175 with an increase of confidence interval limits (series C).

Subsequently, the influence of oxygen (comparing series A versus D, E versus F, G versus I, H versus J), humidification (series A-G, D-I, E-H, F-J) and pulsatile pressure (series A-E, D-F, G-H, I-J) were studied using two mass flow controllers to manage ventilator and NO flow. Humidification, and to a lesser and statistical non significant extent pressure and oxygen content, resulted in increase of RCM deviation from 1.0 and widening of confidence interval limits. There was no significant difference in accuracy (systematic error or bias) of chemiluminescence and electrochemical analysis for each covariate, with the exception of

Table 7.2: Systematic error (or bias) of chemiluminescence (chem) and electrochemical analysis (electro), calculated for each covariate. Systematic error is expressed as a percentage of the calculated value derived from MFC NO and ventilator flow.

Covariate	Measurement sets	Mean bias chem (%)	Mean bias electro (%)	Significance
Overall	A, D-J	-6.6	-9.4	NS ($p > 0.05$)
Dry gas	A, D - F	0.5	-5.0	S ($p \leq 0.05$)
Humid gas	G, H - J	-13.6	-13.9	NS ($p > 0.05$)
21% O_2	A, E, G, H	-5.2	-10.1	NS ($p > 0.05$)
100% O_2	D, F, I, J	-8.0	-8.8	NS ($p > 0.05$)
No pulsatile pressure	A, D, G, I	-6.4	-8.3	NS ($p > 0.05$)
Pulsatile pressure	E, F, H, J	-6.7	-10.6	NS ($p > 0.05$)

NS, difference not statistically significant; S, difference statistically significant.

Table 7.3: Precision of chemiluminescence (chem) and electrochemical analysis (electro), calculated for each covariate. Mean width of the 95% confidence interval is expressed as a percentage of the calculated value derived from MFC NO and ventilator flow.

Covariate	Measurement sets	Confidence interval width chem (%)	Confidence interval width electro (%)	Significance
Overall	A, D-J	4.3	15.3	S ($p \leq 0.05$)
Dry gas	A, D - F	4.0	11.8	S ($p \leq 0.05$)
Humid gas	G, H - J	4.6	14.4	S ($p \leq 0.05$)
21% O_2	A, E, G, H	4.0	15.4	S ($p \leq 0.05$)
100% O_2	D, F, I, J	4.4	15.6	S ($p \leq 0.05$)
No pulsatile pressure	A, D, G, I	2.8	13.6	S ($p \leq 0.05$)
Pulsatile pressure	E, F, H, J	5.8	17.6	S ($p \leq 0.05$)

S, difference statistically significant.

the measurements in dry gas where chemiluminescence accuracy was higher (Table 7.2). NO_2 concentrations, measured with the electrochemical analyser, varied from 0 ppm to a maximum of 0.6 ppm. Highest NO_2 concentrations were found with the use of 40 ppm NO and FIO_2 of l.0 and a ventilator bias flow of 10 l/min.
Precision of electrochemical analysis was lower for all covariates in comparison to chemiluminescence measurement (Table 7.3).

DISCUSSION

Any unit, designed to deliver and measure NO for inhalational therapy in combination with a continuous flow ventilator, will typically consist of a NO source, gas flow controller and a monitor for NO and NO_2 concentration in either the inspired or expired gas. Each of these components will have a certain inaccuracy. When combined in a system and added to a ventilator, inaccuracy of the single components will add to system inaccuracy. Furthermore, during artificial ventilation, NO will be heated, humidified, pressurised and mixed with oxygen affecting NO and NO_2 concentrations and measurement accuracy.

Mass flow controllers and rotameters

In dry gas and 21% oxygen, chemiluminescence is considered to be the reference method for measuring NO concentrations.[10] Under these conditions, the NO concentrations measured with chemiluminescence when two MFC were used are in excellent agreement with the calculated concentrations (maximal overestimation of 1.7%, Table 1 series A). No significant influences of oxygen content on NO concentration was measured (series A and D). In contrast to the chemiluminescence analyser, the MFC will not be influenced by humidification, heating or pressurisation of the gas mixture. In experimental and clinical circumstances therefore, the calculation of concentration with the use of two MFC's can be regarded as a reference method for NO dosage. This will be of principal importance in clinical or experimental research where the highest accuracy in NO dosage is needed.
The standard rotameter used has an inaccuracy of ±10% FS. This inaccuracy has its largest influences when using low flow rates. Furthermore, a standard rotameter will be influenced by static and dynamic ventilator backpressure. In dry air with 21% oxygen and with the chemiluminescence as a reference, the combination of a MFC controlled NO flow and a rotameter controlled ventilator flow results in slightly higher dosage (RCM 0.856) and wider 95% CI (0.835- 0.877) (series B) in comparison to MFC flow controlled ventilator flow (series A). In the worst situation, this could lead to a NO dose 16.5% higher than calculated. However, the wide 95% CI limits found with the use of two rotameters excludes accurate NO dosage, since in the worst case a NO dosage 74% higher than intended may be delivered (series C).
Thus, during HFOV, NO cannot be accurately titrated when NO flow is regulated with a standard rotameter.

Chemiluminescence

Chemiluminescence measurements are in excellent agreement with calculated NO concentrations during HFOV with 21% oxygen and without humidification of the gas mixture (series A and E). The pulsatile pressure generated by the ventilator only minimally influences measurement accuracy (series E, not significant). Although the chemiluminescence analyser is sensitive when oxygen is added to the gas mixture (series D), this difference is also not significant. The decrease in analyser sensitivity due to the change of FIO_2 from 0.21 to 1.0 is about 1% (previous measurements, data not included). In addition, the chemiluminescence analyser appears to be sensitive to humidification of the

gas sample (series G to K). Therefore, sampled humidified gas should be dried prior to entry in the analyser.
Because in the chemiluminescence analyser the NO_2 concentration is determined as the difference between NO and NO_x, NO_2 measurements are not accurate in situations where NO concentration exceeds NO_2 concentration. Accordingly, the value of standard chemiluminescence as a method for monitoring NO and NO_2 concentrations in NO inhalational therapy is limited.

Electrochemical analyser

The SensorNOx was designed to reduce the effects of humidity, pulsatile pressure and high oxygen concentration on gas measurements. Nevertheless, the SensorNOx monitor was found to be sensitive to pressure and humidification.
In humidified gas, the systematic error of the electrochemical analyser did not differ from the chemiluminescence results, although the precision was significantly lower. This can be primarily attributed to relatively small absolute measurement errors in the low concentration range. For purposes of monitoring NO concentration based on calculation and accurate flow regulation, when small measurement errors are not relevant, electrochemical measurement of NO concentrations with the SensorNOx monitor is as useful as that obtained with a chemiluminescence analyser.

Heating and humidification

In the calculation of NO flow required to obtain the desired NO concentration, the contribution of water vapour is not taken into account. Humidification and heating of a gas mixture containing NO will lead to a 4.46% NO concentration reduction at an ambient pressure of 100 kPa and temperature of 36 ^{o}C. This, at least in part, explains the lower concentrations measured with both chemiluminescence and electrochemical analysis in humidified gas.
The standard chemiluminescence analyser underestimates NO concentration by 6.13% of the real NO concentration in humid gas (unpublished communication, Eco Physics, Dürnten, Switzerland). To date, standard chemiluminescence cannot he regarded as the gold standard for NO and NO_2 measurement during artificial ventilation, and calculation of NO concentration from MFC controlled gas flows is more reliable. A chemiluminescence analyser has now been developed with a permapure gas dryer for clinical use.

Should NO and NO_2 concentrations be measured during NO inhalational therapy?

We found the calculation of NO concentration with the use of two MFC's to be an excellent reference method. In a setting with humidified air, variable oxygen concentrations and pulsatile pressure within the ventilatory circuit, a moderate disagreement between calculated and measured concentration exists both with chemiluminescence and electrochemical analysers. Since accuracy of dosage exceeds the accuracy of measurement, the rationale to monitor NO concentration in NO inhalational therapy can be argued. Conversely, to detect human and technical errors in NO dosage, monitoring of NO concentration may be warranted. In these circumstances the electrochemical analyser used in this study provides adequate accuracy. The electrochemical analyser is equipped with acoustic alarms, its accuracy is comparable to the standard chemiluminescence analyser during artificial ventilation, its precision is lower but acceptable, it has a relatively short response time, and its costs are relatively low.

Conclusions

If it is considered important to measure NO_2, an accurate method should be used (not standard laboratory chemiluminescence analysis). For research purposes when a high degree of accuracy and precision is needed, the use of a MFC both for NO and ventilator flow is mandatory. A lower but acceptable accuracy will be obtained when only NO flow is regulated with a MFC, and NO concentrations are calculated. In the laboratory setting it appears that ventilator flow can still be safely regulated with the standard flow controller of the oscillator, during HFOV. NO dosage can be based on calculation of the gas flow needed. Potentially measurement of NO concentration can then be used to monitor for unsafe or unwanted events like a change in ventilator flow without adjustment of NO flow, although further studies are needed to confirm these results in the clinical setting.

APPENDIX

The NO concentration in the inspiratory gas can be calculated as:

$$[NO]_{insp} = ([NO]_{bottle} \times \dot{V}_{NO})/\dot{V}_{total} \quad (1)$$

Since $\dot{V}_{total}$ is formed by ventilator flow and NO flow, this leads to:

$$[NO]_{insp} = ([NO]_{bottle} \times \dot{V}_{NO})/(\dot{V}_{NO} + \dot{V}_{vent}) \quad (2)$$

which can be rewritten to:

$$\dot{V}_{NO} = (\dot{V}_{vent} \times [NO]_{insp})/([NO]_{bottle} - [NO]_{insp}) \quad (3)$$

where $[NO]_{insp}$ = NO concentration in the inspiratory gas (ppm), $[NO]_{bottle}$ = NO concentration in the NO/N_2 bottie (in our experiment 798 ppm), $\dot{V}_{NO}$ = NO/N_2 gas flow (ml/min), $\dot{V}_{total}$ = total gas flow in the ventilator circuit (ml/min), $\dot{V}_{vent}$ = set ventilator gas flow (ml/min).

REFERENCES

1. Kinsella JP, Neish SR, Shaffer E, Abman SH. Low dose inhalational nitric oxide in persistent pulmonary hyper- tension of the newbom. *Lancet* 1992; 340: 819-820
2. Roberts JD, Polaner DM, Lang P, Zapol DM. Inhaled nitric oxide in persistent pulmonary hypertension of the newbom. *Lancet* 1992; 340: 818-819
3. Kinsella JP, Neish SR, Ivy DD, Shaffer E, Abman SH. Clinical responses to prolonged treatment of persistent pulmonary hypertension of the newborn with low doses of inhaled nitric oxide.*J Pediatr* 1993; 123: 103-108
4. Lonnqvist PA, Winberg P, Lundell B, Selldén H, 0lsson GL. Inhaled nitric oxide in neonates and children with pulmonary hypertension. *Acta Paediatr* 1994; 83: 1132- 1136
5. Rossaint R, Falke KJ, Lopez F, Slama K, Pison U, Zapol WM. Inhaled nitric oxide for the adult respiratory distress syndrome. *N EngJ Med* 1993; 328: 399-405
6. KinsellaJP, Abman SH. Inhalational nitric oxide therapy for persistent pulmonary hypertension of the newbom. *Pediatrics* 1993; 91: 997-998
7. Clutton-Brock J. Two cases of poisoning by contamination of nitrous oxide with the higher oxides of nitrogen during anaesthesia. *Br J Anaesth* 1967; 39: 388-392
8. Moutafis M. Hatahet Z, Castelain MH, Renaudin MH, Monnot A, Fischler M. Validation of a simple method assessing nitric oxide and nitrogen dioxide concentrations. *Intensive Care Med* 1995; 21: 537-541
9. Bland JM, Altman DG. Statistical methods for assessing agreement between two methods of clinical measurement. *Lancet* 1986; 1: 307-310
10. Zapol WM, Falke KJ. Inhaled nitric oxide for the adult respiratory distress syndrome. *N Engl J Med* 1993; 329: 206-207

Chapter 8

Occupational exposure during nitric oxide inhalational therapy in a paediatric intensive care setting

DG Markhorst, T Leenhoven, JW Uiterwijk, J Meulenbelt, AJ van Vught

Intensive Care Medicine 1996; 22: 954 - 958

SUMMARY

Objective: To determine the amount of occupational exposure to nitric oxide (NO) and nitrogen dioxide (NO_2) during NO inhalational therapy.

Design: In a standard paediatric intensive care room, 800 ppm NO was delivered to a high-frequency oscillator and mixed with 100% O_2 to obtain 20 ppm NO in the inspiratory gas flow. NO and NO_2 concentrations in room air were measured using a chemiluminescence analyser. Air samples were taken from a height of 150 cm at a horizontal distance of 65 cm from the ventilator in a nonventilated and in a well-ventilated room with and without an expiratory gas exhaust under normal intensive care environmental conditions.

Setting: Paediatric intensive care unit in a university children‘s hospital.

Measurements and results: Maximal concentrations of NO and NO_2 were reached after 4 h NO use. Without exhaust, in a nonventilated room, environmental NO and NO_2 concentration rose to a maximum of 0.462 and 0.064 ppm, respectively. With the use of an expiratory gas exhaust, NO and NO_2 concentrations were 0.176 and 0.042 ppm, respectively. With normal air-conditioning, these values were 0.075 and 0.034 ppm, respectively, without the use of an expiratory gas exhaust. With expiratory gas exhaust added to normal air-conditioning, values for NO and NO_2 were 0.035 and 0.030 ppm, respectively.

Conclusions: The use of 20 ppm NO, even under minimal room ventilation conditions, did not lead to room air levels of NO or NO_2 that should be considered toxic to adjacent intensive care patients or staff. Slight increases in NO and NO_2 concentrations were measurable but remained within occupational safety limits. The use of an exhaust system and normal room ventilation lowers NO and NO_2 concentrations further to almost background levels.

INTRODUCTION

Inhalation of nitric oxide (NO) reduces pulmonary artery pressure and increases arterial oxygenation by improving the matching of ventilation with perfusion, without producing systemic vasodilation in patients with severe adult respiratory distress syndrome (ARDS) [1] as well as in newborns with severe persistent pulmonary hypertension of the newborn and children with pulmonary hypertension.[2-5] It has been found that inhaled NO may be less successful without optimal pulmonary management and that some patients benefit from a combined treatment of inhaled NO and high-frequency oscillatory ventilaton (HFOV).[4,6]. Although these preliminary reports of inhalational NO therapy are encouraging, [1-6] many questions remain to be answered before its routine application can be recommended. NO is present throughout the organism as a signal molecule regulating vasomotor tone and platelet function. It is a messenger molecule in the immune system and it functions as a neurotransmitter. In addition, it is a short-lived and extremely potent radical. In air, in the presence of oxygen, it is rapidly converted into NO_2. The reaction velocity is dependent on oxygen concentration, pressure, and temperature.[7]

Inhalation of gas mixtures containing high concentrations of NO and NO_2 can be rapidly lethal in humans.[8] Long term effects of low-dose NO exposure are unknown, and NO might have carcinogenic properties.[9,10] Therefore, concern remains regarding the safety of NO inhalational therapy. The aim of this study was to assess the potential environmental exposure of intensive care staff and adjacent patients to NO and NO_2 pollution during NO inhalational therapy combined with HFOV.

MATERIALS AND METHODS

Ventilator

We used a 3100A HFO ventilator (SensorMedics Corp, Yorba Linda, CA). Ventilator settings were set to values frequently used for paediatric and neonatal intensive care patients: mean airway pressure 20 cmH2O, pressure amplitude 25 cmH_2O, total gas flow 20 l/min. During the experiment, no humidification of inspiratory gasses was used. The fraction of inspired oxygen (FIO_2) was set at a maximal value of 0.975. NO flow and flow of the air-oxygen mixture were regulated wilt digitally controlled mass flow controllers (accuracy 1% full scale) in combination wilt a NO-dosing controller unit (Bronkhorst Hi-Tec, Veenendaal, The Netherlands; SensorMedics, Bilthoven, The Netherlands). The tube connector remained

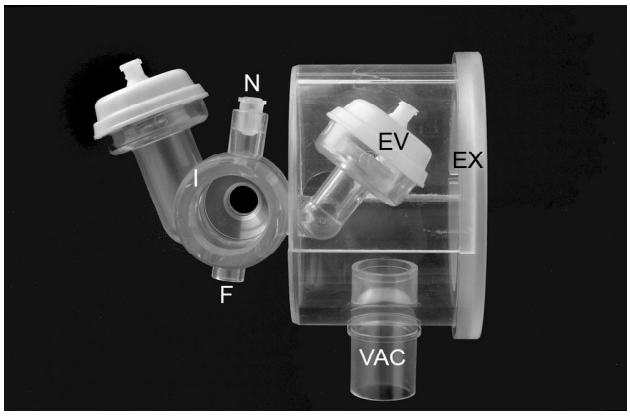

Fig. 8.1: Perspex NO exhaust placed around the expiration valve. Waste gasses are extracted toward the hospital vacuüm system. I: inspiratory limb (transected), F: fresh gas inlet, N: NO inlet, Ex: perspex exhaust, Ev: expiration valve, Vac: connection to vacuüm system.

closed during the experiment. NO was provided in tanks containing 800 ppm NO in N_2 (Linde AG, Düsseldorf, Germany).

NO exhaust

In the 3100A HFO ventilator, expiration gasses and bias flow leave the patient circuit via a balloon valve. To minimise environmental pollution, we used a Perspex capsule placed around this expiration balloon (Fig. 8.1). Waste gas was then directed towards the wall vacuum system. In the text, this device is referred to as an exhaust.

Environmental circumstances

The experiments were performed in one of our standard paediatric intensive care rooms, of dimensions 5 x 4.3 x 2.8 m (volume 60 m^3). Air temperature was around 22 °C, relative air humidity was around 45%. To create a worst-case scenario, in which the influence of NO and NO_2 efflux on environmental conditions would be maximal, we performed the experiment in a closed room without natural room air ventilation and air-conditioning (situation 1). Further measurements were performed using the exhaust without normal room air ventilation and air-conditioning (situation 2), normal room air ventilation and air-conditioning without the use of the exhaust (situation 3) and, finally, with normal room air ventilation and air-conditioning with the use of the exhaust (situation 4). During measurements, care was taken to minimise movements in the room, in an effort to minimise undesired air movement.

Measurement of NO and NO_2 concentrations

The reference method for measurement of NO concentrations in 21% oxygen is chemiluminescence. NO reacts with ozone in a reactor, the release of photons being detected by a photomultiplier tube. NO_x measurement is obtained by reduction of the higher nitrogen oxides to NO in a heated (400 ^oC) molybdenum converter (3 NO_2 + Mo → 3 NO + MoO_3) prior to entrance into the reactor. Thus, NO_2 is not measured directly, but calculated as the difference between NO and NO_x measurements, which can be considered as a specific NO_2 measurement.[11] We measured room air NO and NO_2 concentrations using a chemiluminescence analyser (CLD 700 AL, Eco Physics, Dürnten, Switzerland), which was calibrated using a certified reference gas (Messer en Griesheim, Moerdijk, The Netherlands). Calibration was repeated prior to and after completion of the experiment, revealing no signs of drift. The range of measurement is 0.001-100 ppm, and the 95% response time is 70 s. The decrease in analyser sensitivity due to the change of O_2 concentration from 21 to 100% is about 1 %. NO and NO_2 measurements were recorded with a pen recorder (BD 112, Kipp en zonen, Delft, The Netherlands). Environmental gasses were sampled during a 12-hour period via a sampling tube, which was suspended at a height of 150 cm above floor level, at a horizontal distance of 65 cm from the ventilator circuit expiration valve, at an angle of 45°. This position was chosen because it was considered to be a typical working position of staff nearest to the system.

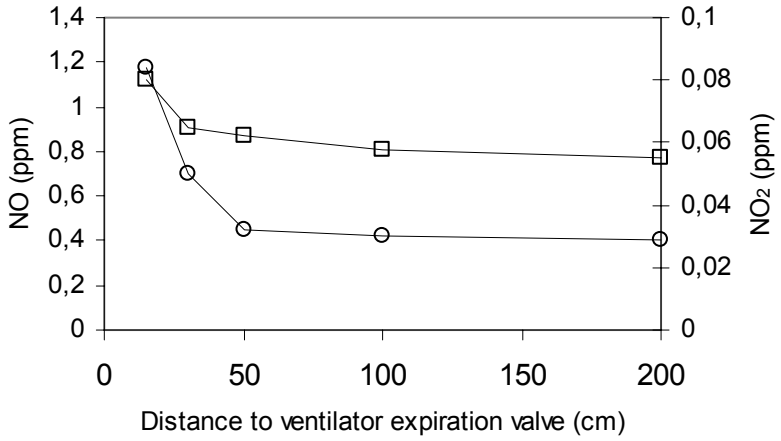

Fig. 8.2: Nitric oxide (circles) and nitric dioxide (squares) concentrations at 100 cm height, as a function of distance from the expiration valve, without ventilation or exhaust.

Prior to and after completion of each measurement, background NO and NO_2 concentrations were measured. Additionally, we measured the NO and NO_2 concentrations after a 12-hour period in the worst-case situation (situation 1), without normal room air ventilation and air-conditioning at a height of 100 cm above floor level at distances of 15, 30, 50, 100, and 200 cm from the expiration valve.

RESULTS

Concentrations of NO and NO_2 were highest in proximity to the expiration valve (Fig. 8.2). Due to air turbulence, measurements did not stabilise less than 15 cm from the expiration valve. Concentrations decreased rapidly with increasing distance from the ventilator, and 50 cm from the expiration valve, NO and NO_2 concentrations did not differ substantially from background concentrations.

Maximal NO and NO_2 concentrations measured 150 cm above floor level, 65 cm from the expiration valve, are shown in Table 8.1. Background concentrations were 0.002 ppm NO and 0.022-0.028 ppm NO_2. Maximal concentrations were reached after 4 h, stabilising thereafter. Room air concentrations of bath NO and NO_2 were highest when natural room air ventilation and air-conditioning were shot off (situation 1). Using the expelled-air exhaust (situation 2), NO room air contamination was reduced by 62%. With normal room air ventilation and air-conditioning but without exhaust (situation 2), an 84% reduction of room air NO concentration could be achieved relative to situation 1. With additional use of the exhaust (situation 4), the NO concentration was 92% lower than in situation 1.

In comparison to situation 1, an expelled-air exhaust reduced the NO_2 room air concentration by 31 %. Room air NO_2 contamination in this situation, after correction for atmospheric NO_2, was reduced by 55%. In situation 3, normal room air ventilation and air-conditioning, without the exhaust device, lowered NO_2 concentration by 47% relative to situation 1. The use of normal air-conditioning in combination with the exhaust lowered NO_2 concentration 53%, when compared to situation 1.

Table 8.1. Maximal concentrations of NO and NO_2 in room air, after a stabilisation period of 12 h, 150 cm above and 65 cm from the expiration valve.

	NO / NO_2 (ppm)	
	Without air-conditioning	With air-conditioning
Without exhaust	0.462 / 0.064	0.075 / 0.034
With exhaust	0.176 / 0.044	0.035 / 0.030

DISCUSSION

Although NO inhalational therapy seems to be a promising tool for the management of patients with severe pulmonary hypertension,[1,5,6,12,13] more data on safety and long-term effects, optimal timing of treatment, as well as dose-response relations are needed. We performed this study to obtain information about the environmental impact of NO inhalational therapy.

Inhalation of gas mixtures containing high concentrations of NO_2, and to a lesser extent NO, can be lethal in humans and can cause severe acute lung injury with pulmonary oedema and marked methemoglobinemia,[8] inhibition of DNA synthesis and deamination of DNA,[9,10] alteration of the inflammatory response of alveolar macrophages,[14] and prolongation of bleeding time.[15] As with most therapeutic agents, these side effects are likely to be dose dependent.[16] NO_2 causes oxidative damage by generating radicals. Damage of pulmonary cells and pulmonary macrophages leads to ARDS and a less efficient response to infections.[17,18] From healthy-volunteer studies, it may be concluded that, in normal persons, bronchial airway resistance may be increased at concentrations greater than 1.5 - 2 ppm.[19-21] At these low NO_2 concentrations, it has not yet been proven that patients with chronic obstructive disease or asthma are more susceptible to bronchial reactivity.[18,22-25]

In the present study, the maximal NO_2 concentration measured near the expiration valve was 0.064 ppm. This concentration was measured in a small room (60 m^3) without normal ventilation, expelled-gas exhaust, or scavenging, thus in the worst situation. These findings are in accordance with other studies.[26] Occupational exposure should be seen in the perspective of atmospheric NO and NO_2 concentrations (Fig. 8.3). The maximal room air

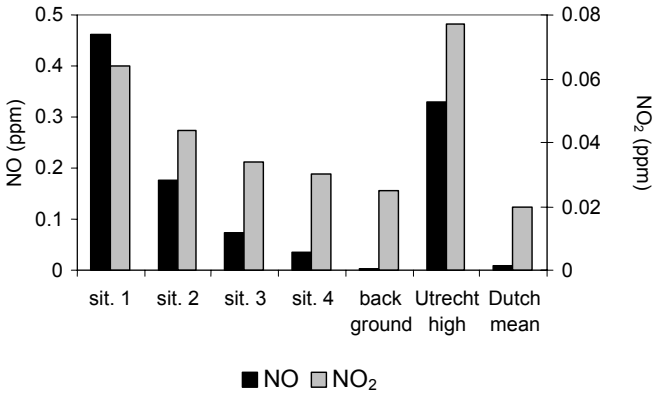

Fig. 8.3: Nitric oxide (NO, black bars) and nitric dioxide (NO_2, grey bars) room air concentrations in the intensive care room during nitric oxide inhalational therapy, in comparison to the highest measured environmental outdoor air concentrations in Utrecht, a Dutch city of 300,000 inhabitants, and to Dutch mean outdoor concentrations (Sit 1 – 4, situation 1 – 4, see text for explanation)

concentrations of NO and NO_2 we measured were comparable to values measured in Dutch cities, although these values were relatively high.[27] In the United States, the ambient air quality standard for NO_2 is 0.05 ppm averaged over 1 year. Maximal 30-min and 24-hour outdoor NO_2 values can be 0.45 ppm and 0.21 ppm, respectively.[28] The Occupational Safety and Health Administration bas listed the 8-hour time-weighted average safe level at 25 ppm for NO and 5 ppm for NO_2.[29] In homes with gas stoves, the NO_2 level ranges from 0.025 to 0.075 ppm.[28] In kitchens with gas cooking appliances, peak NO_2 levels may even reach 0.20-1.0 Ppm.[30] Epidemiologic and laboratory evidence for humans has not conclusively demonstrated adverse effects of NO_2 exposure at these indoor concentrations.[22] Therefore, the NO and NO_2 concentrations measured in the present study may be considered not harmful for intensive care staff and adjacent patients.

In our experiments, a high-frequency oscillator was used, requiring high gas flow rates. As a consequence, NO inflow must also be high, which will result in a high emission of NO into the environment. NO administration with a conventional ventilator will have less influence on environmental NO and NO_2 contamination, because the ventilatory flow rates are lower and, therefore, the required NO inflow rates will also be lower. Furthermore, our experiments were performed in a relatively small room (volume 60 m^3), resulting in limited dilution of expiratory gasses. During our experiment, the tube connector remained closed. When ventilating a patient with NO, same of the inspired NO will be bound to haemoglobin, thereby reducing the amount of expired NO.

Hence, we conclude that the use of 20 ppm NO inhalational therapy combined with HFOV, at least under our experimental conditions - a small intensive care room, with one HFO ventilator, providing 20 ppm in 100% O_2 in use - will not lead to room air NO and NO_2 levels that could be considered toxic to intensive care staff or adjacent intensive care patients. Environmental effects may be measurable but will be minimal and well within occupational safety limits.

REFERENCES

1. Rossaint R, Falke KJ, Lopez F, Slama K, Pison U, Zapol WM. Inhaled nitric oxide for the adult respiratory distress syndrome. *N Engl J Med* 1993;328: 399 – 405.
2. Kinsella JP, Neish SR, Shaffer E, Abman SH. Low dose inhalation nitric oxide in persistent pulmonary hypertension of the newborn. *Lancet* 1992; 340: 819 – 820.
3. Roberts JD, Polaner DM, Lang P, Zapol DM. Inhaled nitric oxide in persistent pulmonary hypertension of the newborn. *Lancet* 1992; 340: 818-819.
4. Kinsella IP, Neish SR, Ivy DD, Shaffer E, Abman SH. Clinical responses to prolonged treatment of persistent pulmonary hypertension of the newborn with low doses of inhaled nitric oxide. *J Pediatr* 1993; 123: 103-108.
5. Lönnqvist PA, Winberg P, Lundell B, Selldén H, Olsson GL. Inhaled nitric oxide in neonates and children with pulmonary hypertension. *Acta Paediatr* 1994; 83: 1132 – 1136.
6. Kinsella JP, Abman SH. Inhalational nitric oxide therapy for persistent pulmonary hypertension of the newborn. *Pediatrics* 1993; 91: 997 – 998.
7. Moncada S, Palmer RMJ, Higgs EA. Nitric oxide: physiology, pathophysiology and pharmacology. *Pharmacol Rev* 1991; 43:109 – 142.
8. Clutton-Brock J. Two cases of poisoning by contamination of nitrous oxide with the higher oxides of nitrogen during anaesthesia. *Br J Anaesth* 1967; 39: 388 – 392.
9. Wink DA, Kasprzak KS, Maragos CM, Maragos CM, Elespuru RK, Misra M, Dunams TM, Cebula TA, Koch WH, Andrews AW, Allen JS, Keefer LK. DNA deaminating ability and genotoxicity of nitric oxide and its progenitors. *Science* 1991; 254: 1001 – 1003.
10. Lepoivre M, Fieschi F, Coves J, Thelander L, Fontecave M. Inactivation of ribonucleotide reductase by nitric oxide. *Biochem Biophys Res Commun* 1991; 179: 442 – 448.
11. Moutafis M, Hatahet Z, Castelain MH, Renaudin MH, Monnot A, Fischler M. Validation of a simple method assessing nitric oxide and nitrogen dioxide concentrations. *Intensive Care Med* 1995; 21: 537 – 541.
12. Donn SM. Alternatives to ECMO. *Arch Dis Child* 1994; 70: F81- F83.
13. Miller OI, Celermajer DS, Deanfield JE, Macrea DJ. Guidelines for the safe administration of inhaled nitric oxide. *Arch Dis Child* 1994; 70: F47 - F49.
14. Turbow R, Waffarn F, Hallman M, Kleinman MT, Rasmussen RE, Mautz WJ, Bhalla OK, Williams JH. Inflammatory responses and suppressed macrophage function following inhaled nitric oxide (abstrct). *Pediatr Res* 1994; 35: 356A.
15. Högman M, Frostell C, Arnberg H, Hedenstierna G. Bleeding time prolongation and NO inhalation. *Lancet* 1993; 341: 1664-1665.
16. Kinsella JP, Abman SH. Recent developments in the pathophysiology and treatment of persistent pulmonary hypertension of the newborn. *J Pediatr* 1995; 126: 853 – 864.
17. Coffing DL, Gardiner DE, Blommer EJ. Time-dose response for nitrogen dioxide exposure in an infectivity model system. *Environ Health Perspeet* 1976; 13: 11 – 15.
18. Meulenbelt J, Sangster B. Acute pulmonary damage by toxic substances: new aspects of therapy. Yearbook of intensive care and emergency medicine. Edited by Vincent JL. Berlin Heidelberg New York, Springer Publisher 1994, 716- 727.
19. Orehek J, Massar JP, Gayrard P, Grimaud C, Charpin J. Effect of short-term, low level nitrogen dioxide exposure on bronchial sensitivity of asthmatic patients. *J Clin Invest* 1976; 57: 301 – 307.

20. Mohesin V. Airway responses to 2.0 ppm nitrogen dioxide in normal subjects. *Arch Environ Health* 1988; 43: 242 – 246.

21. Frampton MW, Morrow FE, Cox C, Cobb FR, Speers DM, Utell MJ. Effects of nitrogen dioxide exposure on pulmonary function and airway reactivity in normal humans. *Am Rev Respir Dis* 1991 143:522- 527.

22. Samet JM, Utell MJ. The risk of nitrogen dioxide; what have we learned from epidemiological and clinical studies? *Toxicol Industrial Health* 1990; 6: 247 – 262.

23. Linn WS, Shamoo DA, Spier CE, Valencia LM, Anzar UT, Venet TC, Hackney JD. Controlled exposure of volunteers with chronic obstructive pulmonary disease to nitrogen dioxide. *Arch Environ Health* 1985; 40: 313 – 317.

24. Linn WS, Shamoo DA, Avol EL, Whynit JD, Anderson KR, Venet TG, Hackney JD. Dose-response study of asthmatic volunteers exposed to nitrogen dioxide during intermittent exercise. *Arch Environ Health* 1986; 41: 292 – 296.

25. Gong H. Health effects of air pollution. *Clin Chest Med* 1992; 13: 201 – 214.

26. Wessel DL, Adatia I, Thompson JE, Hickey PR. Delivery and monitoring of inhaled nitric oxide in patients with pulmonary hypertension. *Crit Care Med* 1994; 22: 930 – 938.

27. Doesburg MJ van, Rentinck ECM, Swaan P. National air quality monitoring network, measurements 1993, part 4. Report number 722101013 28 1994.

28. Samet JM, Marbury MC, Spengler JD. Health effects and sources of indoor air pollution (part I). *Am Rev Respir Dis* 1987; 136: 1486 – 1508.

29. Centers for disease control. Recommendations for occupational safety and health standard. MMWR 1988; 37 (Suppl): 1 – 29.

30. Gold DR. Indoor air pollution. *Clin Chest Med* 1992; 13: 215 – 229.

Chapter 9

General discussion

DISCUSSION

The aim of this thesis was to develop and evaluate a number of methods to improve volume-targeted high-frequency oscillatory ventilation (HFOV) and the combination of HFOV and inhaled nitric oxide (iNO).

In this thesis, we describe our first experiences with HFOV in paediatric patients and introduce three HFOV strategies *(Chapter 2)*. First, the “open-lung strategy” in diffuse alveolar disease, secondly the “low-volume strategy” in air leak syndromes and thirdly the “open airway strategy” in obstructive small airway disease. Although at the time of the study, HFOV was used as a rescue therapy for failure of conventional mechanical ventilation (CMV), in two of 38 HFOV runs in 35 patients a HFOV failure was encountered. Nine patients developed chronic lung disease following HFOV and one patient was discharged with supplemental oxygen therapy. Three patients developed an airleak during HFOV. During transition from CMV to HFOV increased circulatory support was needed in a significant number (32%) of patients, but with this support the transition was tolerated well. Generally, circulatory effects of HFOV in normovolaemic patients are minimal, but in hypovolaemic patients adequate fluid administration may improve haemodynamic stability as well as oxygenation. From these data, we conclude that HFOV is effective and safe with few side effects in paediatric patients. In addition, we found the use of the “open airway strategy” in obstructive small airway disease to be successful as an alternative to more conventional modes of ventilation. However, there may only be a small margin for the optimal airway pressure, since the relatively high pressure needed to maintain airway patency might lead to overdistention of compliant alveoli.

An initial setting of HFOV requires medical expertise with the technique and a thorough understanding of the pathophysiology of the diseased lung. In the operation of a modern military aircraft, complexity of information combined with time stress creates difficulties for the pilot under combat conditions. This bears some analogy with recruiting lung volume during initial HFOV and subsequent reduction of airway pressure, in which the physician has to obtain information from close observation of the patient, the ventilator, vital signs monitor and blood gas analysis. This stream of information then has to be combined into a pathophysiological hypothesis and therapeutic strategy within a short period of time. In an effort to enhance this information gathering process, we developed, tested, and described a system that integrates measurements obtained from the ventilator, continuous blood gas

analyser and lung volume changes *(Chapter 3)*. The system, in part based on respiratory inductive plethysmography (RIP), was modified to sample at high rates, in order to record rib cage and abdominal displacement during HFOV. The linearity and accuracy of the device for the estimation of lung volume changes is confirmed. The relation between continuous distending pressure and lung volume, oxygenation, oxygenation index (OI), and the ratio of pressure amplitudes at the distal end and the proximal opening of the endotracheal tube (OPR) as well as the changes of these dependent variables with time were made available in real time. OI and OPR can be used as estimators of optimal continuous distending pressure (CDP) during HFOV.[1,2] Clinically, however, the value of OPR may be limited, since its measurement necessitates the introduction of a pressure transducer into the main airways for which the patient has to be disconnected from the ventilator, which in turn will lead to the loss of lung volume. Furthermore, the method is sensitive to fluid and mucus accumulation on the pressure transducer. We felt that the integration of ventilator settings and dependent physiological variables may provide useful information for clinical, instructional and research applications.

We studied the accuracy of measurements of lung volumes with the device at different end expiratory pressures (PEEP) with changing severity of acute lung injury, with the intention to predict its accuracy of mean lung volume changes during HFOV *(Chapter 4)*. The standards of measurement of end-expiratory lung volume during mechanical ventilation, inert gas (nitrogen, helium, argon or SF_6) washin or washout techniques or whole body plethysmography were not available in our laboratory. We therefore chose to assess the linearity of tidal volume measured with RIP with the inflated tidal volume measured with a pneumotachograph at the airway opening as an alternative to mean lung volume or end-expiratory lung volume measurement.
The system can be calibrated to a known volume. With changing degree of lung injury, most accurate results were obtained when measurements are preceded by a calibration in pulmonary conditions that are comparable to the measurement period. Furthermore, accuracy proved to be unpredictably PEEP dependent. Calibration of the device during HFOV is not feasible routinely, in the absence of a standard for mean or tidal volume measurements during HFOV. Discontinuation of HFOV and calibration during a period of CMV would be an unattractive alternative. Omitting calibration and weighing both RIP signals (obtained from rib cage and abdominal displacement) equally does not significantly reduce accuracy. Accuracy is dependent on the weight factor used, and this weight factor may be species dependent. Despite these limitations, we find RIP to be comparable to other

techniques of lung volume change measurement currently in clinical use. We have shown that with this technique, it is possible to measure both relative mean lung volume changes and tidal volume changes.

The next question we tried to answer, assuming the accuracy of RIP measurements of lung volume (change) is considered acceptable for clinical purposes, was to assess the value of the pressure-volume (PV) relationship in mechanical ventilation *(Chapter 5)*. The use of PV characteristics to set PEEP during CMV or CDP during HFOV has been addressed in numerous studies. In a mathematical model of the ARDS respiratory system, we demonstrated that opening of collapsed lung units (recruitment) may take place with increasing airway pressures until high pressures are reached. During this procedure previously collapsed lung units may open and immediately become overdistended. This phenomenon is most pronounced in the severest simulated ARDS grades. The characteristics of the inflation limb of the P-V curve are not uniquely related to alveolar recruitment and overdistention, but also to chest wall properties and rate of recruitment. Following complete alveolar recruitment, decreasing airway pressure results in reduction of lung volume, initially with a decrease of alveolar overstretching while alveoli remain open. In other words, the pressure-volume relationship, but also pressure-atelectasis and pressure-overstretching display hysteresis. As a consequence, a procedure aimed at opening collapsed alveoli may facilitate subsequent reduction of airway pressures with avoidance of atelectasis, overstretching and high airway pressures. Between the upper corner point and inflection point of the deflation P-V curve, significant overstretching decreases, while significant atelectasis reappears in the pressure range between the inflection point and lower corner point. In general, optimal PEEP is thus found between the lower and upper corner pressures of the deflation P-V curve, but this knowledge is irrelevant due to the wide range between these boundaries. The good correlation between P-V characteristics and optimal PEEP or CDP reported in the literature may be limited to a group of animals or patients of comparable body size and with comparable degree of acute lung injury. In our model, we found static pressure-volume characteristics to be moderate estimators of optimal airway pressures. We further have shown that optimal PEEP increases with the degree of lung injury, while the safe plateau pressures do not. As a consequence, tidal volumes that can be applied with avoidance of end-expiratory collapse and end-inspiratory overdistention decrease with increasing disease severity to a level that may result in inadequate conventional mechanical ventilation. If the assumptions in our model are correct, this finding suggests that a ventilation mode with smaller tidal volumes may be of benefit, such as high frequency oscillatory ventilation, especially in severe ARDS.

As an alternative to tracing lung volume during lung volume optimisation and subsequent reduction of air way pressure to its optimal value, we hypothesised that RIP estimated chest wall displacement would be maximal at the airway pressure where either respiratory system or lung compliance would be maximal.

RIP measures inductance change in zigzag-shaped gauges fitted in elastic belts placed securely around rib cage and abdomen. As a result of rib cage and abdominal displacement, the belts and gauges will stretch and inductance of the resonator circuit in which the gauges are placed will change. The inductance change of each circuit forms a signal, which has a linear relationship with cross-sectional area. Assuming thoracic and abdominal height is fixed during breathing, an estimate of volume change can be made. Respiratory system volume changes are calculated from the summed signal, assuming synchronicity between both belts. During HFOV, however, a clear mean airway pressure-dependent phase difference between rib cage and abdominal displacement was demonstrated *(Chapter 6)*. In seven of eight piglets a clear maximum tidal chest wall displacement could nevertheless be determined at a mean airway pressure approximating the optimal airway pressure. This optimum airway pressure had been defined as the lowest airway pressure where physiological shunt was still below 0.1. Following a lung volume recruitment manoeuvre, rib cage amplitude increased with decreasing mean airway pressure, without a clear maximum. Interestingly, abdominal displacement was relatively stable during this procedure, but was reduced at airway pressures around the pressure coinciding with optimal respiratory system compliance, oxygenation and ventilation. These changes probably reflect pressure-dependent impedance changes of the components of the respiratory system. Monitoring of tidal volume and abdominal displacement during HFOV may prove to be of clinical value during HFOV. Since these experiments were performed in paralysed surfactant deficient animals the findings cannot be extrapolated to human ARDS patients, but may form a basis for further research.

Not in all patients, it is possible to improve oxygenation by lung volume optimisation. For these patients, adjunctive therapies have been designed. One of these adjunctive therapies is the addition of nitric oxide to the respiratory gases (iNO). The effect of iNO is augmented by optimal recruitment of lung volume, as has been described in the combination of HFOV and iNO.[3,4] At the time, iNO was considered an investigational drug, its use limited to studies and compassionate use. Nitric oxide was not available as a medical gas, and therapeutic dosing systems were not available. In an attempt to provide an accurate means of dosing

nitric oxide during HFOV, we described the accuracy of nitric oxide dosage and measurement during HFOV comparing various set-ups *(Chapter 7)*. We demonstrated that the inaccuracy and pressure sensitivity of standard rotameters even in the absence of HFOV pulsatile pressures resulted in clinically unacceptable inaccurate iNO dosage during HFOV. Highest dosage accuracy could be obtained when both NO and ventilator bias flow were controlled by a mass flow controller. For practical clinical purposes however, we concluded that the combination of rotameter-controlled ventilator bias flow and mass flow controlled-NO flow was adequately predictable although a dose 16% above the calculated dose may be delivered. This is not not necessarily a clinically significant effect, since typically iNO is titrated on effect. For purposes of monitoring NO concentration based on calculation and accurate flow regulation, when small measurement errors are not relevant, electrochemical measurement of NO concentrations with an electrochemical sensor, designed to reduce the effects of humidity, pulsatile pressure and high oxygen concentration on gas measurements, is as useful as that obtained with a chemiluminescence analyser. Based on our work, a commercially available device has been developed for nitric oxide dosage and monitroing of therapy during HFOV.

Nitric oxide is present throughout the body and acts as a messenger molecule, affecting not only vascular tone but also platelet function and the immune system. In the presence of oxygen it is rapidly converted into nitric dioxide. Inhalation of gas mixtures containing high concentrations of NO and NO_2 can be rapidly lethal in humans. Long-term effects of low-dose NO inhalational exposure are unknown, but NO might have carcinogenic properties. The safety of medical and nursing staff and adjacent patients in the proximity of a patient receiving iNO in combination with HFOV, where high gas flow rates are typically used, were of concern. For this reason we assessed the potential environmental exposure of intensive care staff and adjacent patients to NO and NO_2 pollution during NO inhalational therapy combined with HFOV *(Chapter 8)*. We found increased levels of both molecules, but within occupational safety limits. Concentrations decrease with increasing distance to the ventilator exhaust valve, and can further be decreased by the use of waste gas exhaust system.

In the years following these studies, therapeutic use of nitric oxide did meet the initial expectations and its use has been limited to a selected group of diseases.

PERSPECTIVES

HFOV has gained a definitive place in paediatric intensive care, and with the recent availability of a more potent oscillator it may gain a place in adult intensive care as well. Conventional mechanical ventilation has changed in recent years. The importance of reducing tidal volumes in combination with recruitment procedures in acute lung injury has gained interest, but is still not generally accepted. Irrespective of the ventilation mode, clinical evidence on the long-term beneficial effects of these strategies has to be sought. In HFOV, the optimal recruitment manoeuvre (e.g. gradual increase of airway pressure, single sustained inflation, rapid sequence inflations) has not been defined, nor is it clear to which value the recruitment pressure should be increased.

Our studies have shown the limited value of volume measurement and the P-V relation as estimators of optimal airway pressures. Nevertheless, it may prove of value during recruitment pressures, since in our mathematical model with inflation above the upper corner pressure of the inflation P-V curve little volume was gained that could be maintained without significant overdistention with end-expiratory pressure.

For determination of the optimal CDP during HFOV, the oxygenation index has been shown to be of value, but this parameter usually is not available directly at the bedside. With electrical impedance tomography (EIT) global and regional information on lung mechanics and potentially perfusion can be assessed. At present, however, the application of 16 separate electrodes in a potentially unstable patient is impractical and the interface to the user is far from optimal. Development of an easy to apply “electrode belt” and improved graphical interface would strongly improve the applicability of EIT.

Initial optimisation of lung volume with HFOV has been addressed in this thesis and work of others.

Little is known about the phase of HFOV weaning with reduction of airway pressures. Protocol-based ventilator weaning, for instance daily or even more frequent determination of CDP at which the lung collapses and reopens, may reduce intensive care unit length of stay. These protocols yet have to be designed.

Maintenance of spontaneous breathing and avoidance of muscular paralysis results in improved pulmonary function, gas exchange, systemic blood flow and tissue oxygenation. In larger patients however, patient breathing activity during HFOV interferes with operation of the ventilator and may lead to increased work of breathing. The development of a system that would allow the oscillator to support breathing efforts may lead to a better tolerance of

HFOV in adult patients, a reduced use of sedatives and muscle relaxants and even hasten recovery.

REFERENCES

1. van Genderingen HR, van Vught AJ, Duval EL, Markhorst DG, Jansen JR. Attenuation of pressure swings along the endotracheal tube is indicative of optimal distending pressure during high-frequency oscillatory ventilation in a model of acute lung injury. *Pediatr Pulmonol* 2002; 33: 429 - 436.

2. van Genderingen HR, van Vught JA, Jansen JR, Duval EL, Markhorst DG, Versprille A. Oxygenation index, an indicator of optimal distending pressure during high-frequency oscillatory ventilation? *Intensive Care Med* 2002; 28: 1151 - 1156.

3. Hoehn T, Krause M, Hentschel R. High-frequency ventilation augments the effect of inhaled nitric oxide in persistent pulmonary hypertension of the newborn. *Eur Respir J* 1998; 11: 234 - 238.

4. Kinsella JP, Truog WE, Walsh WF, Goldberg RN, Bancalari E, Mayock DE, Redding GJ, deLemos RA, Sardesai S, McCurnin DC, Moreland SG, Cutter GR, Abman SH. Randomized, multicenter trial of inhaled nitric oxide and high-frequency oscillatory ventilation in severe, persistent pulmonary hypertension of the newborn. *J Pediatr* 1997; 131: 55 - 62.

Chapter 10

Summary

Chapter 1

In a significant number of patients, defienct or abnormal surfactant leads to respiratory insufficiency. In preterm infants, a surfactant deficiency may lead to the neonatal respiratory distress syndrome (nRDS), whereas an abnormal surfactant may lead to the acute respiratory distress syndrome. Patients suffering from a respiratory distress syndrome lack a normal function of lung surfactant and their lungs tend to collapse leading to severe hypoxia. Measurements of respiratory system mechanics reveal a disturbed pressure-volume relation. Experimental and clinical studies have demonstrated the benefits of elevated end-expiratory pressures during mechanical ventilation, provided that collapsed lung units have been opened using adequately high airway pressures; recruitment of lung volume. High-frequency oscillatory ventilation (HFOV) is an alternative ventilation mode, in which lung volume can be recruited and maintained while high end-inspiratory pressures and cyclic reexpansion of end-expiratory collapsed lung units may be avoided. In Chapter 2 our initial results using this technique of mechanical ventilation are described and ventilatory strategies introduced. Despite the relative straightforwardness of the technique there is a need for a clinically applicable method to find the optimal lung volume obtained by setting of continuous distending pressure (CDP). In Chapter 3 we describe a system that integrates ventilator settings and dependent physiological variables. The accuracy of lung volume measurements using this system at various levels of end-expiratory pressures and different degrees of lung injury are described in Chapter 4. In Chapter 5, the value of static pressure-volume characteristics as estimators of optimal airway pressures is addressed. Dynamic changes in abdominal and rib cage displacement resulting from changes in CDP during HFOV are described in Chapter 6. Even when lung volume and CDP are considered optimal, a selected group of patients may benefit from the combination of HFOV and inhaled nitric oxide (iNO). In Chapter 7 technical aspects of dosage of iNO during HFOV are presented. With HFOV, relatively large gas flows are generated. When HFOV is combined with iNO, additional large NO flows are generated. In Chapter 8 the occupational consequences for both adjecent patients and intensive care staff of combined iNO and HFOV therapy are discussed.

Chapter 2

Three strategies of setting CDP or targeted lung volume during rescue HFOV in 35 children subsequently admitted to two tertiary care paediatric intensive care units in a four year period were described. First, the “open-lung strategy” designed to rapidly recruit and

maintain optimal lung volume in diffuse alveolar disease (DAD) and pulmonary haemorrhage. Second, the “low-volume” -strategy in persistent airleak where CDP was reduced until the airleak ceases. Third, the “open-airway”-strategy in obstructive airway disease where CDP was used to recruit and stent the airways. Respiratory insufficiency was classified as resulting from DAD in 27 (77%) patients and obstructive small airway disease in five (8%) patients. In one patient with concurrent small airway disease, HFOV therapy was aimed at resolution of persistent airleak. In four patients HFOV was combined with iNO therapy, two of the seven non-survivors died as a result of respiratory failure. Three patients developed a new airleak during HFOV. Nine patients developed chronic lung disease. One of four patients treated with the combined HFOV iNO therapy responded to therapy. Increasing oxygenation index over time predicted adverse outcome resulting from respiratory failure. We concluded that HFOV is a safe and effective modality of mechanical ventilation with very few side effects. HFOV may be used early in the disease process.

Chapter 3

A system that integrates measurements obtained from the ventilator, continuous blood gas analysis and lung volume changes, was developed, tested and described. The system, in part based on respiratory inductive plethysmography (RIP), was modified to sample at high rates, in order to record rib cage and abdominal displacement during HFOV. The linearity and accuracy of the device for the estimation of lung volume changes was confirmed. The relation between continuous distending pressure and lung volume, oxygenation, oxygenation index (OI) and the ratio of pressure amplitudes at the distal end and the proximal opening of the endotracheal tube (OPR) as estimators of optimal continuous distending pressure (CDP) during HFOV as well as the changes of these dependent variables with time were made available in real time.

Chapter 4

Accuracy of lung volume measurements with the designed measurement system was assessed during conventional mechanical ventilation at varying positive end-expiratory pressure (PEEP) levels and with progressive severity of lung injury. Measurement bias increased and precision decreased from the initial calibration with increasing severity of injury and proved to be PEEP dependent. To obtain optimal accuracy, the system has to be recalibrated at the mean lung volume and severity of illness under study. The accuracy of the measurement system is comparable to other monitoring devices that are currently in clinical use, but are not validated during HFOV.

Omitting calibration and weighing both RIP signals (obtained from rib cage and abdominal displacement) equally did not significantly reduce accuracy. Accuracy was dependent on the weight factor used, and this weight factor may be species dependent. Weight factors obtained from the literature and obtained in animal experiments should therefore not be extrapolated to human measurements. We have shown that with this technique it is possible to accurately measure both relative mean lung volume changes and tidal volume changes, provided some conditions are met.

Chapter 5

In a mathematical model of the ARDS respiratory system, we demonstrated that opening of collapsed lung units (recruitment) may still take place with increasing airway pressures until high pressures are reached. During this procedure previously collapsed lung units may open and immediately become overdistended. The characteristics of the inflation limb of the P-V curve are not uniquely related to alveolar recruitment and overdistention, but also by chest wall properties and rate of recruitment. Following complete alveolar recruitment, decreasing airway pressure initially resulted in a decrease of alveolar overstretching while alveoli remained open. As a consequence, a procedure aimed at opening collapsed alveoli may facilitate subsequent reduction of airway pressures with avoidance of atelectasis, overstretching, and high airway pressures.
Static pressure-volume characteristics proved to be moderate estimators of optimal airway pressures. The good correlation between P-V characteristics and optimal PEEP or CDP reported in the literature may be limited to a group of animals or patients of comparable body size and with comparable degree of acute lung injury. Optimal PEEP increased with degree of lung injury, while the safe plateau pressures did not. As a consequence, tidal volumes that can be applied with avoidance of end-expiratory collapse and end-inspiratory overdistention decrease with increasing disease severity to a level that may result in inadequate conventional mechanical ventilation. If the assumptions in our model are correct, this finding suggests that a lung volume recruitment manoeuvre and a ventilation mode with smaller tidal volumes, such as HFOV, may be of benefit, especially in severe ARDS.

Chapter 6

Mechanical ventilation leads to both rib cage and abdominal displacement. We have shown that during HFOV rib cage and abdominal displacement are not synchronous and of equal magnitude. The phase difference between rib cage and abdominal displacement and the mutual relation of these movements depend on the imposed airway pressure and

subsequent lung volume. In seven of eight piglets, maximal tidal displacement of the chest wall was a moderate estimator of optimal airway pressure. Abdominal displacement was minimal in the pressure range coinciding with optimal airway pressure. Monitoring of tidal volume and abdominal displacement during HFOV may be of value during HFOV, but further research in human patients is warranted.

Chapter 7

During HFOV, standard rotameter flow control of both nitric oxide (NO) and ventilator flow may lead to unpredictable and clinically unacceptable NO concentration. Moderate, and clinically acceptable, dosage accuracy was obtained when an electronic mass flow controller (MFC) was used for NO flow control, with ventilator flow controlled with a rotameter. Maximal dosage accuracy was obtained with both NO and bias gas flow controlled with a MFC. The standard method for measurement of nitric oxide and nitric dioxide concentrations in dry air is chemiluminescence. Alternatively, these concentrations can be measured by the use of electrochemical sensors. The standard chemiluminescence analyser used was sensitive to humidification of ventilation gasses. The electrochemical analyser we assessed displayed a systematic error comparable to that obtained with chemiluminescence, but its precision was significantly lower. Absolute measurement error was nevertheless small and without clinical relevance. For purposes of monitoring NO concentration during iNO therapy, based on calculation and accurate flow regulation, when small measurement errors are not relevant, electrochemical measurement of NO concentrations with the an electrochemical sensor is as clinically useful as that obtained with a chemiluminescence analyser. Based on our work, a commercially available device has been developed for nitric oxide dosage and monitroing of therapy during HFOV.

Chapter 8

Nitric oxide and its higher oxides are toxic when levels of safe concentration or exposure time are exceeded. When iNO therapy is used in combination with HFOV, high gas NO flows may be needed to obtain sufficient NO concentration in the inspired gas. We assessed the potential environmental exposure of intensive care staff and adjacent patients to NO and NO_2 pollution during NO inhalational therapy combined with HFOV in four situations. We found increased levels of both NO and NO_2, but within occupational safety limits. Concentrations decreased with increasing distance to the ventilator exhaust valve, and could be further decreased by the use of waste gas exhaust system.

In ***chapter 9*** our findings, their interrelationship and future perspectives are discussed. (***Chapters 10 and 11*** are the English and Dutch summaries of the thesis.)

Hoofdstuk 11

Op weg naar optimaal long volume tijdens hoog-frequent oscillatoire beademing

Samenvatting

Hoofdstuk 1

Bij een belangrijk aantal patienten leidt een tekort aan of afwijkend long surfactant tot acute ademnood. Bij te vroeg geboren patienten leidt een tekort aan surfactant tot het neonataal respiratoir distress syndoorm (nRDS), bij het acuut respiratoir distress syndroom (ARDS) is er sprake van afwijkend surfactant. Bij patiënten die aan een dergelijk ademnood syndroom lijden kan een abnormale functie van long surfactant ertoe leiden dat hun longen neigen tot samenvallen met ernstige zuurstofnood als gevolg. Bij metingen van de mechanische eigenschappen van het respiratoir systeem wordt een gestoorde druk-volume relatie gezien. Experimentele en klinische studies hebben de voordelen van verhoogde druk aan het einde van de uitademing tijdens mechanische ventilatie aangetoond, op voorwaarde dat de samengevallen longdelen door voldoende hoge luchtwegdruk zijn geopend; rekrutering van longvolume. Hoog -frequent oscillerende ventilatie (HFOV) is een alternatieve manier van mechanisch beademen, waarmee het longvolume kan worden gerekruteerd en gehandhaafd terwijl hoge drukken aan het eind van de inademing en cyclisch heropenen van longdelen die aan het eind van de uitademing zijn samengevallen kan worden vermeden. Hoofdstuk 1 verschaft de nodige achtergrondinformatie en geeft de bedoeling en opbouw van dit proefschrift aan. In hoofdstuk 2 zijn onze eerste ervaringen met deze techniek van mechanische ventilatie beschreven en de gebruikte geïntroduceerde strategieën geïntroduceerd. Ondanks de relatieve eenvoud van de techniek is er een behoefte aan een klinisch toepasbare methode om het optimale longvolume te vinden dat door instelling van de gemiddelde luchtwegdruk (CDP) wordt verkregen. In hoofdstuk 3 beschrijven wij een systeem dat ventilator instellingen en afhankelijke fysiologische variabelen integreert. De nauwkeurigheid van de metingen van het longvolume met dit systeem bij diverse niveaus van eind-uitademings druk en bij verschillende graden van longschade wordt beschreven in hoofdstuk 4. In hoofdstuk 5 wordt de waarde van statische druk-volume karakteristieken als schatters van optimale luchtwegdruk besproken. De dynamische veranderingen in de verplaatsing van de buik en ribbenkast, die optreden bij CDP veranderingen tijdens HFOV, vormen het onderwerp van hoofdstuk 6. Zelfs wanneer het longvolume en CDP als optimaal worden beschouwd, kan een geselecteerde groep patiënten van de combinatie van HFOV en geïnhaleerd stikstofoxide (iNO) profiteren. In hoofdstuk 7 worden de technische aspecten van dosering van iNO tijdens HFOV besproken. Bij HFOV wordt gebruik gemaakt van vrij grote gasstromen, bij toediening van NO kunnen dan ook grote hoeveelheden van dit gas in de omgeving terecht komen. In hoofdstuk 8 worden de gevolgen voor het directe milieu en daarmee voor een blootstelling van andere

patiënten en voor het personeel van NO en NO2 tijdens gecombineerde iNO en HFOV therapie besproken.

Hoofdstuk 2

Drie strategieën worden beschreven met een verschillende gemiddelde luchtwegdruk en longvolume tijdens rescue HFOV bij 35 opeenvolgend opgenomen kinderen gedurende 4 jaar in twee afdelingen voor pediatrische intensieve zorg. Ten eerste, de "open-long strategie" die bedoeld is om bij diffuse aandoeningen van de longblaasjes (DAD) snel een optimaal longvolume te bereiken en te handhaven. Ook bij longbloeding werd deze strategie gebruikt. Ten tweede, de "lage-volume-strategie" die haar toepassing vond bij patiënten met een blijvend luchtlekkage naar het longweefsel of naar buiten de long. Ten derde, de "open-luchtweg-strategie" waarbij CDP bij obstructieve aandoeningen van de kleine luchtwegen werd gebruikt om de luchtwegen te openen en open te houden Bij 27 (77%) patienten was er sprake van DAD, bij 5 (8%) patiënten was er sprake van een obstructieve aandoening van de kleine luchtwegen. Bij een van deze vijf patiënten was er ook sprake van een ernstig luchtlekkage syndroom, en werd de HFOV therapie gericht op resolutie van de luchtlekkage. Bij vier patiënten werd HFOV gecombineerd met iNO, twee van de zeven niet-overlevenden stierven als gevolg van falende beademing. Drie patiënten ontwikkelden een nieuw luchtlek syndroom tijdens HFOV. Negen patiënten ontwikkelden chronische longziekte. Één van vier patiënten die met de gecombineerde HFOV en iNO therapie werden behandeld, reageerde gunstig op de combinatietherapie. Een met de tijd stijgende oxygenatie-index voorspelde een ongunstig resultaat tengevolge van tekort schietende beademing. Wij concludeerden dat HFOV bij een juist gebruik effectief en veilig is en weinig ongewenste neveneffecten kent. HFOV kan vroeg in het ziekteproces worden ingezet.

Hoofdstuk 3

Een systeem dat metingen integreert, afkomstig van de beademingsmachine, de continue bloedgasanalyse en longvolume metingen, werd ontwikkeld, getest en beschreven. Het systeem, voor een deel gebaseerd op respiratoire inductieplethysmografie (RIP), werd aangepast om verplaatsingen van ribbenkast en buik tijdens HFOV te registreren. De lineariteit en de nauwkeurigheid van het apparaat voor de schatting van de veranderingen van het longvolume werden bepaald. De relatie tussen gemiddelde luchtwegdruk en longvolume, oxygenatie, oxygenatieindex (OI) en de verhouding van drukamplitude aan de openingen aan het begin en einde van de beademingsbuis (OPR) als schatters van optimale

luchtwegdruk tijdens HFOV waren direct beschikbaar. Ook de veranderingen van deze afhankelijke variabelen als functie van de tijd kon worden afgelezen.

Hoofdstuk 4

De nauwkeurigheid van de metingen van het longvolume met het ontworpen meetsysteem werd beoordeeld tijdens conventionele mechanische ventilatie op variërende positieve eind-uitademings druk (PEEP) niveaus en met toenemende ernst van longschade. De afwijking van de oorspronkelijke calibratie en de spreiding van de meetfout nam toe met toenemende ernst van longschade en bleek PEEP afhankelijk te zijn. Om optimale nauwkeurigheid te verkrijgen, moet het systeem bij het gemiddelde longvolume en bij de mate van ziekte in studie opnieuw worden geijkt. De nauwkeurigheid van het systeem is vergelijkbaar met andere meetmethodieken die momenteel klinisch gebruikt worden bij conventionele mechanische ventilatie, maar die niet gevalideerd zijn voor gebruik tijdens HFOV. De nauwkeurigheid was wel afhankelijk van de gebruikte weegfactor, en deze weegfactor kan soort-afhankelijk zijn. Gebruik van in de literatuur genoemde weegfactoren bij proefdieren is af te raden bij humane metingen. Wij hebben aangetoond dat met deze techniek het mogelijk is om zowel relatieve veranderingen van het gemiddelde longvolume als teugvolume veranderingen nauwkeurig te meten zijn als aan een aantal voorwaarden voldaan is.

Hoofdstuk 5

In een wiskundig model van het ademhalingssysteem met ARDS, toonden wij aan dat het openen van samengevallen longdelen (rekrutering) met stijgende luchtwegdruk kan voortduren tot een zeer hoge druk wordt bereikt. Tijdens deze procedure kunnen de eerder samengevallen longdelen openen en onmiddellijk overrekt zijn. De kenmerken van het inademingsbeen van de P-V kromme worden niet uitsluitend bepaald door het openen en overrekken van de kleinste longdelen, maar ook door eigenschappen van de borstkas en de snelheid waarmee de longdelen open gaan. Nadat het grootste deel van de samengevallen longdelen was geopend, resulteerde een dalende luchtwegdruk aanvankelijk in een afname van het aantal overrekte longdelen terwijl deze wel open bleven. Een procedure die op het openen van samengevallen longdeeltjes is gericht kan verdere vermindering van luchtwegdruk vergemakkelijken terwijl samenvallen en overreking van de long en de noodzaak tot het gebruik van hoge luchtweg druk worden vermeden. De kenmerken van de statische P-V kromme bleken matige schatters voor de optimale luchtwegdruk te zijn. De goede correlatie tussen P-V kenmerken en optimale eind-uitademings druk of CDP die in de

literatuur wordt gemeld kan mogelijk worden verklaard doordat groepen proefdieren en patiënten met vergelijkbare ernst van longschade werden vergeleken. De optimale eind-uitademings druk steeg met de ernst van longschade, terwijl de veilige plateaudruk eerder afnam. Dat kan er toe leiden dat de teugvolumes waarbij samenvallen aan het einde van de uitademing en overrekking aan het einde van de inademing wordt vermeden afnemen met toenemende ernst van acute longschade. Bij de ernstigste vormen van acute longschade kan dat resulteren in ontoereikende veilige conventionele mechanische beademing. Als de veronderstellingen in ons model correct zijn, zou een manoeuvre gericht op het openen van samengevallen longdelen in combinatie met een manier van beademen waarbij kleine teugvolumes worden gebruikt, zoals HFOV, vooral bij de ernstigere vormen van acute longbeschadiging van nut kunnen zijn.

Hoofdstuk 6

Tijdens mechanische beademing bewegen zowel ribbenkast als buik. Wij hebben aangetoond dat ribbenkast en buik tijdens HFOV niet gelijktijdig en in dezelfde mate bewegen. Het faseverschil tussen buik en ribbenkast beweging en de onderlinge verhouding van deze bewegingen is afhankelijk van de opgelegde luchtwegdruk en dus het longvolume. Bij zeven van de acht biggen werd een maximum teugvolume gevonden in het drukgebied, overeenkomend met de optimale luchtwegdruk. De optimale luchtwegdruk was daarbij gedefinieerd als de laagste druk, waarbij de fysiologische shunt fractie nog juist kleiner was dan 0.1. De uitslagen van de buikbewegingen waren ook het minst rond deze druk. Tijdens hoog-frequent beademen zou het bewaken van het teugvolume en de buikbewegingen van klinisch belang kunnen zijn, maar verder onderzoek bij humane patiënten is noodzakelijk om deze veronderstelling te toetsen.

Hoofdstuk 7

Tijdens HFOV kan het gebruik van standaard gasstroomregelaars (rotameter) voor zowel stikstof monoxide (NO) als ventilator gas stroom tot onvoorspelbare concentraties NO in het beademingsgas leiden. Deze onvoorspelbaarheid maakt deze methode klinisch onaanvaardbaar. Een redelijke en klinisch aanvaardbare doseringsnauwkeurigheid werd verkregen met een elektronisch gestuurde gasstroomregelaar (massflow controller) voor de NO gasstroom, terwijl de ventilator gasstroom met rotameter werd gecontroleerd. De hoogste nauwkeurigheid werd bereikt indien beide gasstromen electronisch werden gestuurd. De standaardmethode voor meting van NO en stikstofdioxide (NO_2) concentraties in droge lucht is chemoluminescentie. Electrochemische meting van deze concentraties is

een alternatieve methode. De standaard gebruikte chemoluminescentiemeter bleek gevoelig te zijn voor bevochtiging van het beademingsgas. De elektrochemische sensor toonde een systematische fout vergelijkbaar met die van chemoluminescentie, maar de precisie van de electrochemische methode was beduidend lager. Dit werd veroorzaakt door meetfouten bij lage NO concentraties die in absolute zin klein waren, maar groot in relatie tot de werkelijke waarde. Wanneer kleine meetfouten acceptabel zijn bij de controle van NO-inhalatietherapie, en de NO dosering nauwkeurig kan worden geregeld, is elektrochemische meting van NO concentraties klinisch even nuttig als metingen verkregen met een chemoluminescentie meter. Op basis van onze studies is een commercieel systeem beschikbaar gekomen, waarmee nauwkeurig NO kan worden toegediend tijdens HFOV en NO en NO_2 concentraties gemeten.

Hoofdstuk 8

Stikstofmonoxide en zijn hogere oxiden zijn giftig bij hoge concentraties of lange tijden van blootstelling aan het gas. Als de NO inhalatie (iNO) therapie in combinatie met HFOV wordt gebruikt, zijn hoge NO gasvolumes vereist om voldoende NO concentratie in het beademingsgas te bereiken. Wij hebben de mogelijke gevolgen voor de omgeving van personeel op een afdeling voor intensieve zorg en patiënten die in de buurt liggen van een patient die behandeld wordt met de combinatie van iNO en HFOV in vier situaties gemeten. Wij vonden verhoogde niveaus van zowel NO als NO_2 in de omgeving, maar deze concentraties bleven binnen de veiligheidsrichtlijnen. De concentraties verminderden met toenemende afstand van de gasuitlaat van de beademingsmachine, en konden verder worden verlaagd door het met NO en nitreuze gassen verontreinigde uitademingsgas op te vangen bij de uitademingsklep van de beademingsmachine en af te voeren.

In ***hoofdstuk 9*** worden de bevindingen in onderling verband bediscussieerd en worden toekomstperspectieven besproken. (***Hoofdstuk 10*** en ***11*** vormen de Engelstalige respectievelijk Nederlandstalige samenvattingen van het proefschrift.)

DANKWOORD

Veel mensen hebben bijgedragen tot de voltooiing van dit proefschrift. Daarom wil ik iedereen bedanken die mij op enigerlei wijze heeft geholpen. Een aantal wil ik graag met name noemen, in het besef dat een dergelijke opsomming nooit compleet kan zijn.

John Roord bood mij de gelegenheid om dit onderzoek uit te voeren en had altijd het volste vertrouwen in een gunstige uitkomst. Zijn begeleiding, met name in de afrondende fase van dit proefschrift, is van grote waarde geweest.

Hans van Vught stond aan de basis van mijn HFOV gerelateerde onderzoek. Hij organiseerde de “HFOV-groep” en bracht daarbij een samenwerking tussen het WKZ Utrecht en het Vumc tot stand, waarbij onderzoekers uit diverse disciplines bij elkaar werden gebracht. Geregeld waren er besprekingen van onderzoeksvoorstellen en resultaten in het WKZ, die vrijwel zonder uitzondering tot een geanimeerde discussie in een vriendelijke atmosfeer aanleiding gaven. Voor een belangrijk deel ontstonden de onderzoeksideeën tijdens wandelingen in Snowbird en Ovifat, waarbij het voor kon komen dat we zo verdiept waren in de discussie dat we uiteindelijk verdwaalden. Het mag een wonder heten dat wij uiteindelijk steeds weer de bewoonde wereld hebben bereikt. Ik heb de positieve maar ook kritische en altijd kundige begeleiding bijzonder gewaardeerd. Ik hoop dat onze samenwerking zal worden voortgezet.

Huib van Genderingen ben ik meer dan dankbaar voor zijn ondersteuning bij mijn gedachten vorming en zijn hulp bij het schrijven. Hij was mijn dagelijkse gesprekspartner op de werkvloer. Regelmatig kwamen wij bij elkaar om ideeën te toetsen. Meestal kon Huib mijn ideeën ontkrachten. Het was vooral plezierig als dat niet lukte, omdat ik altijd wist dat Huib een kritisch filter was. Zijn bijdrage is van onschatbare waarde geweest. Ik hoop ook bij volgende projecten nog lang met Huib samen te kunnen werken.

De promotiecommissie, prof.dr.ir. J. H. van Bemmel, dr. J. R. C. Jansen, prof.dr. R. J. B. J. Gemke, prof.dr. A. R. J. Girbes en prof.dr. R. M. Heethaar ben ik dank verschuldigd voor het beoordelen van het manuscript.

Tom Leenhoven, onnavolgbaar in het bedenken van onderzoeks vragen, praktische oplossingen en het samenbrengen van experts overal vandaan, heeft bijzonder veel bijgedragen bij de uiteindelijke totstandkoming van dit werk. Onze samenwerking gaat vele jaren terug. Eigenlijk hebben wij aan het einde van de tachtiger jaren samen een van de

eerste prototypes van de hoog frequent oscillator gebouwd. Ook aan het project van de AD convertor die via de parallelle computer poort kon worden uitgelezen en waarbij we een computer hebben opgeblazen, bewaar ik goede herinneringen. Bij onze wandeling op de Axamer Lizum, waar we de eerste ideeën over geïntegreerde metingen tijdens HFOV bespraken, had ik niet verwacht dat dit uiteindelijk tot dit resultaat zou leiden.

Dr. John Arnold. John, Thank you for the hospitality rendered at your department in Boston and for the effort you took to introduce me to high frequency oscillatory ventilation. Since then we had many stimulating discussions on the subject of HFOV, mechanical ventilation and critical care in general, whisky and the art of making espresso. Its is always stimulating meeting with you, and I do hope our co-operation will continue.

Dr. Keith Hickling. Keith, chapter 5 is mainly based on your previous work. Although we never actually met, your insights and the many stimulating discussions via E-mail during the preparation of this manuscript were of considerable value. Thank you for your contribution from down under.

Els Duval ondersteunde mij bij de eerste dierexperimenten in Utrecht en heeft veel werk verzet voor de analyse van de klinische gegevens. Ik dank haar voor haar hulp daarbij en hoop dat zij binnen afzienbare tijd haar eigen proefschrift zal kunnen afronden.

Jos Jansen was gelukkig bereid kritisch en creatief mee te denken toen wij verklaringen zochten voor de long mechanische veranderingen die optreden tijdens HFOV. Al bij de eerste experimenten mocht ik gebruik maken van je expertise en praktische hulp. Het was en is een voorrecht met je samen te mogen werken.

Reinoud Gemke en Frans Plötz, in successie medisch hoofd van de intensive care kinderen dank ik voor de mogelijkheid die zij mij boden dit onderzoek in relatieve rust te kunnen doen en hun kritische bijdrage bij mijn voordrachten. Het zou fijn zijn als het beademings gerelateerde onderzoek op onze afdeling kan worden voortgezet. De eerste stappen daartoe zijn gezet.

Renata Sibarani-Ponsen, als anesthesioloog-kinder intensivist verbonden aan onze afdeling, belangrijke trait d’union tussen de IC kinderen en de rest van de wereld en een uitstekend clinica. Lieve Renata, wat zou ik zonder jou hebben moeten beginnen. Dank je wel voor alles wat je met oneindig geduld hebt geleerd. Je bent een kanjer.

Marre Hassing en Moniek op de Coul, mijn kamergenoten en maatjes in de tijd dat ik de onderzoeken deed en de resultaten moest verwerken, hebben veel dagelijks werk zonder morren overgenomen. Zij hebben de merkwaardigste geluiden gehoord van zowel mij als mijn computer –bijna een twee-eenheid ondertussen - als er weer eens een berekening misging. Beiden hebben uiteindelijk gekozen voor voortzetting van hun carrière in de algemene praktijk. Gelukkig ontmoeten wij elkaar nog geregeld, bijvoorbeeld tijdens APLS cursussen.

Martin Kneyber, Dana-Anne de Gast-Bakker en Marc van Heerde, fellow op de IC kinderen, hebben van mij minder begeleiding gekregen dan ik eigenlijk graag had willen geven, maar zij hebben –zover ik weet- daar niet over geklaagd. We gaan er weer tegenaan.

Mariska en Tom, betere paranimfen kan ik niet wensen, fijn dat jullie me ook bij de openbare verdediging willen bijstaan.

Mijn moeder en grootouders hebben mij altijd aangemoedigd tot studie, eerlijkheid en zelfredzaamheid. Ik ben dankbaar dat zij aanwezig konden zijn bij de uitreiking van mijn artsen bul. De afronding van mijn specialisatie mochten zij niet meer meemaken. Wat zouden ze trots geweest zijn op dit resultaat.

Berend en Thomas, jullie hebben me leren relativeren en zijn veel belangrijker dan enig proefschrift. Als kritische lezers vinden jullie dit boekje natuurlijk maar niets; je kunt er niet eens kan uit worden voorgelezen en de plaatjes zijn ook niet leuk. Het boekje op zich is ook niet zo belangrijk. Wat wel belangrijk is dat je altijd kritische vragen blijft stellen en onbevooroordeeld kunt luisteren naar nieuwe meningen. Voorlopig zijn jullie daar gelukkig erg sterk in.

Lieve Karin, jij hebt de hele weg meegemaakt vanaf de middelbare school. De laatste jaren heb je zelfs je eigen carrière op een laag pitje gezet om een stabiele basis voor de jongens en mij te kunnen verzorgen. Zonder jouw opofferings gezindheid zou het mij nooit gelukt zijn dit werk te combineren met een gezinsleven zoals ons dat voor ogen stond. Dit boekje zou er dan dus nooit gekomen zijn. Ik kan je niet genoeg vertellen hoe blij ik met je ben, en heus niet alleen omdat ik nou eindelijk dit boekje af kon maken.

AFFILIATIONS

Department of Pediatric Intensive Care, VU medical center, Amsterdam
F. B. Plötz
R. D. Sibarani – Ponsen
R. J. B. J. Gemke

Department of Physics and Medical Technology, VU medical center, Amsterdam
H. R. van Genderingen

Department of Pediatric Intensive Care, Wilhelmina Children's Hospital, Utrecht
A. J. van Vught,
T. Leenhoven
J. P. M. D. van Gestel

Department of Pediatrics, Paola Childrens's Hospital, Antwerp, Belgium
E. L. I. M. Duval

Department of Anesthesiology, Erasmus MC-Faculty Rotterdam, Rotterdam
J.J. Haitsma
B. Lachmann

Department of Intensive Care, Leiden University medical center, Leiden
J. R. C. Jansen

National Institute of Public Health and the Environment (RIVM), Air Research Laboratory, Bilthoven
J. W. Uiterwijk

National Institute of Public Health and the Environment (RIVM), National Poisons Control Centre, Bilthoven
J. Meulenbelt

CURRICULUM VITAE

Dick Markhorst was born on march 1st, 1959 in Apeldoorn. He graduated high school (HAVO) in 1976 and completed Atheneum B (Alexander Hegius Scholengemeenschap Deventer) in 1978. In the same year he started medical studies at the Vrije Universiteit in Amsterdam. In 1985, he graduated as a medical doctor. The following two years, he worked as a resident in general surgery and medicine in the Lutherse Diaconessen Hospital in Amsterdam. In 1987, he started his training in paediatrics in the St. Elisabeth Hospital in Tilburg (*J. A. Rammeloo*, residency program director). Paediatric training was completed from 1989 to 1992 at the Vrije Universiteit in Amsterdam (director *prof. dr. A. J. P. Veerman*). Subsequently he started subspecialisation in neonatology in the same hospital (*prof. dr. H. N. Lafeber*). He was a staf neonatologist in this department until 1995. In 1995, he started his training in paediatric intensive care at the Vrije Universiteit *(K. Haasnoot*). In 1997, he was officially registered as a paediatric intensivist and proceeded his career as a staff member at this unit.
Dick Markhorst is married to *Karin Fenijn*. They have two sons, *Berend* and *Thomas*.